Magnetic investigation of igneous intrusions in Teesdale, Northern England

Elijah Mwandoe

MAGNETIC INVESTIGATION OF IGNEOUS INTRUSIONS IN TEESDALE, NORTHERN ENGLAND

By: Elijah Mwandoe

Presented to the Graduate School, Durham University
In Partial Fulfilment of the Degree of M.Sc. (RES) in Geophysics

March 2005

Supervisors: Professors: R. C. Searle and N. Goulty

Department of Earth Sciences
University of Durham
United Kingdom

Abstract

A total field magnetic survey was conducted in Harwood valley in Northern Teesdale, and the neighbouring area, to investigate the igneous intrusions which could be the cause of a magnetic anomaly and metasomatism in the mineralization of the area.

Niccolite and other nickel-bearing minerals had been found in magnetite-rich ore at three localities in Harwood valley by a team of the British Geological Survey. This mineral assemblage has only been sighted in a few other zones and the cause of mineralization was assumed to be metamorphism due to the emplacement of the Whin Sill and associated dykes during the late Carboniferous-early Permian age.

Magnetic profiles recently acquired in the area confirm the existence of a dyke intruding the Teesdale fault along the Harwood valley. The average amplitude of the anomaly is 350nT, reversed with respect to the present field. Further investigations to the south-east and north-west of the valley relate the intrusion with the known outcrops of the Cleveland dyke (Tertiary). An outcrop of an igneous intrusion that bears similar properties with samples of the Cleveland dyke rock was recently sighted by the author at lower Langdon Beck near the confluence of the Tees and Harwood rivers. Thin sections of this rock displayed an identical match in grain size and pigment composition with the Cleveland dyke samples from other known outcrops, confirming the dyke's presence along the Teesdale Fault.

2.5D modelling of the magnetic profiles was carried out and the results reflect the depth to the top of the dyke at Harwood to be about 30m. Thickness of the body varies from 5 to 25m but is 12m at Harwood and about 14m in Etters Gill.

Further south of the valley at Langdon Beck is another geological formation; the Burtreeford Disturbance. This is a series of faulting and folding that was a result of compressional stress (Permian age) from a WSW direction. It also produced the E-facing monoclinal folds of the Dent Fault zone and the easterly directed Pennine thrusts of the Cross Fell Inlier before, during and after the emplacement of the Whin. The study here reflects the Disturbance as a magnetic high and its confluence with the Teesdale fault, the inferred Cleveland dyke and the Whin Sill offers a complex interpretation challenge.

A GIS data base for the project area was created using Arc-GIS, GRAVMAG, SURFER, DIDGER and other Microsoft Office applications. General interpretation of the anomalies is conducted but conclusions raise several questions. The cause of the mineralization in Harwood Valley is still uncertain, though it could be due to the cooling Cleveland dyke (58Ma) or the dyke could be forming a passage for the fluids of unknown age from the lower crust or mantle that cool and crystallize at shallower depths.

Acknowledgements

I would first wish to acknowledge my two supervisors; Professors R. C. Searle and N. Goulty for their tireless efforts in guiding me throughout the course, especially during the trying moments when I seemed to despair. Many thanks to all the staff and post graduate students at the department of Earth Sciences for their keen interest in my project and undiminished enthusiasm whenever I sought their help.

Much gratitude to Dr. B. Young of the British Geological Survey for his repeated visits to offer the much needed geological expertise in the survey area, and to all the farmers in Harwood in whose land I was kindly permitted access during data acquisition.

Last, but not least, I would wish to thank my wife and children in Kenya for their support and sacrifice in seeing the project to fruition as well as the Kenyan Government for the availed scholarship.

Table of contents Page

List of figures

Figure Page

List of tables

The Whin Sill out-crop at Cronkley Scar near the Cow Green Reservoir in Upper Teesdale. The camera is pointing to the south down the Burtreeford Disturbance.

1. INTRODUCTION

The Harwood valley is located in Teesdale, Northern Pennines, between eastings NY790 (longitude 2º 21'W) and 820 (long. 2º 18'W) and northings NY 320 (latitude 54º 40' N) and 355 (lat. 54º 43' N). The topography (See Fig. 1) is controlled by the Teesdale fault that runs NW to SE across the valley at an altitude of 430 m a.s.l. (fig.2). The highest flank to the NE is the Three Pikes peak [NY 830 340] at an altitude of 651 m a.s.l. The Viewing Hill [NY 780 330] is the highest flank to the South-west of the valley rising to a height of 649 m asl.

Geochemical tests by the British Geological Survey in Harwood led to the discovery of the mineral assemblage (developed in a skarn environment) of nickel-bearing minerals in magnetite-rich ore. Niccolite and other nickel-bearing minerals had been found in magnetite-rich ore at three localities in the Harwood valley; Lady's Rake Mine, Cadger Well Level and at the Trial Shaft (Figs.3 & 4). Associated ore minerals include galena, sphalerite, chalcopyrite and others (Young and others, 1985). The niccolite mineralization suggested formation temperatures of over 550ºC; twice as high as those at nearby Cow Green (Young and others, 1985). Only the Hilton mine near Appleby [NY 760 220] and Settlingstones mines in Hexam [NY 840 680] are known to bear such mineralization. The common factor is that where these ore dumps were found, the mine shafts cut the Teesdale fault and associated fractures. The objective in my investigation is to map the source of the magnetite-rich ore and niccolite mineralization and investigate if this source is associated with the intrusive rocks of this area (e.g. the out-cropping Cleveland dyke to the NW and SE or the Whin Sill and associated dykes).

Access to the centre of the valley is possible through tracks that were used during mining of lead, zinc and other minerals during the 19th century. Both flanks of the valley are littered by streams

Fig.1. Topographical map of Teesdale. The boxes denote areas where ground magnetic profiles were conducted by the indicated researchers.

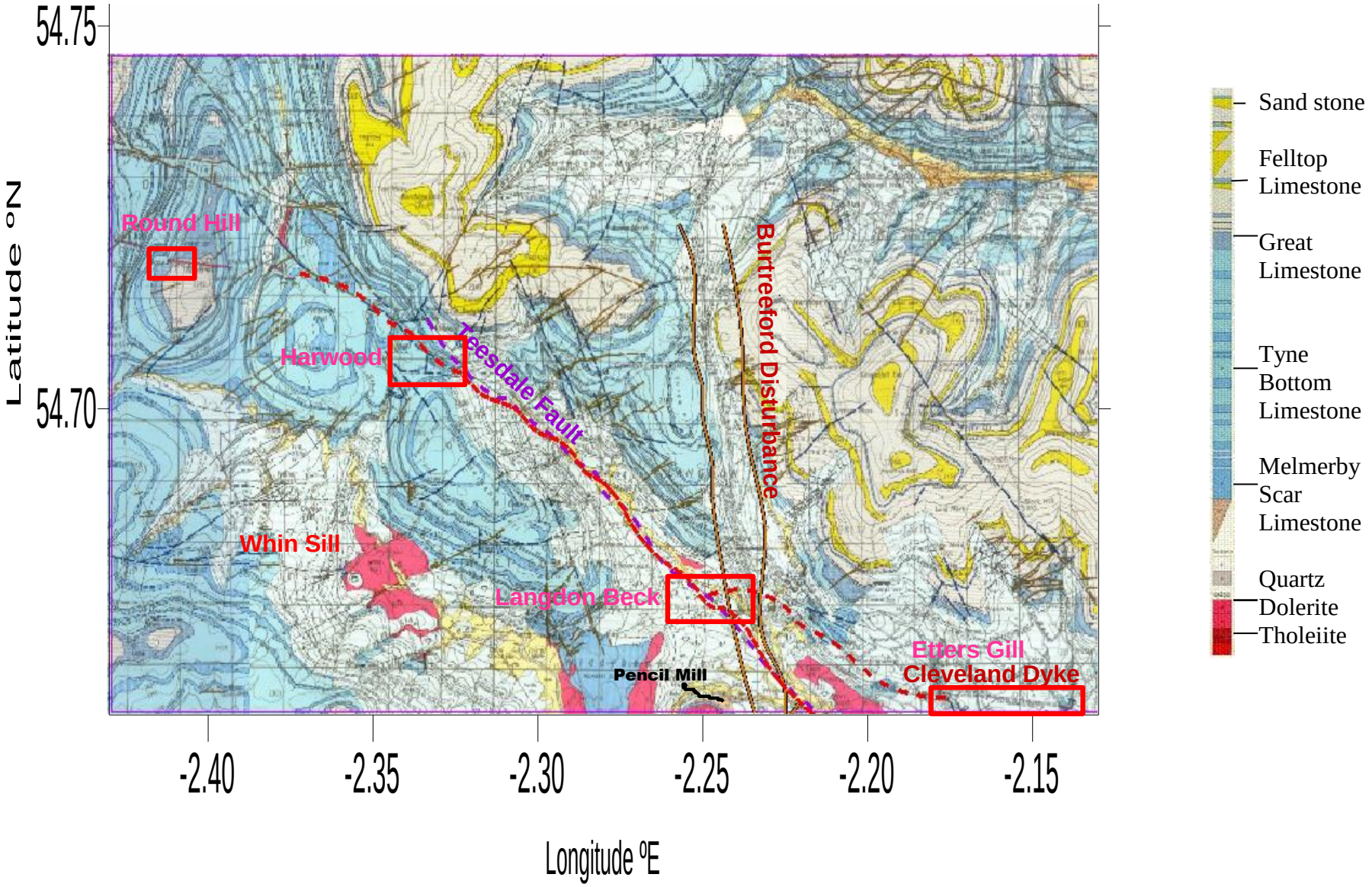

Fig.2 Geological map of Teesdale (Whin dolerite intrusion in red). The inset boxes in indicate the areas where intense magnetic surveys were conducted.

emanating from the hills. They all drain into the Harwood Beck that flows parallel to the Teesdale fault towards the south- east.

Along the course of Teesdale, the Tees river (Fig.1) has produced two large water-falls, both due to the hard Whin Sill resisting the erosive power of the river, i.e. High Force near Middleton-in-Teesdale [NY 880 280] and Cauldron Snout NY[810 280] in the Upper Teesdale.

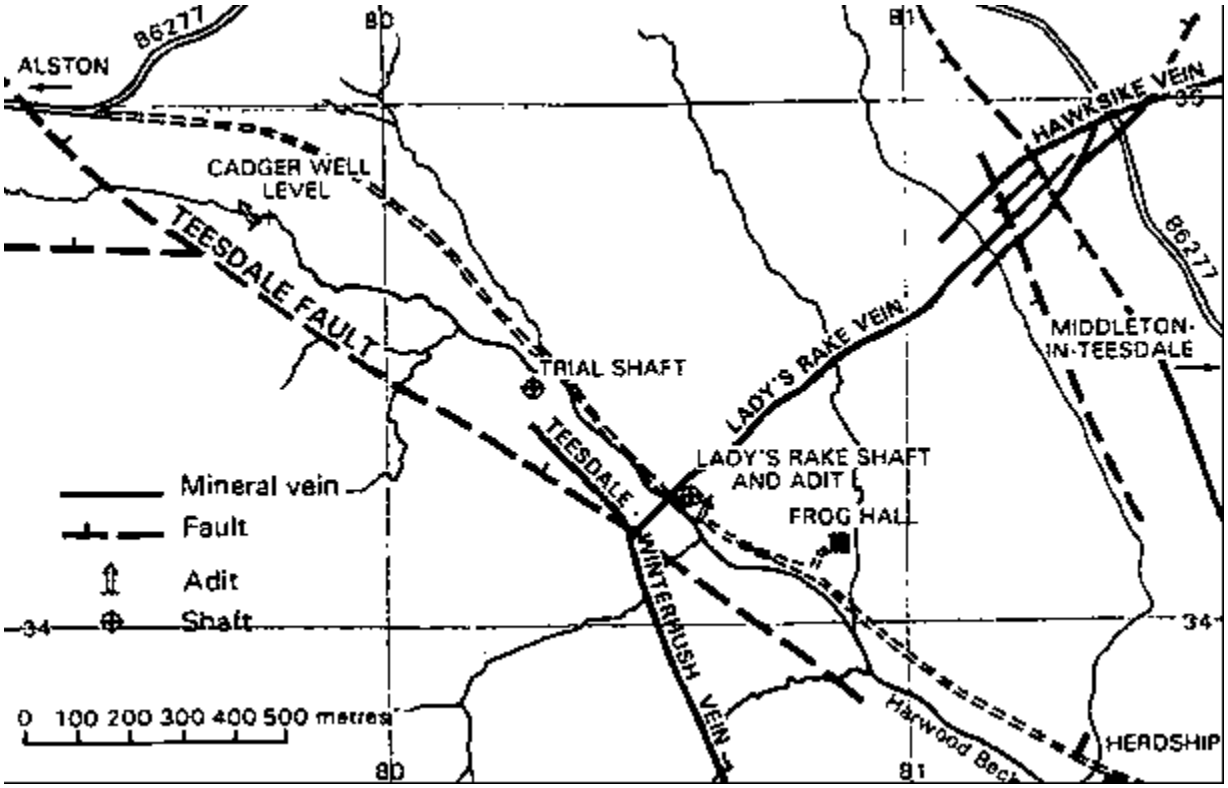

Fig.3. Veins and mine workings in the Harwood valley, Teesdale (After Young et al, 1985).

The Teesdale fault runs along the Tees valley, down-throwing north-east by 50m or more (Evans, 1984). Because the Whin Sill and other intrusive rocks contain magnetic minerals, they create a small change to the magnetic field of the earth, especially where there are discontinuities in the sill, such as faults, dykes and irregular erosion surfaces. By measuring the fluctuations of the magnetic field (i.e. magnetic anomalies), it is possible to model these discontinuities on a computer, and obtain an estimate of the shape and extent of the intrusions.

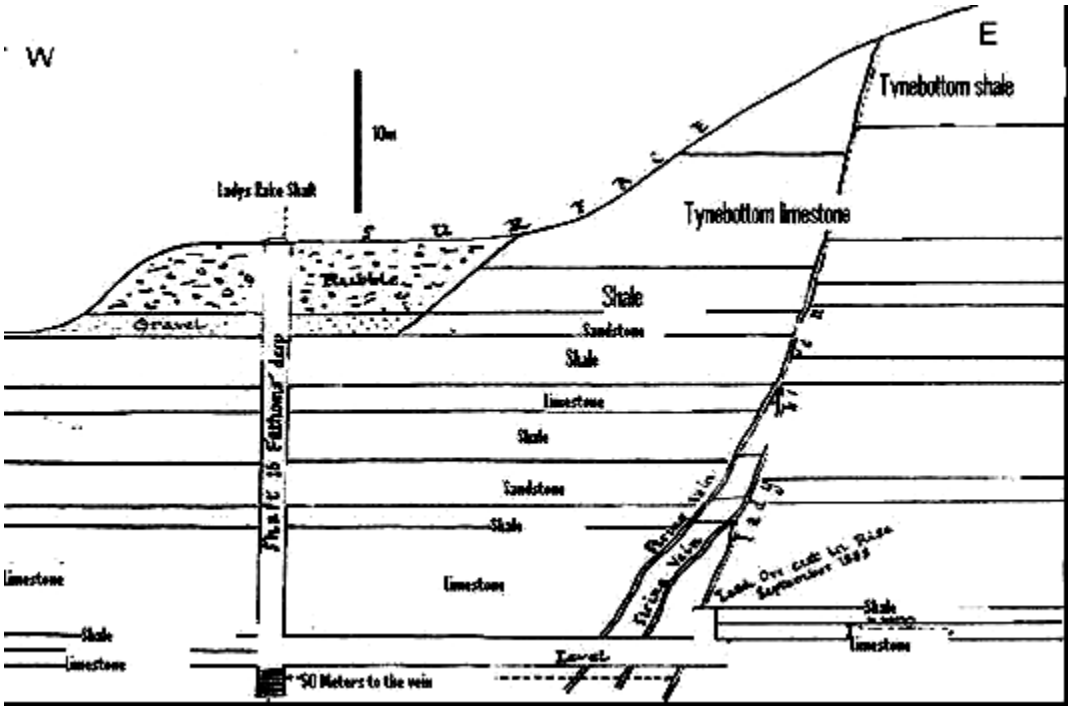

Fig.4. Statigraphic column through the Lady's Rake Shaft. The 'Yoredale' cyclothem sequence can be observed here with layers of shale, sandstone and limestone depositions.

2. GEOLOGY

2.1.1 REGIONAL GEOLOGY

The structural history of Northern England is directly responsible for all the major rock types that occur in the region (Dunham, 1990). In the Ordovician and Silurian, the Midland Valley of Scotland was probably the site of a closing ocean with subduction zones either side, and an island area in the Lake District. The collision of the two continental land masses was the final phase of the Caledonian orogeny. The orogeny had caused considerable deformation and heating in the crust across Northern England, as a result of which, a series of granites were intruded in the Lower Devonian, including the Lake District granites connected by subsurface ridges to two concealed granites to the east under the Pennines. These, the Weardale and Wensleydale granites form, respectively, the Alston and Askrigg blocks (Fig.5). These are bounded by faults along which the blocks rose up during the Lower Carboniferous (Johnson & Dunham, 2001).

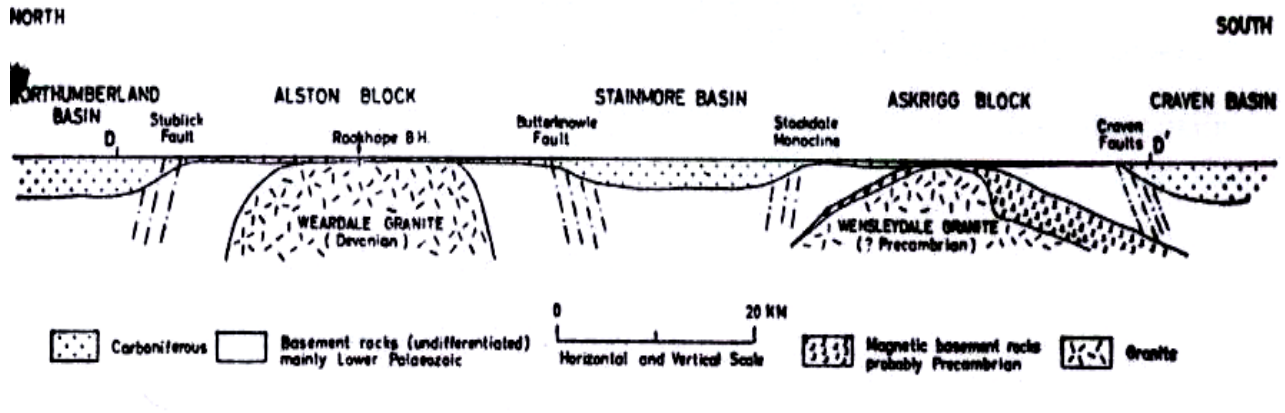

Fig.5. A true-scale section showing the interpretation of the topmost third of the crust beneath the Northern Pennines in a North-South direction (After Johnson & Dunham, 2001).

The tendency for the blocks (Fig.5) uplifting relative to the surroundings is attributed to isostatic mechanism depending on the low density of underlying granite masses. The low density basement rises to a state of equilibrium and this occurs through faulting.

The Askrigg basement feature showed a tendency to uplift even before Carboniferous. Evidence from the Rookhope borehole portrays the Weardale granite as older than Carboniferous sediments. Investigations of basement structures of the Northern Pennines have provided an insight to the proposition that mineralization (lead, zinc) comes from the lower crust rather than from cooling magmas in the upper crust (Bott, 1961). The primary cause of subsidence is the flow of the underlying mantle material towards the mountain ranges suffering erosion. Fig.6 below shows the geological formations in Northern England.

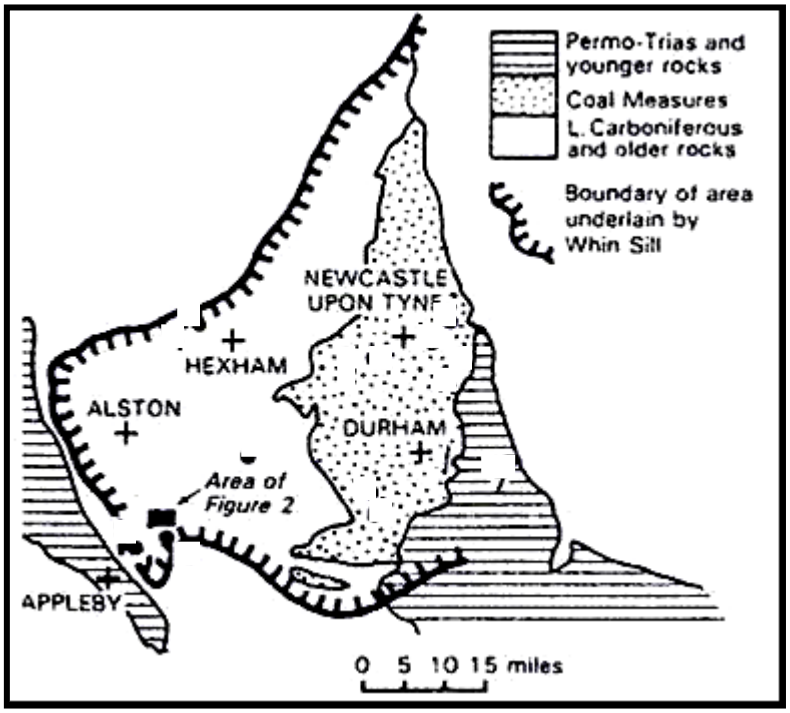

Fig.6. Regional geological rocks of Northern England. The Whin intruded the lower Carboniferous in Upper Teesdale. (After Young and others, 1985)

During the Lower Devonian, the continental shelf was probably under slight tension, with most of it lying very close to sea level. There was an overall graben and horst structure in England and Wales, whilst further north in the Midland Valley of Scotland, the Clyde Plateau lavas were erupted (Dunham & Kaye, 1965). There was pronounced differential movement of the fault-bounded blocks which diminished during the Namurian and was followed by very extensive Coal Measure deposition over much of Britain and North Europe as this part of Laurasia moved northwards over the Equator.

This quiescence was halted at the end of the Carboniferous by the collision of a South European plate with Laurasia in the region of Cornwall, causing intense deformation. This episode (called the Variscan, Armorican or Hercynian Orogeny), had milder effects in Northern England and Scotland, rejuvenating old hinge-lines on fault-bounded blocks, and applying general compression whose effects were governed largely by older Caledonian structures. Widespread uplift raised the area above sea level producing the Permian desert landscape and associated igneous activity included the intrusion of the Lugar Sill in west Scotland, and the Sills of the Midland Valley and Northern England including the Whin Sill, dated at 300- 295 Ma (Johnson & Dunham, 2001).

2.1.2 STATIGRAPHY

The geological formations occurring within Teesdale and the surrounding district are summarized in Table 1 below (After Burgess and Holliday, 1979):

Fig.7 below displays detailed stratigraphic columns in bore-holes in the study area, showing horizon sections of the different limestone formations in the Alston Group

Solid Formations	**Table 1.**	**Approximate thickness (m)**
Pleistocene and Recent	landslips, peat, alluvial fans and river terraces, glacial and fluvioglacial sand and gravel, boulder clay and morainic drift	50
Permian and Triassic		
St Bees Sandstone	brick-red sandstones and siltstones	250
Eden Shales	red, grey and brown sandstones and siltstones with thin beds of gypsum-anhydrite and dolomite	180
Penrith Sandstone	brick-red dune-bedded millet-seed sandstones with bands of Brockram	100- 275
Carboniferous		
Westphalian		
Coal Measures	sandstones and siltstones, with thick coals	305
Namurian		
Millstone Grit	sandstones, siltstones, mudstones and marine limestones with thin Coals	300- 500
Dinantian		
Alston Group	sandstones, siltstones, mudstones and thick marine limestones	300- 570
Orton Group	sandstones, siltstones, mudstones and thin marine limestones	20- 190
Basement Beds	sandstones and quartz conglomerates	65- 250
Silurian		
Wenlock		
Brathay Flags	grey laminated muddy siltstones with graptolites	75
Browgill	Beds pale grey and red mudstones with thin bands of black graptolitic mudstone	85
Skelgill Shales	black mudstones with graptolites	42
Ordovician		
Coniston Limestone Group		
Swindale Shales	grey partly calcareous mudstones with bands of bioclastic Limestone	35- 40
Dufton Shales	grey calcareous siltstones and mudstones with lenticular limestone bands; sandy at base and top	400
Borrowdale Volcanic Group	rhyolite, acid ash-flow tuffs and volcanic Sandstones	1050
Skiddaw Group		
Kirkland formation	black graptoliptic mudstones with interbedded basic tuffs and andesitic lavas	
Murton Formation	grey slates with thin sandstones	

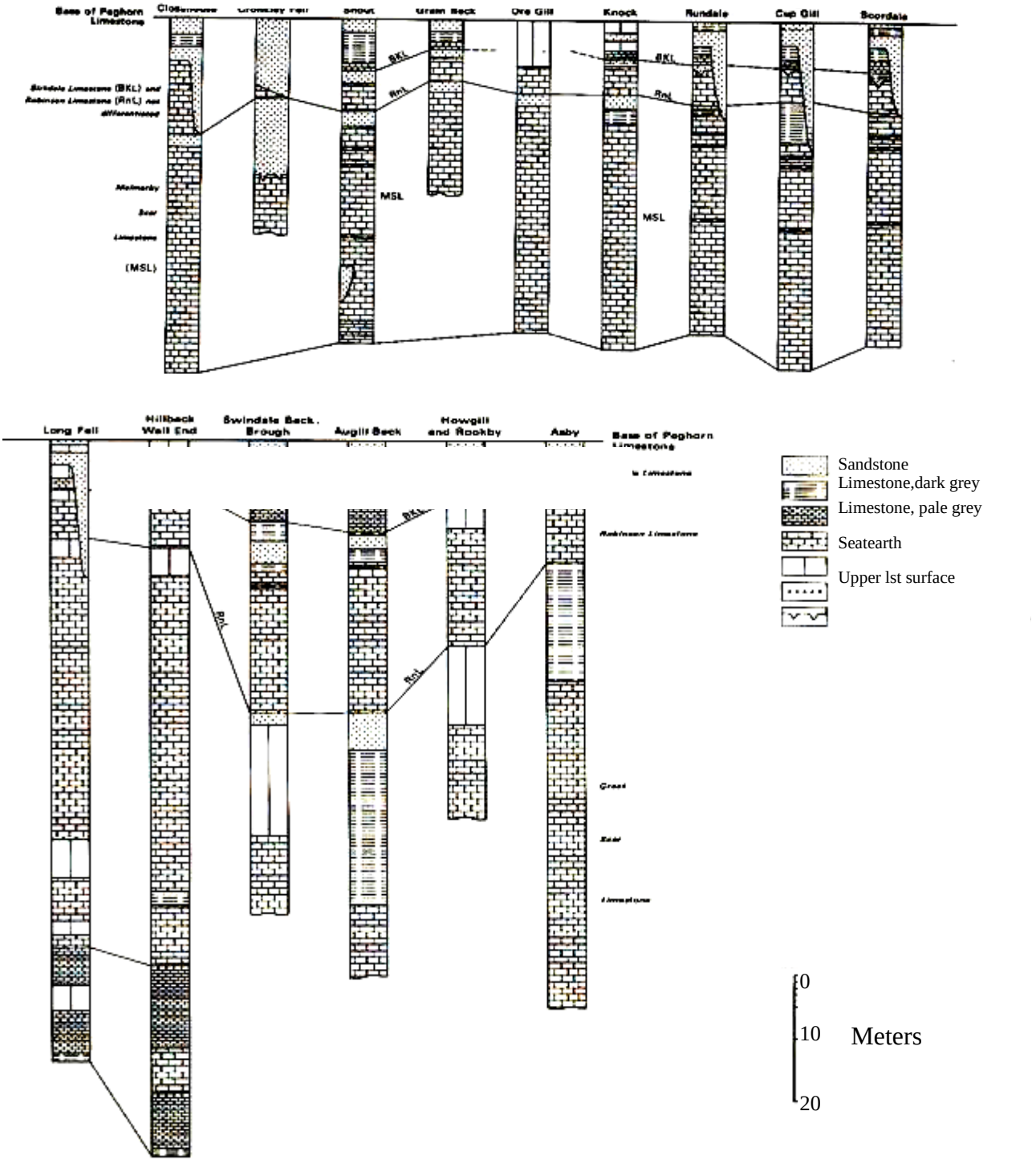

Fig.7. Comparative vertical sections of the Lower Alston Group. The sequence ranges from the base of Peghorn limestone through Birkdale limestone, Robinson limestone to Melmerby scar Limestone (Alston group) (From Burgess and Holliday, 1979).

2.1.3 INTRUSIONS

Three major intrusive rocks in this region are: Tholeiitic dolerite of Tertiary age, mostly dykes; quartz-Dolerite sills and dykes of late Carboniferous or early Permian age; Porphyritic acid intrusions, lamprophyres and dolerites of Lower Palaeozoic age, e.g the Weardale Granite (not seen at surface). Fig.8 below shows the Whin Sill (Quartz Dolerite) intrusion levels in various boreholes in the area of study.

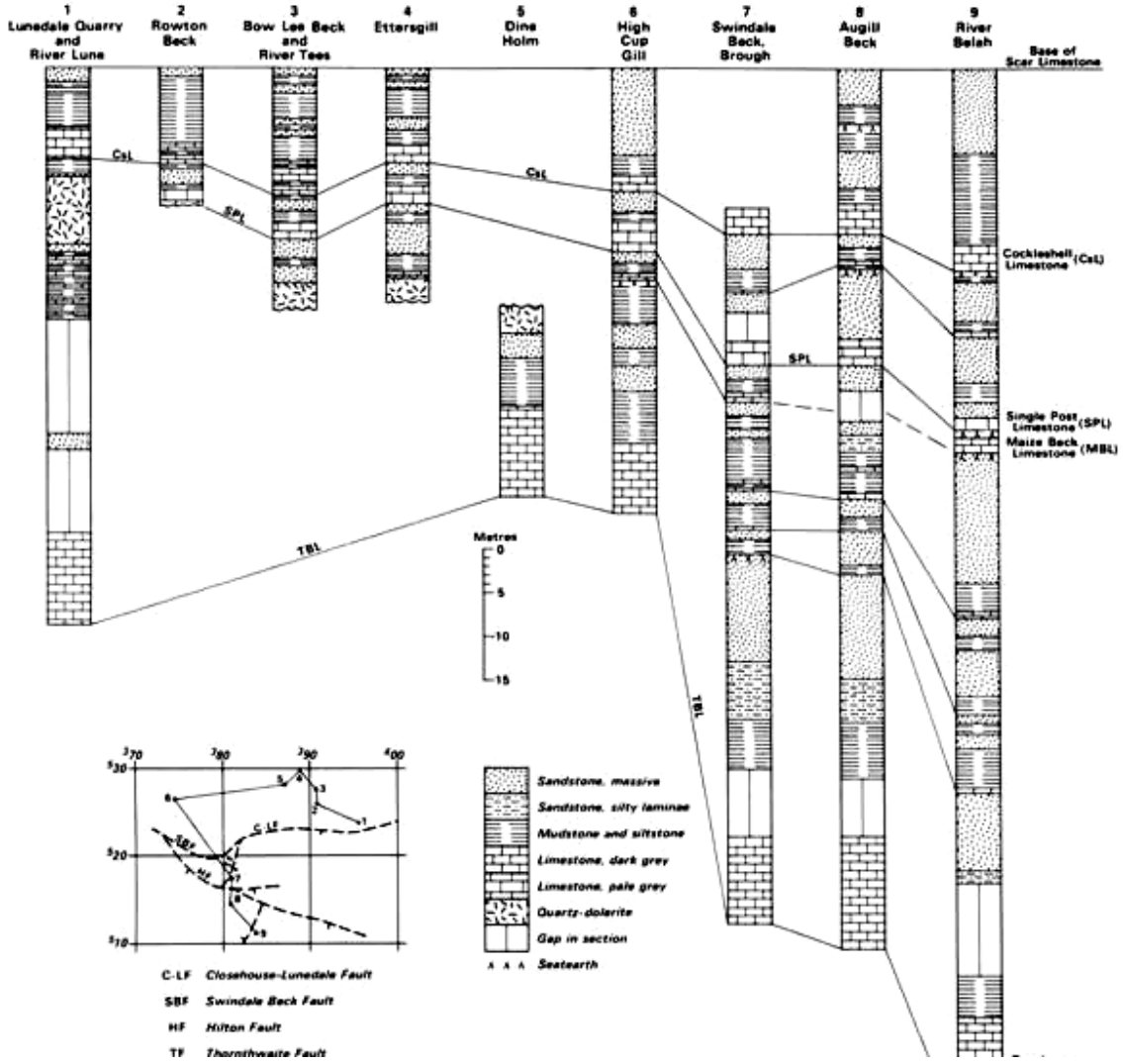

Fig.8. Bore holes correlating intrusion of the Whin Sill (quartz Dolerite) in limestone at Langdon Beck in Upper Teesdale (After Burgess and Holliday, 1979).

The Cleveland Dyke

In their paper, 'The magnetic properties of tholeiite dykes of northern England', Bruckshaw and Robertson (1949) state that "The period 65 to 2.6 Ma began with a major lowering of sea-level together with uplift, and nearly all of Britain, apart from the south-east, emerged as land. Because of this, it is most likely that no Tertiary sediments were deposited in northern England, although thick sequences are known offshore beneath the North Sea".

"The western side of the British Isles was affected by the opening of the north Atlantic since, by the early Tertiary, the spreading North Atlantic ridge had developed far enough north to begin splitting Northern Europe from Greenland. Separation of Greenland from Western Scotland and Ireland was preceded by igneous activity, i.e. volcanic eruptions and the intrusion of dykes, e.g. in Skye, Mull, Staffa (Fingal's Cave) and Northern Ireland (the Giant's Causeway)"

It was during this period that a number of linear igneous dykes, e.g. the Cleveland, Tynemouth and Acklington Dykes composed of a type of basalt, were intruded. These are the only tertiary rocks to be seen in Northern England. The Cleveland dyke is the southernmost, radiating from the British Igneous Tertiary province. Members of the Cleveland-Armathwaite dyke-echelon occur near Middleton in Teesdale (Fig.9 & 10). In common with other Tertiary tholeiite dykes, the Cleveland Dyke is reversely magnetized (Bruckshaw and Robertson, 1949). Three specimens of the Cleveland Dyke have been dated by the K-Ar method by Evans and others (1973) who concluded that an age of 58.4 ± 1.1 Ma can be regarded as a fairly close minimum estimate of the age of intrusion. The Cleveland Dyke, with a chilled margin, can be seen cutting the Whin Sill in Ettersgill beneath the footbridge at Outberry [NY 880 280]. To the east the dyke, 14m wide, is seen in Smithy Sike [NY 890 290], and again in Bow Lee Beck near Mirk Holm [NY 900 290], where it is split into two parts and includes a screen of baked sediments belonging to the Upper Alston Group (Dunham, 1990).

Fig.9. Tertiary dykes in the British Isles (After Robson, 1964)

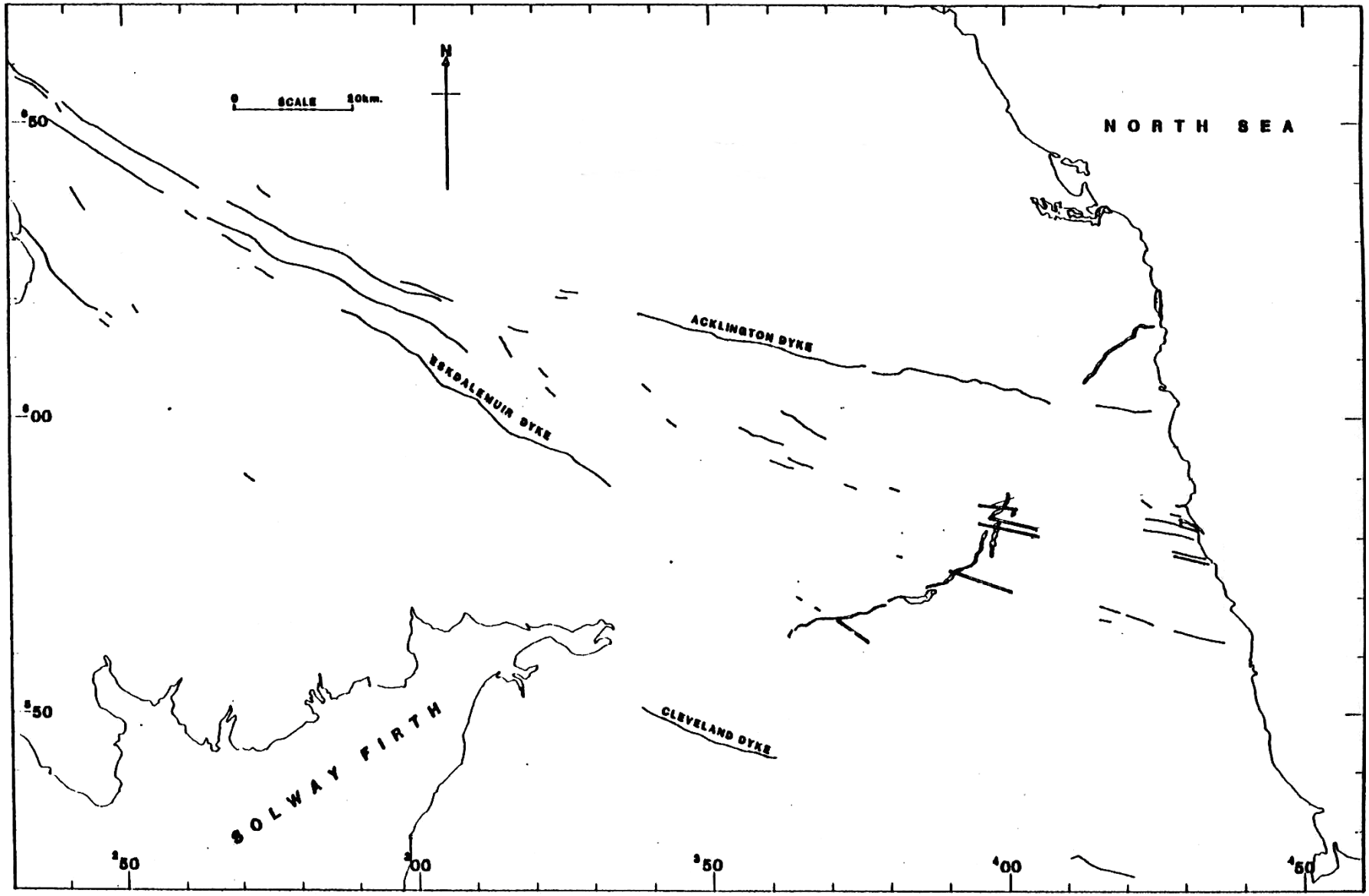

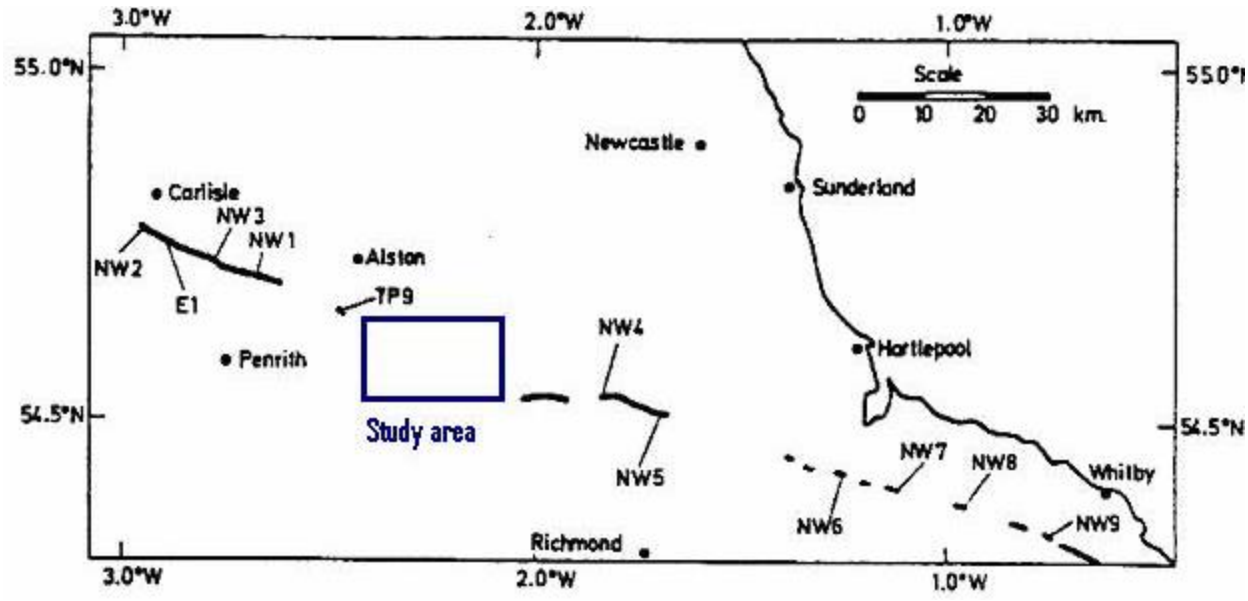

Fig.10. Outcrops and sampling sites along the Cleveland-Armathwaite dyke (Adapted from Giddings et al, 1972).

The Cleveland Dyke is always readily distinguishable in the field from rocks of the Whin Sill (quartz-dolerite) suite by its porphyritic character, with phenocrysts of plagioclase and pyroxene set in a dark fine-grained or glassy matrix (plate 1).

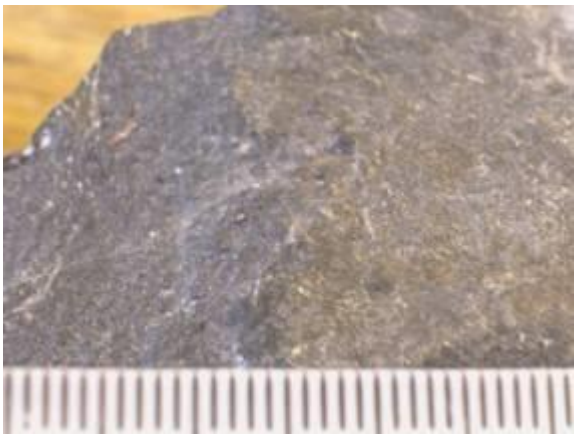
A


B

Plate 1. Cleveland dyke (A) and Whin Sill (B) rock samples collected from Cadgers' well and Lady's Rake mine respectively in Harwood (Ruled scale in mm).

Whin Sill

The other major intrusion occurring in the area of study is the Whin Sill. There is an identifiable presence of chloritized phenocrysts of olivine in the little Whin Sill (Robinson, 1970). The Great Whin is mainly composed of quartz-dolerite material and is lower in total iron than the Little Whin which is again low in SiO, K_2 and Rb. Ferrous oxide has been found to be more abundant in southern outcrops.

Major outcrops of the Sill can be seen in Cronkly Scar on the western side of the region (fig.1 & 2) [NY 840 290] and in Dine Holm Scar [NY 870 280], which runs along the eastern side of the River Tees (Fig.1). There is also another outcrop at High Crags, which is just to the south of Cronkly farm [NY 863 290], and in the River Tees by Cronkly Bridge [NY 862 294].

At Middleton-In-Teesdale the Sill is 43m thick whilst at Ettersgill it is 69m thick (Astle, 1978). Bore holes at Dine Holm have located the base of the Sill at a height of 335m above sea level giving it a thickness of at least 65m (Fig. 8). Studies of the Whin Sill have shown that it is at its thickest in Upper Teesdale, and that the Melmerby Scar Limestone is the lowest horizon in which it is found (Burgess and Holliday, 1979).

A vertical rise of the Sill through the Melmerby Scar Limestone to the Robinson Limestone can be seen at White Well Green [NY 840 280], and nearby the sill partly truncates and partly underlies the highly metamorphosed Robinson Limestone. At a number of localities concordant tongues of quartz-dolerite project out from the tops of these vertical rises (Figure 11). Most of these can only be inferred from mapping but a number are more directly visible. Similar tongues of dolerite were demonstrated in borings associated with the Cow Green Reservoir (Burgess and Holliday, 1979).

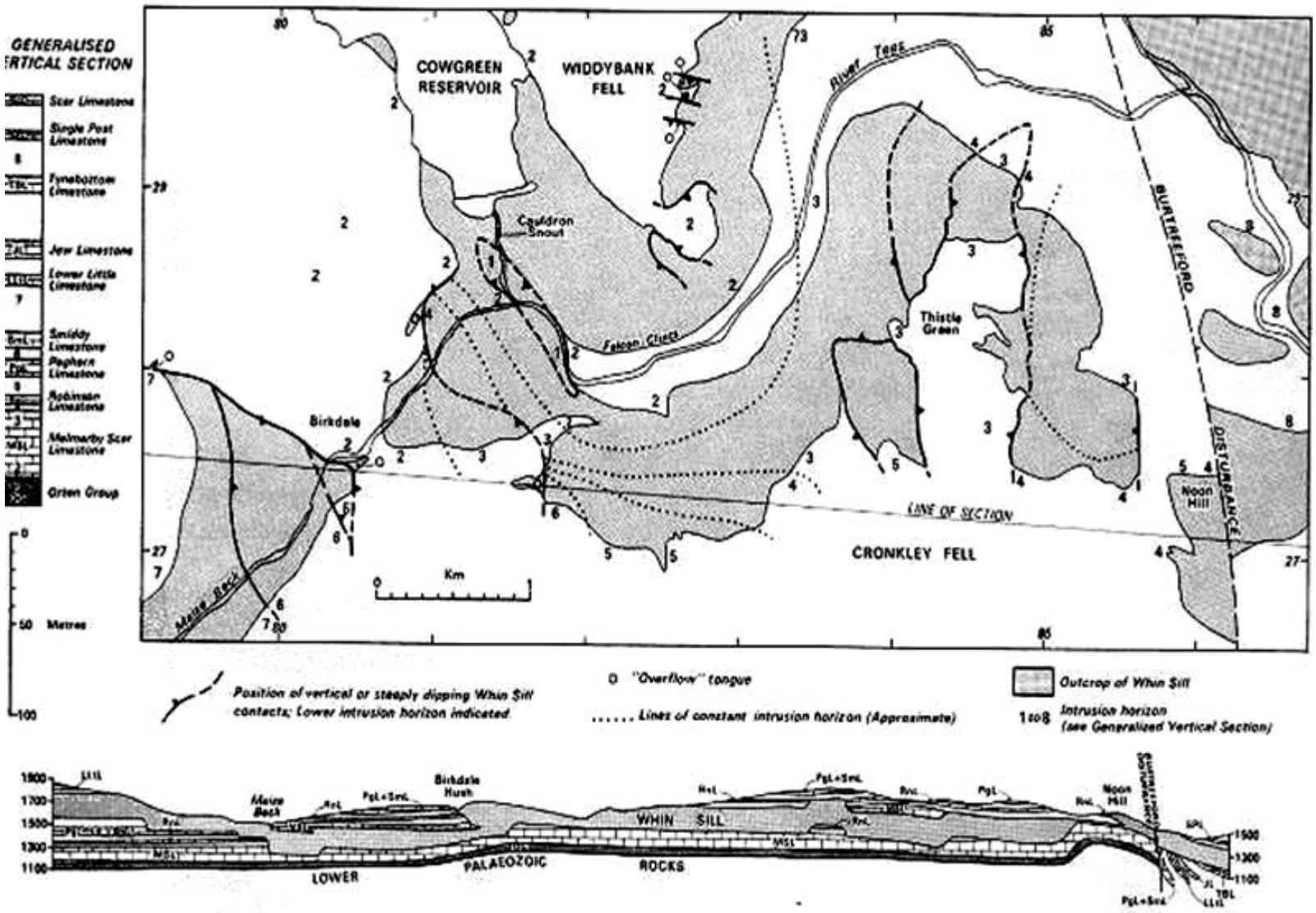

Fig.11. Sketch-map of outcrops in the Cronkley Fell area showing horizon changes by the Whin Sill Dolerite (After Burgess and Holliday, 1979)

The intrusion of the Sill has produced some thermal metamorphism in the surrounding rocks. This metamorphism is almost entirely restricted, however, to Upper Teesdale where the Whin Sill is at its maximum thickness and intrudes in the lowest horizon. The effect of metamorphism on the country rocks varies according to the type. Limestone in the Cow Green and Cronkley areas has been altered for over 30m from the contact.

A rock containing wollastonite (i.e. $CaSiO_3$ formed by contact metamorphism of limestone) has been found near Cow Green, suggesting high temperatures in the area (about 250ºC) (Young and others, 1985). Shales also show some alteration and any pure sandstones which occur near the Whin Sill have been converted to quartzites especially where the sill intruded at the lower levels of the limestone (e.g. Melmerby scar). From the geology of Harwood, the formation temperatures in the valley are almost the Curie temperature of magnetite (Giddings and others, 1972) and the possibility of mineralization occurring above this temperature raises questions on the previous assumption that it was a result of the intruding Whin Sill in the late Carboniferous/early Permian. The lowest horizon (Melmerby scar Limestone) in which the Whin Sill intruded in upper Teesdale (hence highest temperatures) is found at Cow Green.

The Little Whin occurs further to the north of the study area [NY 860 385] and it is known to be some 6Ma older than the Great Whin. There is a distinct variation in lithology between Great and Little Whin. It has been suggested that the Little Whin represents the principal parent magma (greater pressure of magma injection) (Burgess and Holliday, 1979)

2.2 GEOLOGY OF HARWOOD

The Harwood valley is cut into Yoredale (cyclothem) beds of the Alston Group into which the quartz dolerite of the Whin Sill is intruded. The Sill extends beneath the Lady's Rake mine workings and crops out beneath the boulder clay about 1km away to the south-east at about 370m above sea level (Young and others, 1985).

The valley is structurally controlled by the Teesdale Fault which can be traced for almost 20km from Alston to Middleton-in-Teesdale (figs. 2 & 3). The fault is mineralized locally in Teesdale and also in the South Tyne Valley to the north (Young and others, 1985). The veins formerly worked at Lady's Rake and Cadger Well lie within the Barium zone of the Northern Pennine mineralization. The Allens Cleugh fault and Vein, one of the lineaments intersecting the Teesdale fault, branches to the west at upper Harwood. Some of the minerals extracted from the mines here include: galena, barite, sphalerite, siderite, ankerite and ores of iron. High levels of niccolite and other nickel-bearing minerals were found in magnetite-rich ore at various localities in the Harwood valley.

Niccolite has only been recorded from two other localities in England: at Settlingstones mine near Hexam [NY 840 680] and at Hilton mine near Appleby [NY 760 220]. Analyses of the mineralization in Lady's Rake mine compared well with that in the other two areas, but the extensive substitution of As for Sb found in the compounds suggests that the solid solution between these two compositions is more extensive than that experimentally determined at 550ºC, indicating that the minerals found here were formed above this temperature (Young et al, 1985).

Fig.12 below is a mine plan describing mineral shafts and veins at Harwood. The miners in the 19th Century encountered a hard rock in form of a dyke with a width of 12m parallel to the Teesdale fault at a depth of around 40m. They circumvented the rock after failing to chip it out of their way and dumped

the rubble at Cadger's Well (fig.3). Geological analysis of the subsurface rock would give some indication of what rock type this 'dyke' is.

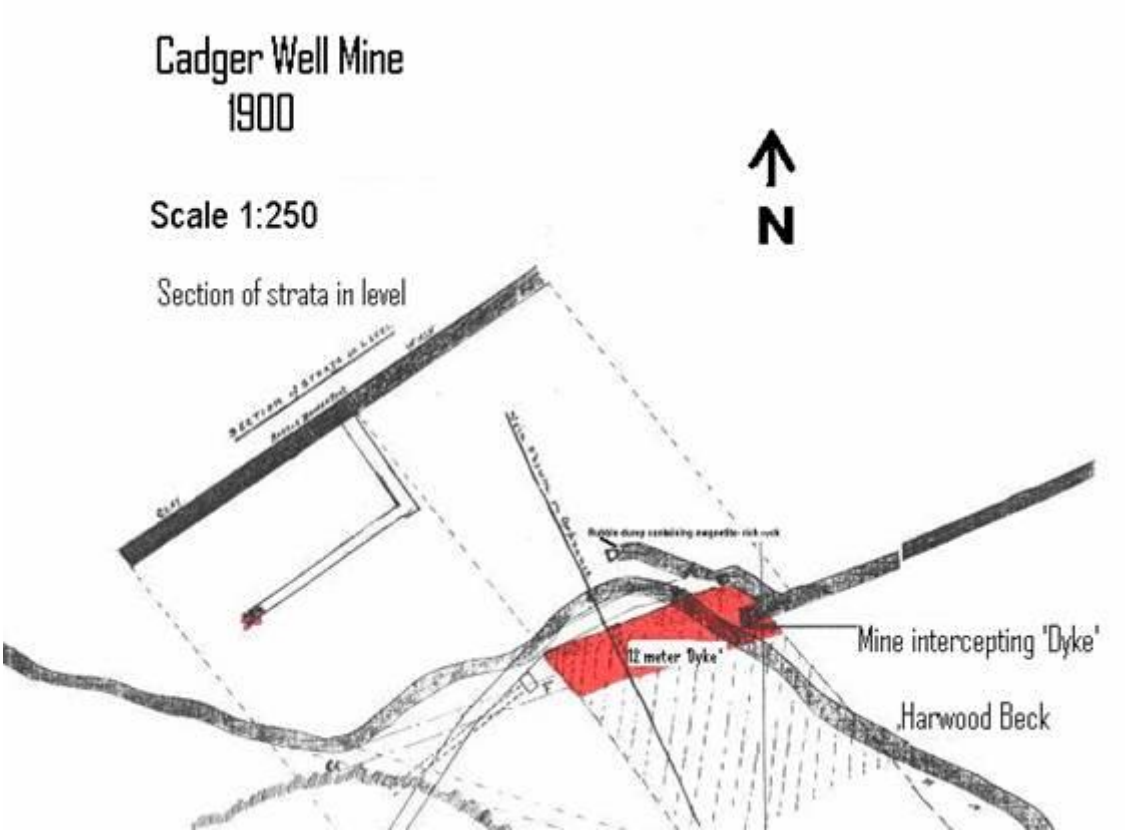

Fig.12. An old mine plan at Harwood displaying the location of a 12m 'dyke' intercepted at depth. (From the Raby estate, Middleton-In Teesdale).

2.3 GEOLOGY OF CRONKLEY AND LANGDON BECK

This survey area is geologically dominated by the Teesdale Fault, Burtreeford Disturbance and the Whin Sill (fig.2). The oldest rocks (Ordovician) in the area are found on the western, up-thrown side of the Fault. They consist of highly cleaved slates (Skiddaw slates), poorly exposed due to the drift covering them. One of the few outcrops is to the west of Cronkly at Pencil Mill [NY 840 290] (Fig.2).

2.3.1 Sediments

On the eastern side of the Burtreeford Disturbance (see fig.1) the rocks consist of members of the Carboniferous Limestone Series, including the Tyne Bottom Limestone which belongs to the Middle Limestone group (Alston group). This is a dark, fine grained limestone representing one of the members of a cyclic sequence or cyclothem (Astle, 1978).

The cyclic sequence in strata comprises: the Smiddy Limestone overlain by the Lower Little Limestone, Jew Limestone, the Tyne Bottom limestone, Single Post Limestone, Cockleshell Limestone, Scar Limestone, Five-yard Limestone, Three-yard Limestone with the Four-Fathom Limestone appearing right at the top. The local name for this Middle Limestone Group cyclothem in Teesdale is the Yoredale.

To the west of the Disturbance, the Melmerby Scar Limestone lies above and possibly below the Whin Sill (See fig.11). This is one of the lowest members of the Carboniferous Limestone Series. It is pale grey in colour and is about 35m thick (Burgess & Holliday, 1979).

2.3.2 Burtreeford Disturbance

The Burtreeford Disturbance is the major structural feature in the Cronkley area. It can be mapped for over 35km from Allendale, in the North, to Hagworm Hill, above Lunedale in the south. The only exposure near Teesdale, however, is at Drygill Sike [NY 850 317].

It is a faulted, east facing monocline with an eastward down-throw of up to 150m although on average this value is 75m (Astle, 1978). A series of less important monoclinal folds lie parallel to the Disturbance and are believed to be contemporaneous with it. The Disturbance is a compressional feature which was produced slightly earlier than, or contemporaneous with the intrusion of the Whin

Sill (Fig.13- Folding & thrust faulting in WSW-ENE stress field). This is inferred by the change in horizon of the Whin Sill across the fault (Fig.11).

2.3.3 Drift

The most recent deposits in the Teesdale area are the boulder clays deposited during the last glacial period. These clays cover the older rocks in the lower parts of the area. The moraine drift, which forms a ridge running along the base of Cronkley Scar, was probably part of the lateral moraine of a glacier. Boreholes at Dine Holm [NY 865 283] (Fig.8), in the south of the region, have shown that there is as much as 50m of drift filling what was probably a pre-glacial river channel.

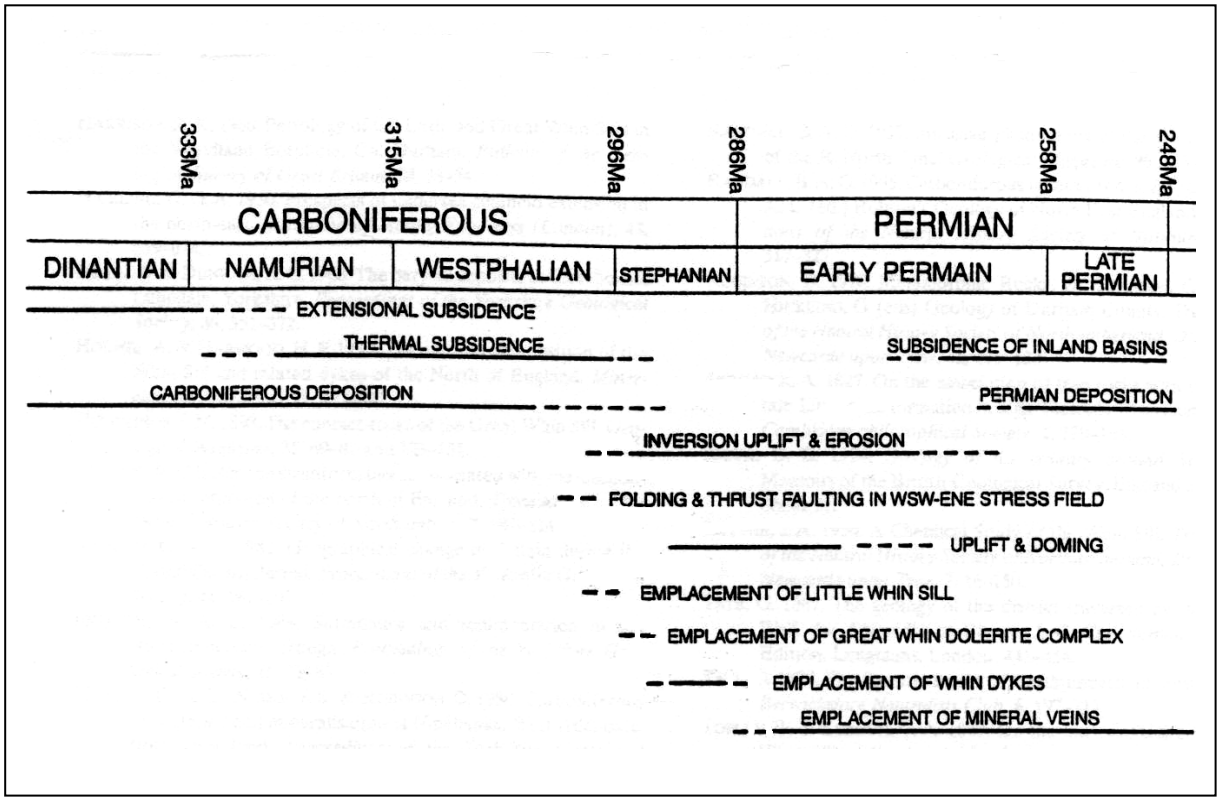

Fig.13. Diagram showing the late Carboniferous and early Permian geology in northern England (After Johnson and Dunham, 2001)

3. *PREVIOUS GEOPHYSICAL WORK*

3.1 WHIN SILL AND ASSOCIATED DYKES

3.1.1 Whin Sill

A lot of geophysical work has been done to investigate the nature of the Whin Sill in Northern England. The Whin Sill is defined as a concordant, tabular sheet of igneous rock intruded into sedimentary rocks or lava (Johnson and Dunham, 2001). However, it usually rises and falls in the stratigraphic succession in gentle transgressions and abrupt jumps to new levels. The age of the Whin has been dated to be 295 ± 6 million years (Johnson and Dunham, 2001). The Little Whin is believed to be a slightly older intrusion compared to the Great Whin group.

Magnetic anomalies in Northumberland have been found to relate to igneous rocks (Giddings et al, 1972). Samples collected from various outcrops of the Whin Sill were demagnetized to remove acquired magnetization. They indicated a mean magnetic pole (at the time of intrusion) located at latitude 38° N, longitude 177° E. Earlier researchers obtained a palaeo-position of an un-cleaned Whin Sill specimen at 37° N, 169° E.

Measured thicknesses of outcrops of the Whin (in England) range between 35 to 81m. Magnetisation of the Whin Sill is greatly reduced by the process of metamorphism which led to formation of 'White Whin' where iron oxides are completely destroyed, perhaps with associated mineralization. Localized magnetic anomalies can occur in areas of significant zones of 'White Whin' due to the absence of magnetite within an otherwise essentially homogenous magnetic body (Bott , 1967).

The dolerite intrusions in the Carboniferous sediments of the Alston Block itself had a thickness of up to 73m (Cornwell and Evans, 1986). Magnetisation of the Whin comprises a component induced by the

present geomagnetic field and a remanent component preserved basically since intrusion. Samples from five sites in Hexham area, Northumberland [NY 940 630], indicate the following (After Cornwell and Evans, 1986):

Susceptibility	0.025 SI Units
Direction of NRM (Decl.)	183°
Inclination of NRH	14° up (i.e. -14°)
Intensity of NRM	2.74 A/ m
Declination of Total Magnetization	185°
Inclination of Total magnetization	4° down
Intensity of Total Magnetization	2.76 A/ m

Table 2. Magnetic parameters of the Whin Sill in Northumberland, England (Adopted from Cornwell and Evans, 1986)

The Whin Sill outcrop corresponds to a series of low magnetic anomalies. The southern margin of the near-horizontal Sill produced anomalies which are negative relative to the undisturbed background field, while the northern margin largely produced positive anomalies.

Where the edge of the Sill strikes North-South, the anomalies are less well defined due to the fact that the Sill is magnetized in a N-S direction and minimal magnetic flux emerges from its N-S trending E and W margins.

Aeromagnetic surveys were flown over the NE England by the BGS in 1984 with ground clearance of 305m along 2km spaced N-S flight lines. Several mapped faults in the Alston Block (including the Teesdale Fault) are seen to be associated with magnetic anomalies analyzed from those data.

The faults in the Alston Block could not be older than the intrusions in the Northern margin of the Alston Block (Cornwell & Evans, 1986). Consideration of the shape of the magnetic profiles did give an indication of alteration of the Sill to White Whin. The symmetry of the anomaly due to a southerly down-throwing fault is changed according to the width of an assumed zone of alteration (hence demagnetisation) either side of the fault (fig.14 a & b).

There is, therefore, a good overall correlation between the magnetic anomalies of near-surface origin and the mapped outcrop of the Whin Sill but the magnetic data additionally indicate that the nature of the Sill intrusion is largely controlled by joints or faults. This probably also applies in places to dykes of both Whin dolerite and Tertiary.

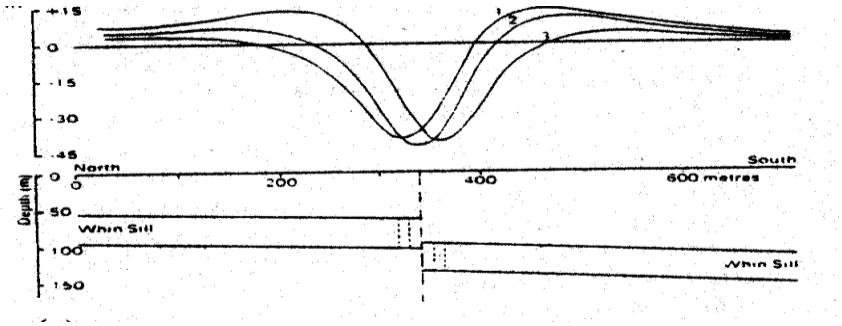

(a) Demagnetised zones of varying widths (1 to 20m wide zone either side of the fault, 2 to 10m wide and 3 to 0m wide)

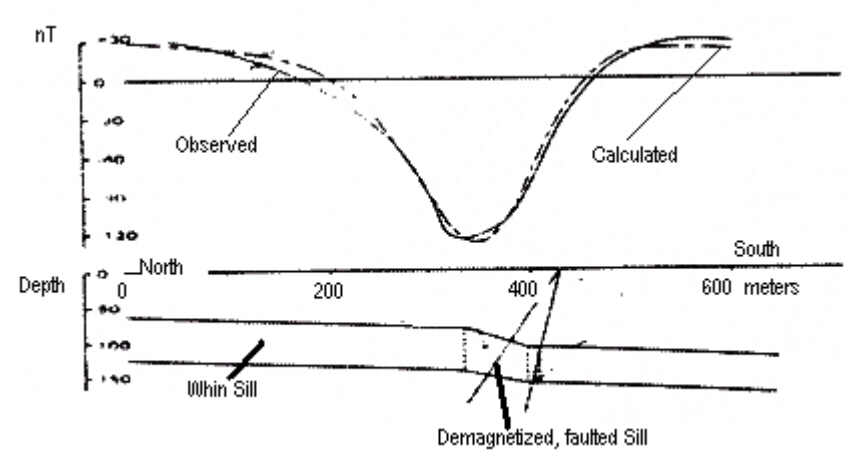

(b) The total magnetization for the main Sill had to be set at 3.5 A/m to achieve similar amplitude fit with the observed plot.

Fig.14. Model magnetic profiles across a fault in the Whin Sill (After Cornwell & Evans, 1986).

3.1.2 Permian Dykes

The Permian Dykes in N.E England trend WSW-ENE and are thought to be associated with the Whin Sill. A magnetic survey study of the mainland parts of the Holy Island en-echelon dyke system [NZ 260 185] shows that the dyke system comprises a series of four sub-parallel ENE-WSW trending dykes (El-Harathi and Tarling, 1988). The dykes appear to be associated with simple tensional fractures.

In the interpretation, the profiles were studied mainly to determine the dyke locations, widths and depths to their upper surfaces. The location of each dyke was mapped by identification of the anomaly itself.

When analysis was carried out, the depth to the top of the dyke was seen to vary from 5 to 8m and widths were fairly constant at 13-17m. Where a dyke terminated, there was no evidence of burial depth increasing. The magnetic signature of each dyke is abrupt, i.e. where the dykes seemed to terminate the signature would abruptly change (Fig.15). This suggests interruption by faults or the fissures at the ends, where the dyke permeates during intrusion, were too narrow; resulting in faster cooling of magma at depth.

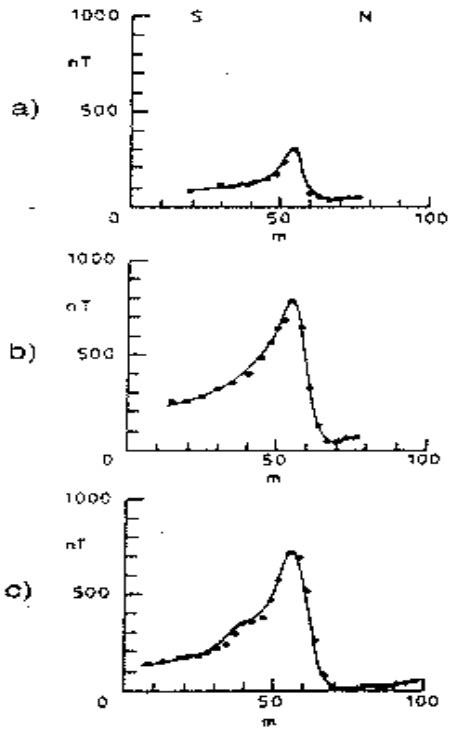

Fig.15. Magnetic profiles across dyke terminations where the magnetic signature is gradually cut out; the base-line is 48000 nT (After El-Harathi & Tarling, 1985).

3.1.3 Tertiary Dykes

In the British Isles, Tertiary dykes were formed when the geomagnetic field was reversed with respect to the present field. This has given all the Tertiary dykes; e.g. the Acklington, Eskdalemuir and Cleveland (See fig. 9), a general negative anomaly. Bruckshaw and Robertson (1949) did some ground magnetic work in northern England and their result showed susceptibility values ranging from 0.01 to 0.03 (SI) and remanent intensities of between 1 and 10 A/m. The northern-most dyke, the Acklington, produces anomalies of over 700nT in some places along its 24km length (Robson, 1964).

The Cleveland-Armathwaite dyke is identified with the swarm of doleritic dykes radiating from a plutonic complex on Mull island (Tertiary; 65- 52 Ma) (Giddings and others, 1972). The width of the dyke at the outcrops ranges from 5 to 25m and directions of remanence were so scattered that the dyke was thought to have continued to flow below the Curie point. The initial palaeomagnetic results (before demagnetization) showed a scattered trend though others portrayed a tight grouping of directions. Others still showed a streaking toward the earth's present field.

Remanence is generally in the range of 5 to 10 A/m while maximum and minimum values were 31.7 and 1 A/m respectively. The values were systematically obtained by demagnetising specimens from various sites along the exposed dyke (fig.10 & 16). As contact with the dyke is approached, the magnetisation intensity increases from less than 1 A/m to 1.6 A/m within 15m of the contact and 6 A/m within 1m of contact.

Stability of the remanence was observed to increase as its direction moves towards that of the dyke itself. The variations of these results at different sites were interpreted as due to emplacement of the

dyke in sediments of different composition, cementation, wetness, etc. The samples were found to contain magnetite at cooling temperatures of 580-590^{0}C (Curie). Also a few traces of ilmenite were found. The more highly oxidised sites showed greater mineral stability on heating.

Giddings and others (1972) found that specimens from different sites tested for low-field magnetic anisotropy of susceptibility were similar in all directions with maximum anisotropy being 1.03 and an average of 1. Hence no significant alignment of crystal axes or shapes was found in these rocks. The average pole position of 75° N 120° W (A_{95}= 5.50) appears to be a reliable model for the geomagnetic field at dyke intrusion time (Tertiary).

Fig.16 below shows palaeomagnetic results of the Cleveland dyke from samples obtained along various outcrops by Giddings and others (1972). Sample NW4 obtained at Cockfield, just to the east of Middleton-In-Teesdale, displayed a declination angle of 153º and an inclination of 67º upwards (i.e. -67º). Fifteen samples were analyzed from this site and this result gives an average palaeomagnetic nature of the Cleveland (Tertiary) dyke in the vicinity. However, the upper and lower declination and inclination levels in the entire stretch of the dyke are respectively: 177º & 141º and -52º & -69º. The baked contacts analyzed gave correspondingly similar values to those exhibited by the dyke itself. This result explains the behavior of other rocks and sediments into which the dyke intrudes, i.e. the dyke re-magnetizes the host rock that eventually, after cooling, inherits its palaeomagnetic parameters near the contact.

		Grid reference	N	Dec.	Inc.	k	A_{95}	Stability index (8)
Cleveland-Armathwaite dyke (after alternating magnetic field treatment)								
NW1	Blunderfield	83-564436	7	160	−60	91	6	10·2
	T8 (P.D.)		5	164	−62	767	3	—
	(E.M.)		22	158	−64	28	6	—
NW2	Dalston Hall	76-381514	5	149	−65	381	4	5·2
NW3	Armathwaite	83-504454	6	152	−67	81	8	6·9
NW4	Cockfield	84-123251	15	153	−67	269	3	3·0
NW5	Bolam	85-194230	12	161	−59	179	3	2·9
NW6	Stainton	85-483141	6	165	−67	263	4	3·4
NW7	Great Ayton	86-574117	12	173	−65	52	6	2·3
	T11 (P.D.)		5	165	−68	310	4	—
NW8	Castleton	68-684086	7	177	−52	198	4	7·7
NW9	Egton Bridge	86-799053	6	144	−69	41	11	1·2
T9	(P.D.) Tynehead	35-761362	6	152	−66	84	7	—
	Mean of each location (NW1-9)		10	160	−64	145	4	
Baked contacts (after thermal treatment)								
NW1	Blunderfield	83-564436	3	147	−65	—	13	5·0
NW3	(Armathwaite (N. margin)	83-504454	5	141	−63	—	3	8·9
	(Armathwaite (S. margin)		12	163	−61	—	10	1·1
E1	Wreay	83-526348	3	161	−63	—	5	5·5

N is the number of observations used in the calculation (samples or sites); *k* and A_{95} are the estimates of precision and radius of 95% confidence (Fisher, 1953); (P.D.) = P.

Fig.16. Palaeomagnetic results of the Cleveland dyke at various locations (After Giddings and others, 1972). Cockfield site is in Upper Teesdale.

3.1.4 The Burtreeford Disturbance

Astle (1978, unpublished dissertation) investigated the relationship between the Whin Sill and the Burtreeford disturbance in Upper Teesdale. Magnetic, electromagnetic (VLF) and electrical resistivity surveys were carried out at Cronkley Pasture [NY 860 290].

A proton precession magnetometer was used to read the total magnetic field of survey stations in eleven profiles. The magnetic and VLF results located the Burtreeford Disturbance running in a SSE direction from the Tees river. The Whin was interpreted to be the thickest along the Disturbance in the

area. Astle (1978, unpublished dissertation) suggests that the feeder for the Whin Sill could be located 100m east of High House [NY 857 294].

3.1.5 The Teesdale Inlier

In order to determine the extent of the outcrop of the Lower Palaeozoic rocks which form the Teesdale Inlier in Lower Harwood [NY 384 529], Ledigo(1978, unpublished dissertation) acquired magnetic data using a proton precession magnetometer. Electrical resistivity, sesmic as well as VLF techniques were also used and the result located the possible boundary of the Inlier.

The resistivity method was very instrumental in delineating the Skiddaw Slate-Borrowdale volcanic series boundary while the VLF technique gave a better interpretation of the slates topography with varying limitations. The seismic method gave drift thicknesses averaging 30m, confirmed by boreholes in the area. However, the technique could not distinguish between the slates and basement conglomerates velocities.

Lee (1978, unpublished dissertation), collected total field magnetic data along twelve profiles across the Harwood Beck to the east of Cow Green [NY 840 310] using the proton precession magnetometer. At this location, the Whin Sill is not far below the surface and it has been eroded from its full thickness of about 60m to between 15 and 30m during the glaciation age when morainic debris swept down the valley. A positive magnetic anomaly near the road to the NE of the river was thought to be due to the Burtreeford Disturbance. The Whin is seen outcropping in the stream bed and at one point a block was uplifted about 60m then later eroded. A negative anomaly in the Harwood Beck itself could not be explained by the Whin faulting alone. The combined data with borehole logs also traced the pre-glaciation boundary of the Harwood valley at some places.

4. THE MAGNETIC METHOD

The study of variations in the Earth's magnetic field can help to determine the structure and magnetization of bodies in the crust. Magnetic induction gives rise to a magnetic field, **B**, exhibited by a magnetic body. The SI unit for magnetic field is the Tesla but due to small values of geophysical anomalies, the high sensitivity of the latest magnetometers and the need for higher accuracy, the nano-tesla is used (10^{-9} T)

4.1 THEORY OF THE MAGNETIC METHOD

The magnetic moment of a small current carrying loop of area δA and current I, is defined to have magnitude I.δA and a direction perpendicular to the loop. The right hand corkscrew rule defines the directions of the field and current.

Magnetic moment units are Am^2. Magnetization is, hence, defined as the magnetic moment per unit volume and has the unit A/m. It can also be referred to the vector sum of the induced and permanent magnetizations, i.e.

$$\mathbf{J} = \mathbf{J}_P + \mathbf{J}_i \quad \ldots\ldots\ldots\ldots\ldots\ldots\ldots\ldots\ldots\ldots\ldots\ldots\ldots\ldots 1$$

where **J** is the total, or effective magnetization, $\mathbf{J}_P$ is the permanent, or remanent magnetization, $\mathbf{J}_i = k\mathbf{B}/\mu_0\mu$ is the induced magnetization and k is the susceptibility. **B** is the Earth's magnetic field vector, μ_0 is the permeability of free space, and μ is the relative permeability.

Also, $\mathbf{B} = \mu\mu_o\mathbf{H}$ ……2

where **H** is the magnetising field (A/m), so that

$\mathbf{J} = \mathbf{J}_p + k\mathbf{H}$ and $\mathbf{J}_i/\mathbf{H} = k$ …… 3

The permeability of free space is $4\pi \times 10^{-7}$ H/m, and the relative permeability is assumed, in geophysics, to be unity for common rocks and minerals. Magnetic susceptibility is a dimensionless measure of the degree to which a rock or mineral can be magnetized by an external field.

Magnetic field is a vector quantity which varies in magnitude and direction spatially over the surface of the Earth and with depth, and also with time. At any point it can therefore be described by three orthogonal components, or a magnitude, inclination and declination.

4.2 THE GEOMAGNETIC FIELD

Four major components contribute to the Earth's magnetic field: (1) the dipole field, originating within the outer core at depths greater than 3000 km; (2) the non-dipole field, also originating in the outer core, contributing 5-10% of the overall field; (3) near surface (less than ~40 km depth) anomalous magnetic bodies; (4) and short period, such as diurnal, variations which are of external origin but induce an internal magnetic field in the Earth's outer layer.

Often considered as a separate component, secular variations of the dipole and non-dipole field also contribute to the magnetic field. . The secular variation of the field is the continual fluctuation of the Earth's magnetic field, in magnitude and direction, with periodicities of decades to millennia. The dipole and non-dipole fields, and their secular variations, collectively called the main geomagnetic field, produce long wavelength signals which can be predicted based on theoretical models. This theoretical reference field, known as the International Geomagnetic Reference Field (IGRF), is updated and published every five years corresponding to the newly defined model for successive five year epochs (http://nssdc.gsfc.nasa.gov/space/model/models/igrf.html).

The Earth's magnetic field is non-constant in magnitude and direction over time scales as short as hours (or less) and as long as millions of years. Disregarding diurnal and secular variations, it frequently changes its polarity over durations commonly hundreds of thousands of years. The reversal process takes place over approximately 5000 years; the duration is instantaneous in geological terms. The field can remain in a mono-polarity state for as short as 20,000 years or as long as 60 Ma (Telford and others, 1995). Periods of time where the field is predominantly one polarity, lasting of the order of 1 Ma, are called magnetic polarity epochs or chrons, whereas shorter intervals, of the order of 0.1 Ma, are called events or sub-chrons.

4.3 ROCK MAGNETIZATION

The objective of studying magnetic anomalies is to infer differences in characteristics of a source from its surroundings. These characteristics fall into two categories; spatial and magnetic. Spatial characteristics include position, shape, depth and thickness of the magnetic body, whilst magnetic characteristics are defined by the magnetization magnitude and direction of the component minerals making up the rock. Without magnetic characteristics a geological unit (e.g. a dyke or lithological layer) is not a magnetic source body, regardless of its spatial character or other physical properties (e.g. seismic velocity).

All minerals and native elements are magnetic to some extent. However, only minerals that are ferrimagnetic are of importance in geophysics; those that are diamagnetic, paramagnetic or antiferromagnetic have susceptibilities approximately less than 10^{-3} and are therefore below the practical measurable level. In contrast, the strongest magnetism, ferromagnetism, does not occur in common minerals; only native metals, such as iron, acquire a ferromagnetism and are therefore of little interest outside mineral prospecting. Most magnetic minerals possess ferrimagnetism and have

susceptibilities of up to 15. The main magnetic minerals are the titanomagnetites (including magnetite), pyrrotite and the ilmenite-haematite series. For most common rocks, rock magnetism depends almost exclusively on the amount of titanomagnetite present.

Magnetic minerals can possess an induced and (or) a permanent (remanent or NRM) component of magnetization. The magnitude of a mineral's induced magnetization is governed by its susceptibility and the magnitude and direction of the external field**,** which for the purposes here is the Earth's magnetic field. A mineral's induced magnetization is therefore always parallel to the Earth's field**.** In contrast, a remanent magnetization can be in any direction; the orientation of the Earth's field at the time of NRM acquisition determines the direction of magnetization. Of importance here are minerals possessing thermoremanent magnetization (TRM), chemical remanent magnetization (CRM) and viscous remanent magnetization (VRM), all of which are types of natural remanent magnetization (NRM). TRM is acquired when a mineral cools through its Curie temperature in the presence of an external field. The Curie temperature of magnetite is 575 ^{0}C, much lower than the temperature at which minerals crystallize within cooling magma or lava (~ 1,100-800^{0}C). Igneous rocks are the main carriers of TRM. CRM is acquired by the chemical growth of magnetic mineral phases in the presence of an external field**,** subsequent to their initial formation. Thus, CRM can be acquired at any temperature. VRM is a type of NRM that is acquired slowly if a magnetic mineral is exposed to an external field for a long time**.** The effective magnetization of a given rock unit is not only dependant on the amount and type of magnetic minerals present, but also on the grain size of the magnetic minerals; in general, for a given mineral, its magnetization increases with decreasing grain size.

4.4 METHODOLOGY

This report presents my work and that done by other scientists before me in the Teesdale area (i.e Astle, 1978, Lee, 1978 and Searle, 2002; all unpublished). While more than two thousand data sets were surveyed in this area, a total of 1,800 stations were considered to occur in areas likely to exhibit substantial magnetic anomalies. Among these, I surveyed 1018 stations. The magnetic work done by Ledigo (1978, unpublished dissertation) was compared to that done by Lee (1978, unpublished dissertation) and was found to be a close duplication and was, therefore, not considered during interpretation.

4.4.1 Data acquisition technique

The method I used involved two proton precession magnetometers (Geometrics model-856); the base magnetometer to measure diurnal variations and the other in roving mode. Appendix (I) gives full details of the equipment used. Readings along a profile (across a probable or known strike) were taken every twenty meters and the time also noted so as to reduce the values later by comparing them with the base station record. All stations were repeated and recorded on paper three times to confirm the values, and the final reading recorded in the magnetometer's memory. A GPS (Plate 2) was also carried along to map the spatial position of each station as well as elevation. Lengths of profiles range from 300m to more than 2km, depending on the nature of anomalies encountered. Notes were also taken corresponding to a particular station regarding; outcrops, metallic objects in the vicinity or power lines. These were later analyzed during data processing. Data were entered into a PDA for latter processing.

The base magnetometer was set at the beginning of the surveys for the day to automatically take readings every fifteen minutes. This would continue till the end of all surveys in the area on that particular day. During data processing, a graph of magnetic field versus time is plotted and corrections

effected where spikes and other diurnal variations occur, which are also reflected in the data collected using the roving magnetometer.

Plate2. Magnetic survey equipment; magnetometer sensor on its pole attached to the meter itself and the GPS antenna held vertically by hand (Burtreeford fold-axis in the background).

4.4.2 Data integration

The data that was acquired earlier by Astle (1978), Lee (1978) and Searle (2002) (all unpublished) had to be analyzed first before being integrated with the recently observed result. The background magnetic value was noted to be at variance with the current regional values (an average of 400 nT) when two profiles were repeated on the old traverses. This, however, only affected one zone (Langdon Beck) where the 1978 data was included (Fig. 17).

In the GRAVMAG program, the raw magnetic data is entered through a text editor and the "background" value is subtracted by observing where the anomaly ends at both shoulders of the profile. This is achieved by entering, on the console, the value, for example, 48500 nT, both at the minimum

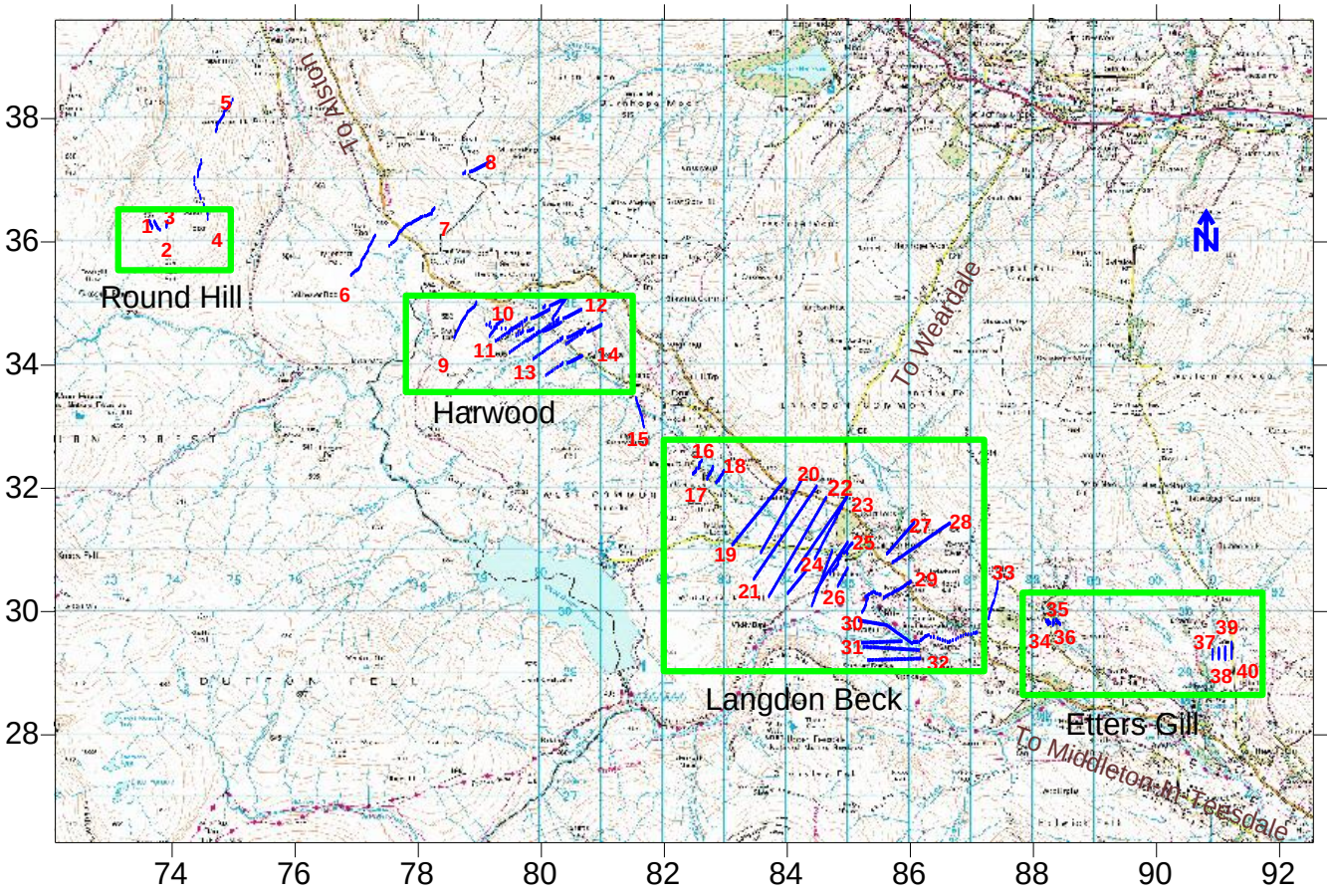

Fig.17. Magnetic traverses made recently in Upper Teesdale integrated with earlier survey results. Profiles are numbered from 1 to 40 (see fig.1 for details).

and maximum x- co-ordinates respectively. The magnetic value here is treated as the y value in the program (See fig.18).

The difference in the regional value for the previous data and the recent values was seen to be consistent on several profiles and this variance was maintained whenever an old traverse was not close to a recent one. The individual removal of the background magnetic value for each profile was adopted as the best method rather than subtracting from the raw data a constant or gradient IGRF. This was

because the background values in the various survey locations tended to vary significantly, probably due to the nature of the intrusions and mineralization in the area. This method eventually resolved the problem of integrating the various data sets and the result gave a very close match of the profiles that were near each other or overlapping.

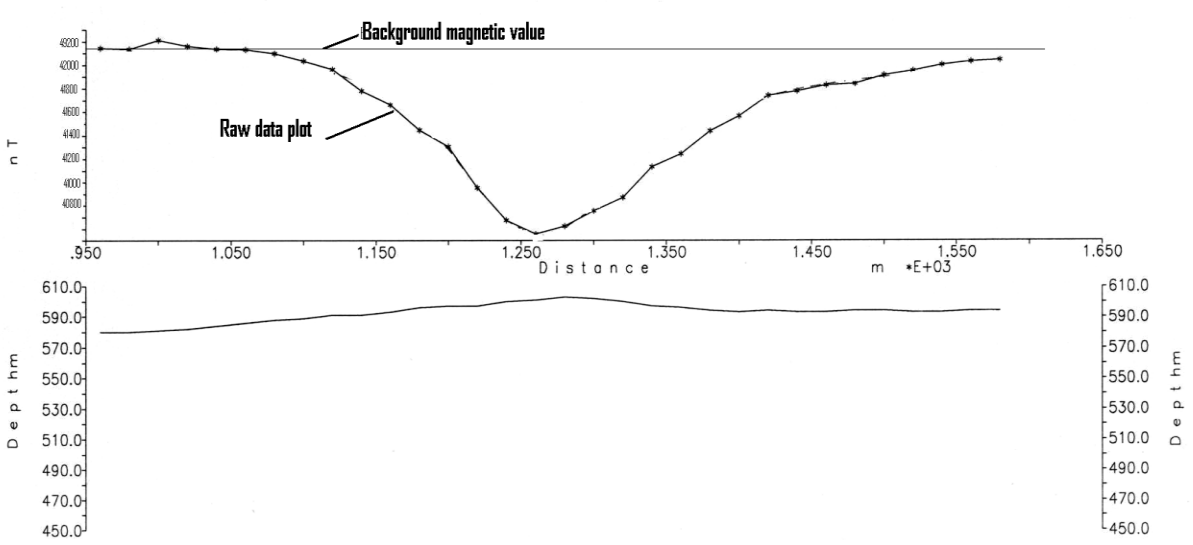

Fig.18. Initial magnetic data analysis, using GRAVMAG program. The constant background magnetic level (regional) is subtracted through the keyboard where the curve 'levels-out' on both shoulders.

4.4.3 Data reduction

Table 3 below displays the format of the data acquisition and archiving in the field. The data was later processed to reduce the magnetic readings to values expected in the absence of diurnal variations. This was achieved by comparing the magnetic readings at the base station (a) over time with those of the field magnetometer (b). Since the two magnetometers were initially synchronised both in time and

BASE STATION	(FROG HALL 17/3/10:40AM)
mag nT	TIMEREF(Hr.dec)
49036.20	10.42
49035.60	10.67
49041.90	10.92
49040.50	11.17
49038.50	11.42
49036.50	11.67
49038.20	11.92
49037.90	12.17
49037.00	12.42
49039.70	12.67
49041.60	12.92
49038.80	13.17
49046.20	13.42
49051.40	13.67
49061.40	13.92
49069.90	14.17
49058.90	14.42

(a) Base magnetometer readings

Table 3. Magnetic field data acquisition format.

	line 012		20m apart							
Stn.	Mag1	mag2	mag3	magav.nT	error nT	magred.nT	long deg.	Lat deg.	Alt.m	time(hr.dec)
133	49172	49171	49171	49171.6	0.6	49172	2.3198	54.7094	580	12.13
134	49230	49230	49231	49230.2	0.7	49230	2.3201	54.7093	576	12.27
135	49196	49198	49199	49197.7	1.0	49198	2.3204	54.7092	568	12.30
136	49193	49197	49197	49196.0	1.3	49196	2.3206	54.7090	559	12.33
137	49171	49170	49173	49171.4	1.4	49171	2.3208	54.7089	556	12.38
138	49153	49154	49155	49154.0	0.7	49154	2.3211	54.7088	552	12.42
139	49109	49112	49111	49110.5	0.2	49110	2.3214	54.7087	543	12.45
140	48860	48860	48863	48861.1	1.4	48861	2.3214	54.7084	546	12.48
141	48811	48812	48811	48811.2	0.6	48811	2.3216	54.7083	549	12.53
142	48887	48884	48884	48884.5	1.0	48885	2.3218	54.7081	546	12.57
143	48950	48952	48952	48951.5	0.8	48951	2.3220	54.7079	551	12.62
144	49003	49004	49004	49003.9	0.5	49004	2.3222	54.7077	554	12.65
145	49040	49040	49041	49040.5	0.9	49040	2.3224	54.7075	560	12.68
146	49070	49074	49073	49072.3	1.0	49072	2.3226	54.7074	562	12.72
147	49111	49113	49115	49113.1	1.9	49113	2.3227	54.7073	565	12.75
148	49144	49143	49143	49143.4	0.3	49143	2.3229	54.7071	571	12.78
149	49178	49181	49182	49180.2	1.7	49180	2.3231	54.7069	575	12.82

(b) Roving magnetometer readings

magnetic response, a magnetic anomaly was easily observed after numerical additions or subtractions were, subsequently, applied to the field data on the spreadsheet. Sensitivity of the readings was to the nearest nT while co-ordinates were acquired to the nearest 2m laterally and 5m in heighting. The Base magnetometer readings acted as a guide to the field magnetometer data. The first column on table 3 represents the magnetic reading (in nT) while the second column bears the corresponding time at which the reading was taken. The time is converted to hour-decimal for ease of manipulation. A graph of Time versus Magnetic reading is then plotted and the trend noted (see chart 1).

The first column of the roving magnetometer table represents the station number surveyed, the second, third and fourth columns hold the three magnetic values read off from the magnetometer at a short interval of time. Column five represents the average of the three readings while the error in column six is the difference between the average value and the largest value among the three taken. To obtain the entry in column 7 of the roving magnetometer in the table, the average value in column 5 is arithmetically adjusted with respect to the increment or decrease in the diurnal value of the base magnetometer at the time that particular reading was taken. In most cases a constant value was either added or subtracted

The graph of the result obtained by the field (roving) magnetometer in the vicinity is expected to appear similar to chart 1. However, due to magnetic anomalies encountered in the subsurface below the field magnetometer, the magnetic value, at a particular time, is not the same as that recorded at the base. The magnetic reading difference between the field magnetometer and the base one, at a particular time, is the magnetic anomaly at the field station.

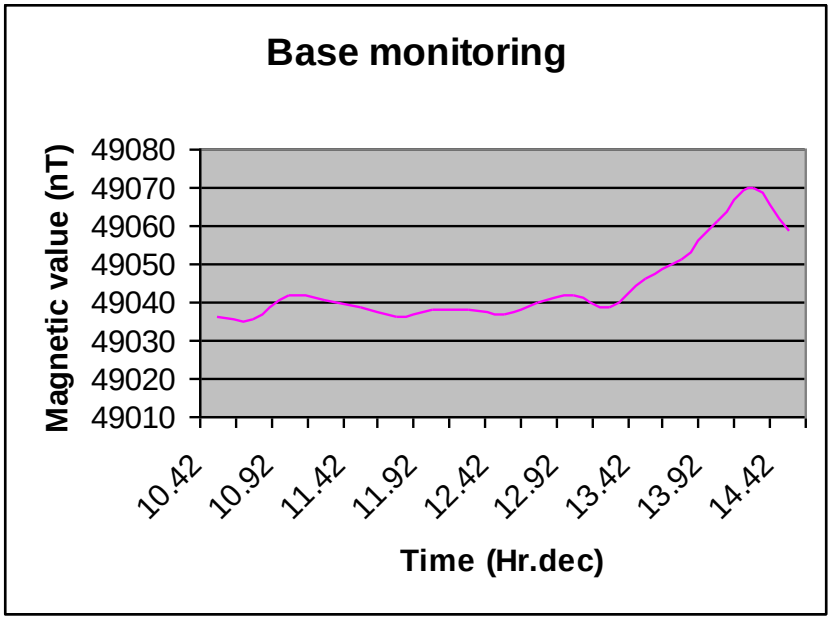

Chart 1. Example of diurnal variations recorded by the base magnetometer

Columns eight and nine represent the longitude and latitude co-ordinates of the individual stations; column ten represents the altitude above sea level in meters while the last column is the recorded time when the third magnetic reading was made. All the data are given in Appendix II. The stations' spatial locations were later transferred to a geo-database that contained geo-referenced geological maps, topographical maps and aerial photographs of the area of survey. This was achieved by transferring the reduced magnetic values from the EXCEL spreadsheet to SURFER spreadsheet where contouring could easily be done in the windows operating system (table 4).

The method employed in the surfer program for plotting uses the Krigging averaging option and Akima Spline smoothing technique to draw the contours. Triangulation of the nearest neighbour points is achieved to form a '.grd' file that enhances the anomalous zones and the contours can be viewed in full colour either in 2D or as 3D DEM's, depending on the operator's final objective. In this case, the magnetic anomalies were displayed in 2D while the elevations were drawn in 3D mode.

Stn. No.	Mag.(nT)	Long.(deg)	Lat.(deg)	Alt.(m)
1	49129	-2.3121	54.7081	526
2	48971	-2.3123	54.708	532
3	48769	-2.3124	54.708	530
4	48574	-2.3127	54.7079	532
5	48502	-2.313	54.7078	529
6	48453	-2.3132	54.7078	528
7	48449	-2.3136	54.7077	519
8	48619	-2.3148	54.7077	518
9	48794	-2.3149	54.7075	524
10	48901	-2.3153	54.7074	529
11	48969	-2.3153	54.7073	530
12	49018	-2.3159	54.7071	532

Table 4. Example of a spreadsheet file imported to Surfer program. Second column represents the reduced magnetic values.

5 RESULTS

A total of 1,880 stations, covering an area of approximately 50 square kilometres and over 35km distance of ground magnetic lines, were analysed at four different locations (See fig.1). The data acquired in Round Hill, Harwood, Langdon Beck and Etters Gill, was analyzed separately for purposes of ease of understanding of the anomalies. The overall interpretation combined all the analysed zones into one region.

5.1 QUALITATIVE DATA ANALYSIS

5.1.1 Round Hill Area

The Round Hill locality is in the North-Western part of the survey area between longitudes 2.36º and 2.42º W and latitudes 54.71º and 54.74º N (Fig.19). The survey area is approximately 10 sq. kilometres and is right at the top of the hill. The Cleveland dyke is exposed here at two different sites and three profiles were surveyed in the North-South direction since the dyke runs east-west.

Geology of Round Hill area (fig.19) shows the en-echelon dyke system in close proximity to the Whin Sill (in red).The contour plot (Fig.20) shows the en-echelon traced trend of the Cleveland dyke where a slight displacement occurs between two adjacent terminations. The 3-D elevation model (fig.21) displays the path of the Cleveland dyke across Round Hill. The main reason why the survey was conducted here was to identify the magnetic nature of the exposed dyke outcrop. The average anomaly obtained here was over 400nT, negative with respect to the background. The magnetic-low anomalies are seen to coincide with the position of the known outcrop of the dyke (green levels for low anomaly). In this and other subsequent contour figures, the latitude scale may appear slightly out of proportion due to importation of the plots to MS Word from Surfer program. However, this does not alter the co-ordinate references.

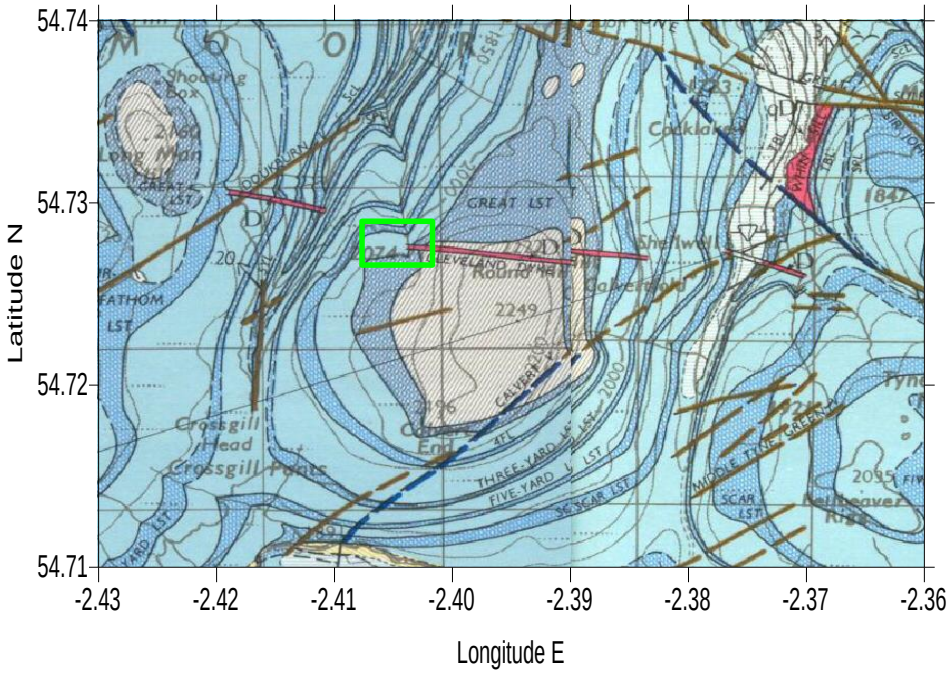

Fig.19. Geological map of Round Hill area showing the en-echelon nature of the Cleveland dyke and the Whin Sill outcrop in red (survey area in green box).

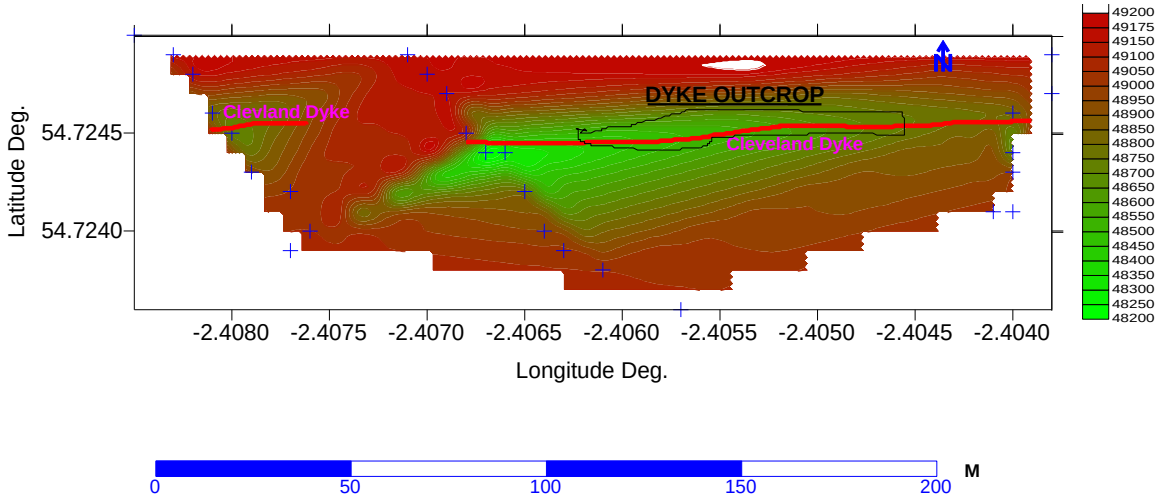

Fig.20. The Round Hill magnetic anomaly. The traced line marks the continuation of the outcrop of the Cleveland Dyke (in black). + signs indicate positions of individual readings. The magnetic low (in green) coincides with this outcrop location.

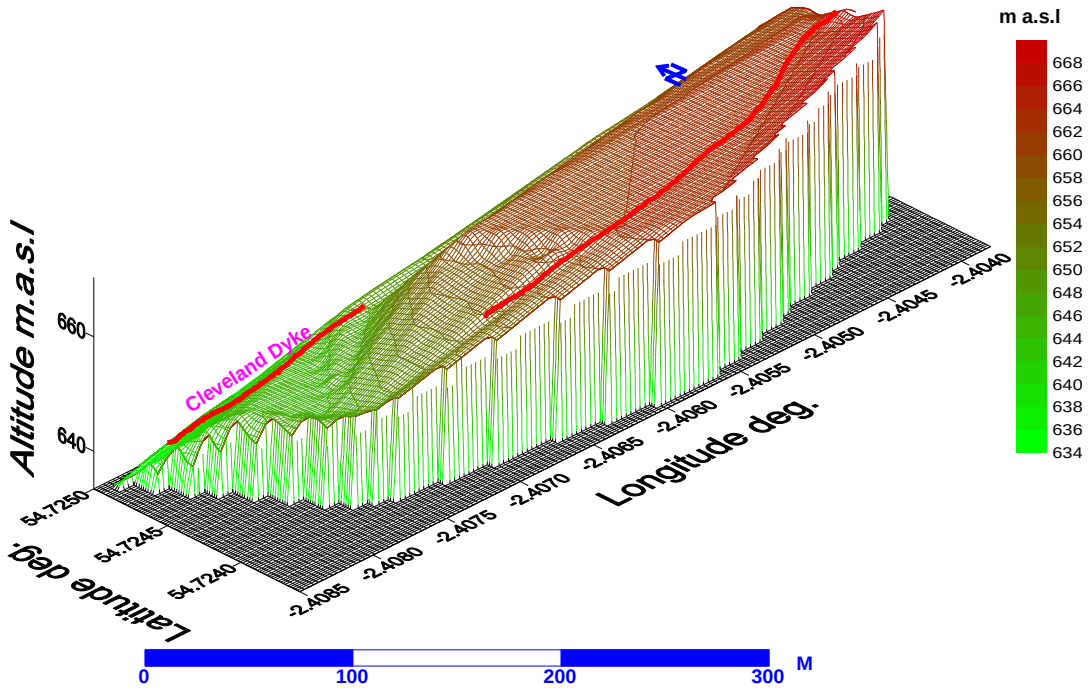

Fig.21. 3-D elevation model at Round Hill

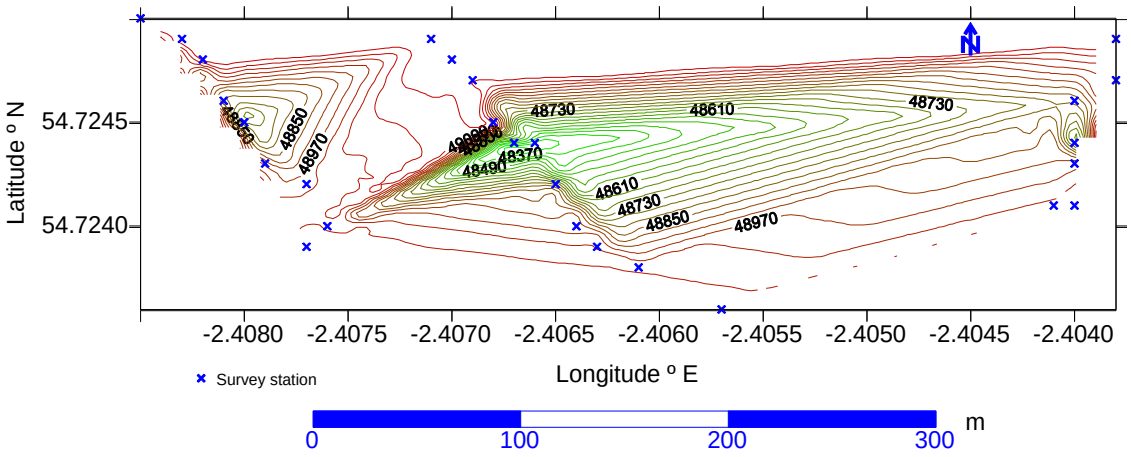

Fig.22. Magnetic contours at Round Hill. The survey stations are shown in blue crosses, the 'low' anomaly appears in green while the 'background' value is in red.

Profiles 4 & 5 (fig.17) were not considered here as they were surveyed to investigate the extent of the dyke to the north of Round Hill. The same applies to profiles 7 and 8 to the east of Round Hill. These profiles gave insignificant magnetic signatures.

5.1.2 Harwood Area

The Harwood locality covers an area of 18 square kilometers and is bounded by longitudes 2.25º and 2.35º W and latitudes 54.68º and 54.73º N. The geology in Harwood is basically controlled by the Teesdale fault that runs in the NW-SE direction, intersecting with several faults and mineral veins. The Harwood beck has its origins here and the valley is littered with streams on both flanks (Fig.23).

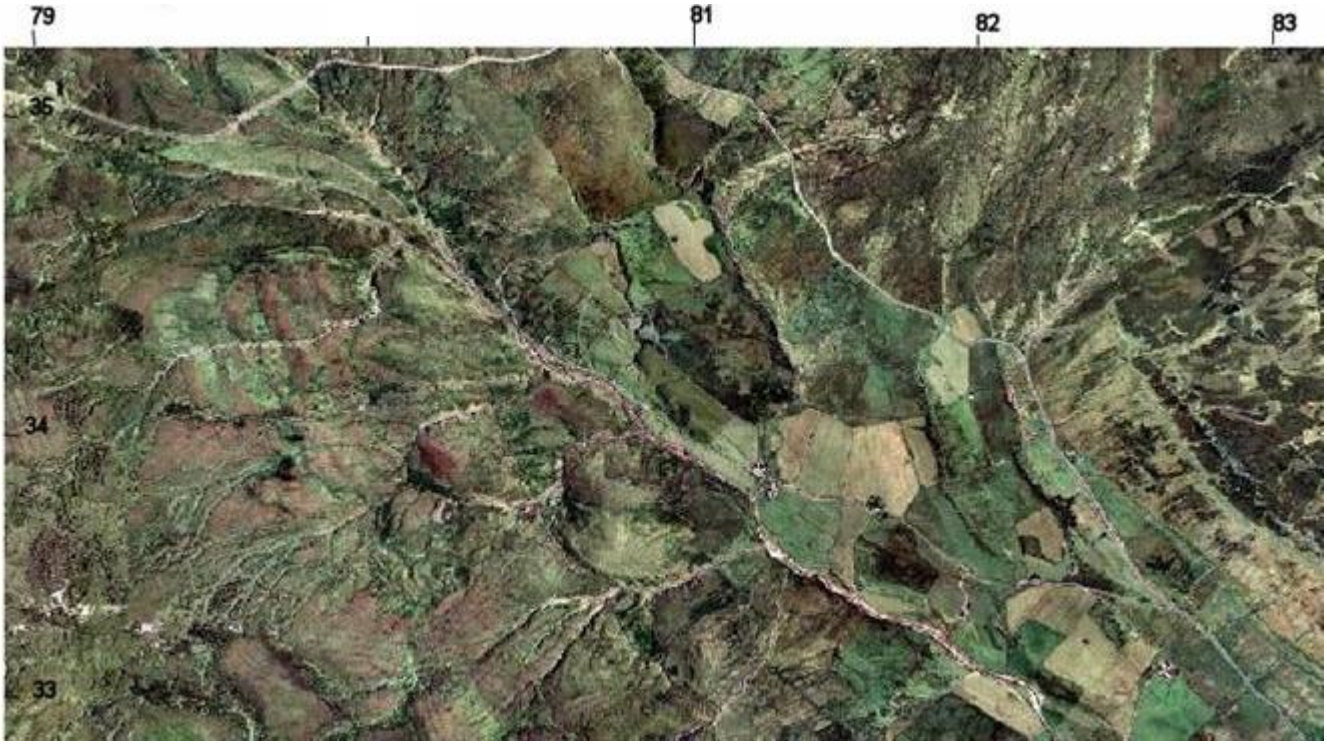

Fig.23. Aerial photograph of the Harwood valley, with the Harwood beck flowing towards the SE through the centre of the image and the road to Alston running parallel to and north of it from Middleton-In-Teesdale (compare with fig.3).

Figure 23 above is an aerial photograph of the valley depicting the drainage system and the Teesdale Fault's control of the topography. Most of the magnetic data in this report was concentrated in this area and the results show a negative anomaly trending NW-SE straddling the Teesdale fault (figs.24 & 25).

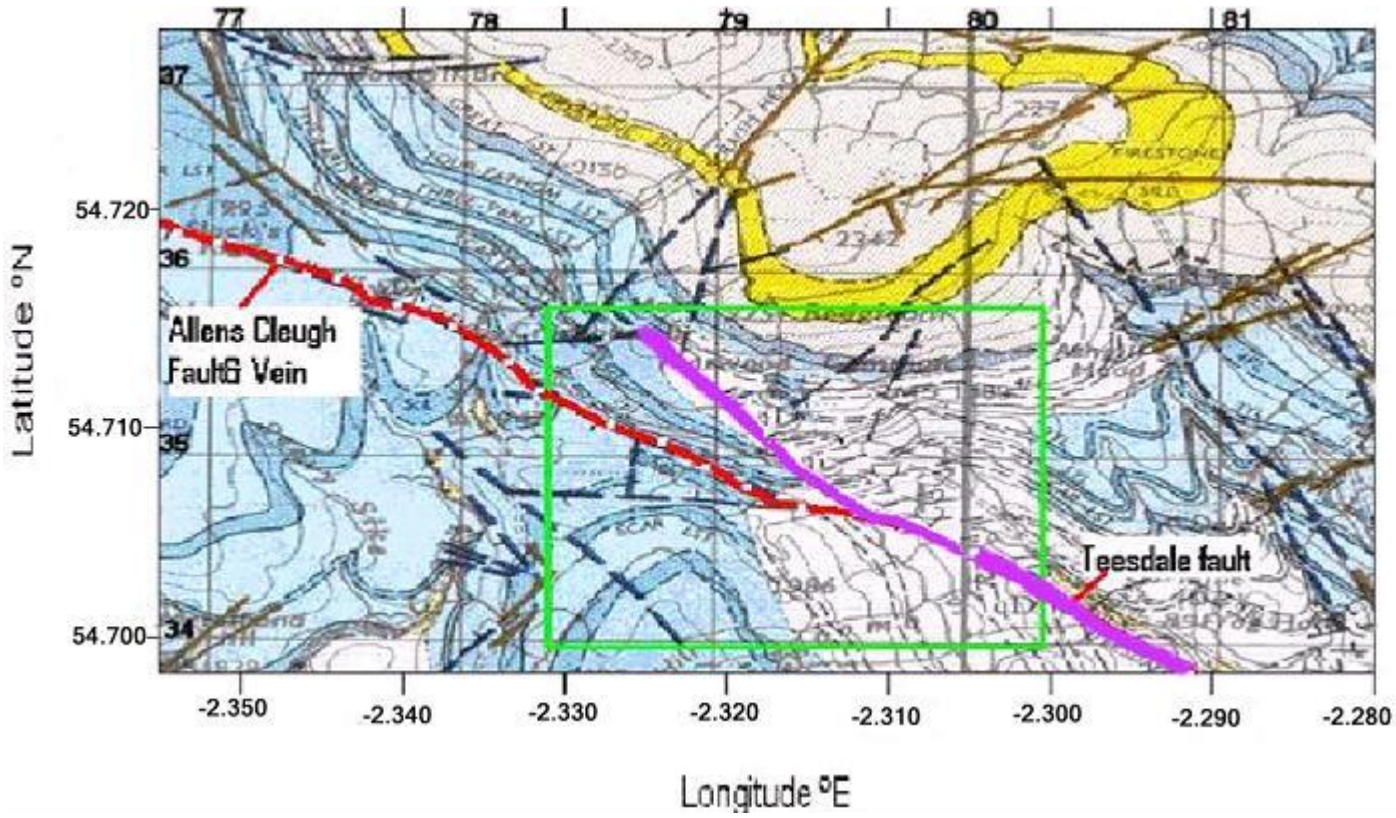

Fig.24. Geological map of Harwood. 'qD' (quartz Dolerite) on the map refers to the Whin Sill under the surface. The box in green indicates the actual data acquisition area (fig.25).

Fig.24 above depicts the geology of Harwood and highlights the Teesdale fault trending right through the middle in the SE direction with the Allens Cleugh Fault and Vein intersecting it about 30º towards the NW. A lot of drift is found here though the thickness could not be established. Fig.25 below indicates the spatial orientation of the survey stations with the magnetic contours showing a remarkable anomaly over the Teesdale fault, trending to the north-west along the Allens Cleugh vein. The anomalous body eventually trends towards the Cleveland dyke outcrop at Round Hill, some 3km north-east of Harwood. The contour-fill gridding in fig.26 below triangulates areas nearest to the surveyed station and ignores no-data zones, hence the empty space within the map area.

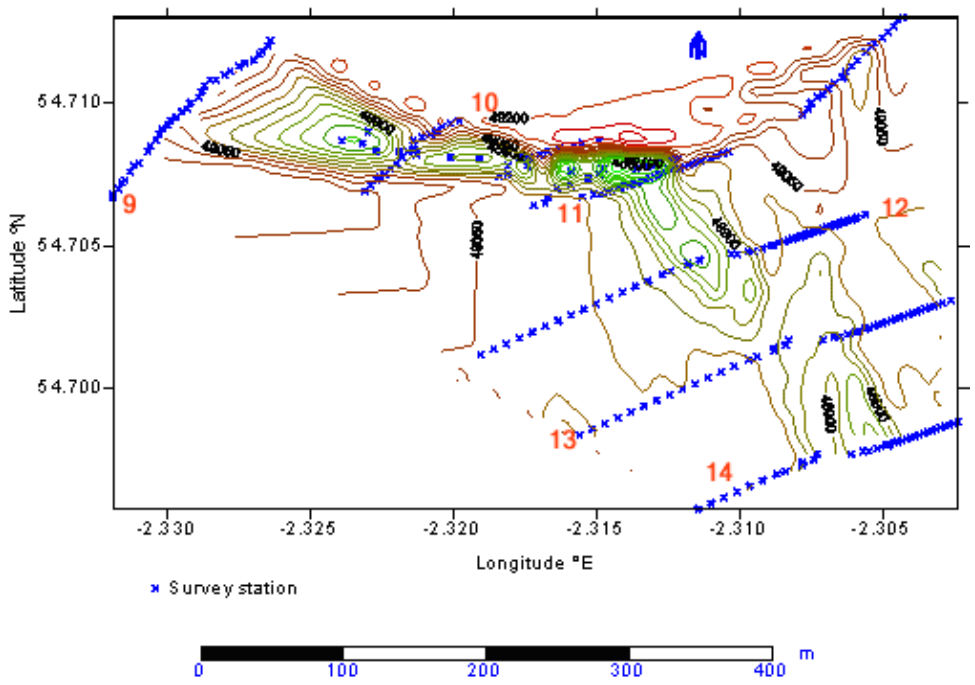

Fig.25. Magnetic anomaly contours in Harwood valley. Bright green indicate low magnetic levels. The numbers identify the profiles surveyed in this locality (see fig.17)

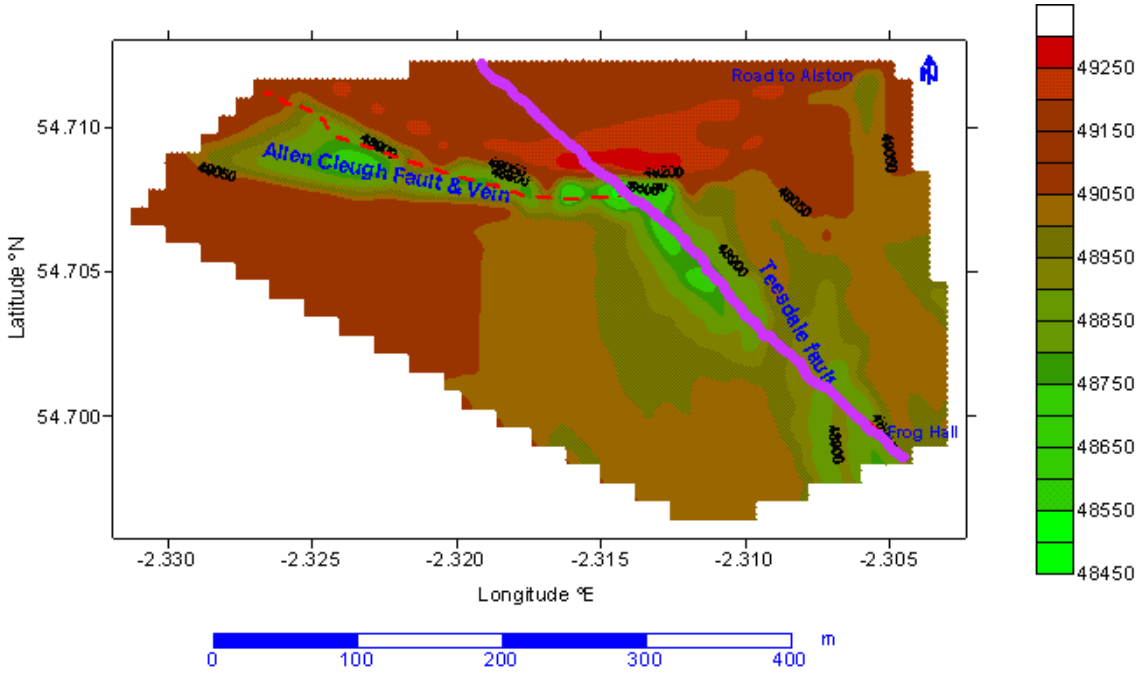

Fig.26. Magnetic anomaly at Harwood (in nT). The magnetic 'lows' occur along the Teesdale fault and the Allens Cleugh mineral vein & fault.

Fig. 27 below shows the elevation of the survey area, the higher altitudes are principally related to isostatic adjustment of the sub-surface.

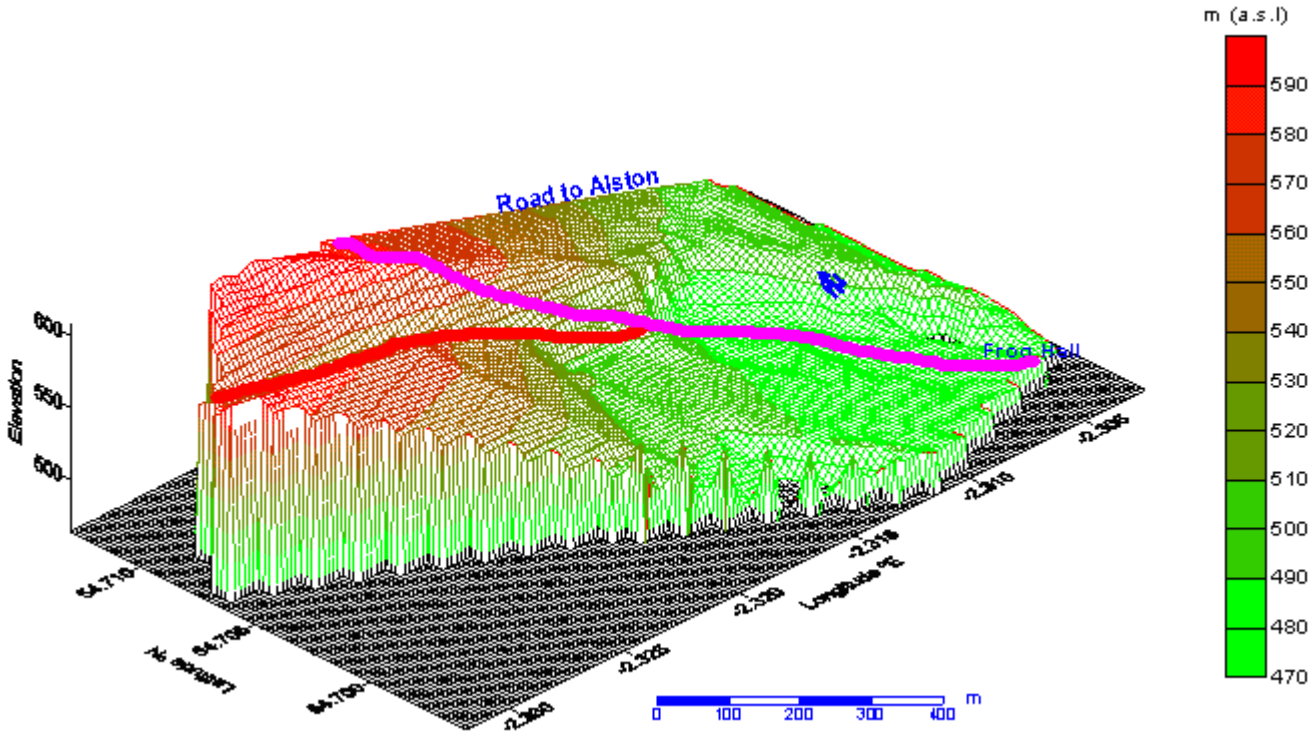

Fig.27. A 3D Elevation model at Harwood. The Harwood river flows down the middle of the valley in the NW-SE direction parallel to the Teesdale fault (in purple). The Allens Cleugh Vein/Fault branches off the Teesdale fault in the NW direction (in red)

5.1.3 Langdon Beck area

This survey area stretches from longitude 2.2º to 2.28º W and latitude 54.66º to 54.68º N covering an approximate area of 15 square kilometres. The Langdon Beck locality is the most geologically complex area under investigation (Fig.28). This survey area hosts the Teesdale fault, the Burtreeford disturbance and the Whin Sill as well as the inferred Cleveland dyke. The profile anomalies obtained needed special attention whenever two or more of these geological features intersected.

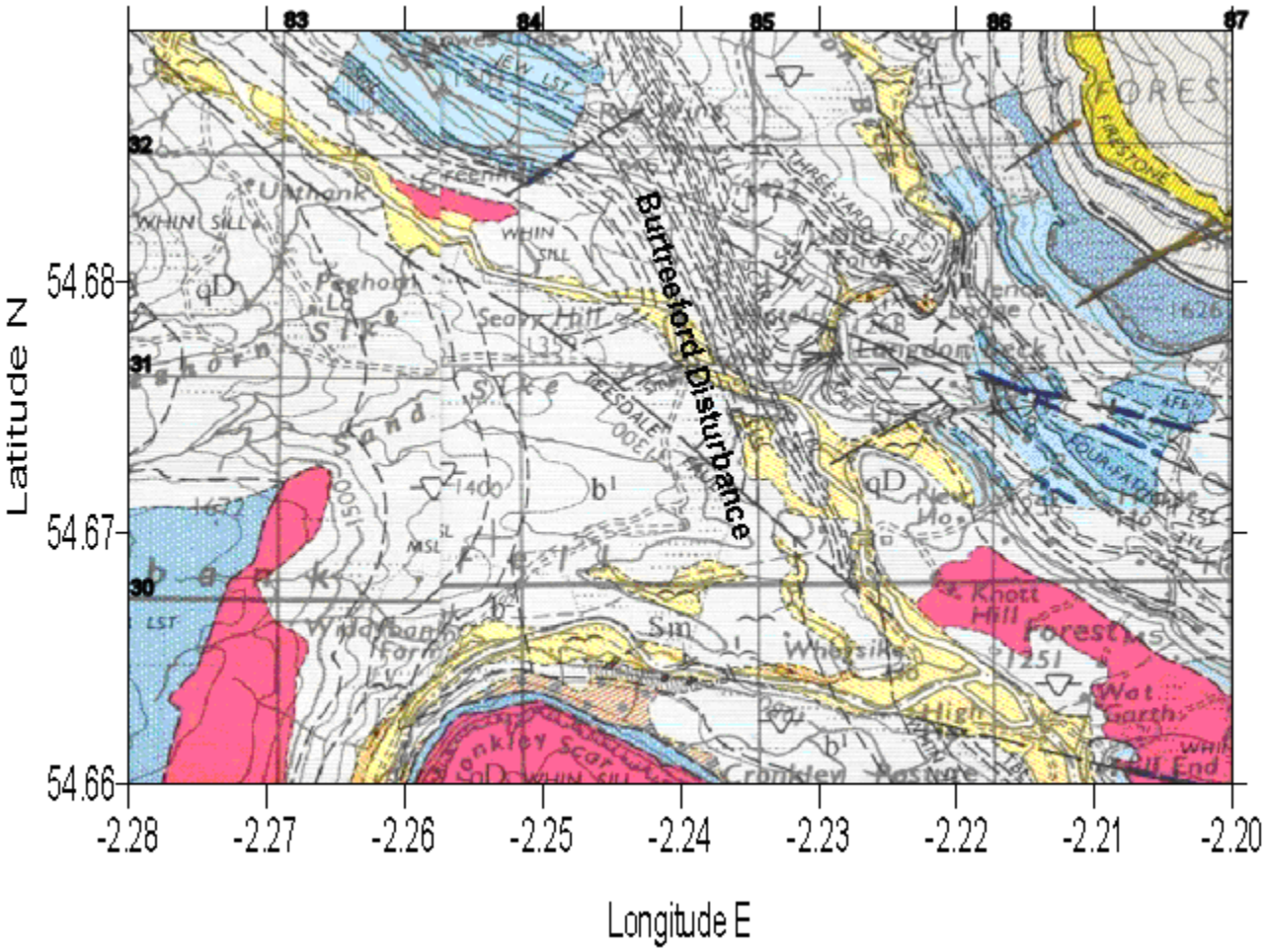

Fig.28. Geological map of Langdon Beck (Whin Sill outcrops in red though the intrusion is continuous under the surface in areas marked 'qD').

Figs. 29 & 30 below display magnetic contours in Langdon Beck. The amplitude of the anomaly here is about 200 nT and the distinct magnetic lows occur along a valley running off to the east of the Teesdale fault. This valley eventually connects with the known outcrop of the Cleveland dyke at Etters Gill.

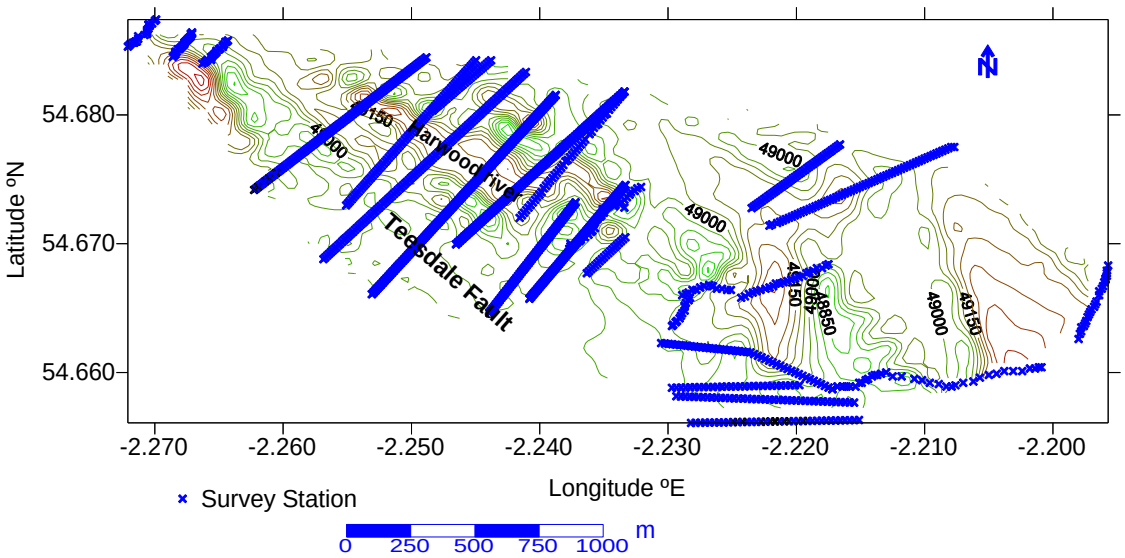

Fig.29. Magnetic anomaly contours at Langdon Beck. The 'low' values are contoured in green. The Teesdale Fault runs parallel to the Harwood river more than a hundred meters away to the west.

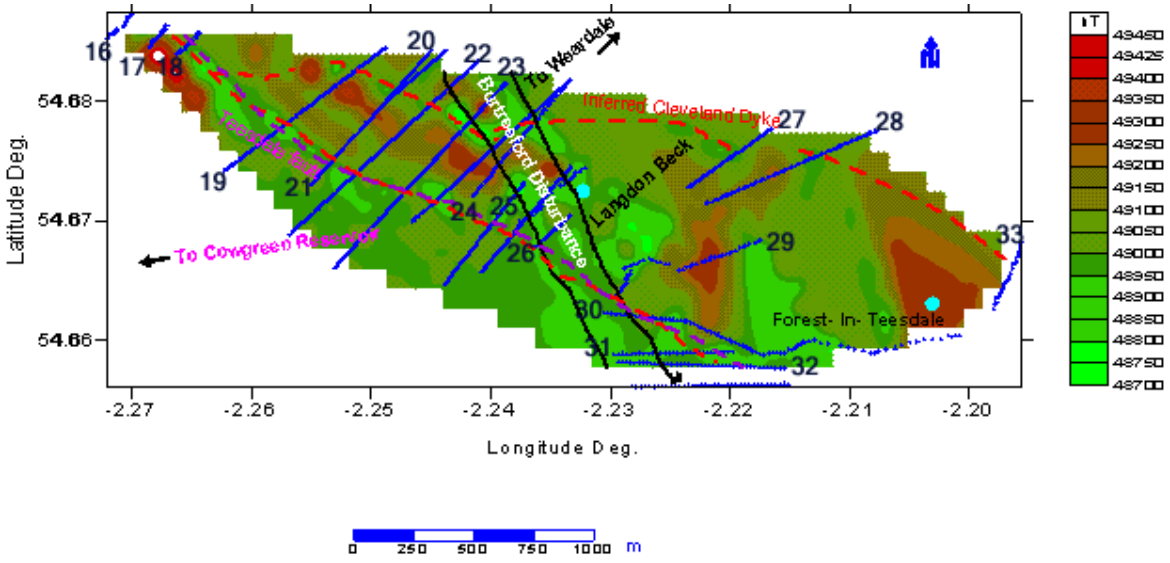

Fig.30. Magnetic anomaly plot at Langdon Beck. The Teesdale Fault, Burtreeford Disturbance and the inferred Cleveland Tertiary dyke here give a very complex magnetic picture. Red (high) magnetic levels depict the Disturbance as a high anomaly while the Teesdale Fault (probably hosting the dyke) bears a green 'low' anomaly. The numbers (16 to 33) indicate the traverses surveyed in this locality (see fig.17)

The contours alone could not conclusively identify the nature and trend of the geological bodies. Closer scrutiny using the profiles individually and severally was required to arrive at a sensible explanation of each anomaly. Very distinct here (fig.30) is the magnetic high anomalies appearing almost north-south, sub-parallel to the Burtreeford disturbance (e.g. at 2.225º W and 54.66ºN). These features are thought to have occurred contemporaneously with the Burtreeford Disturbance (Dunham, 1934) (fig.31) during the Permian. The magnetic 'low' occurring along the Teesdale Fault could be caused by the intruding Cleveland dyke, suspected to be present in the sub-surface.

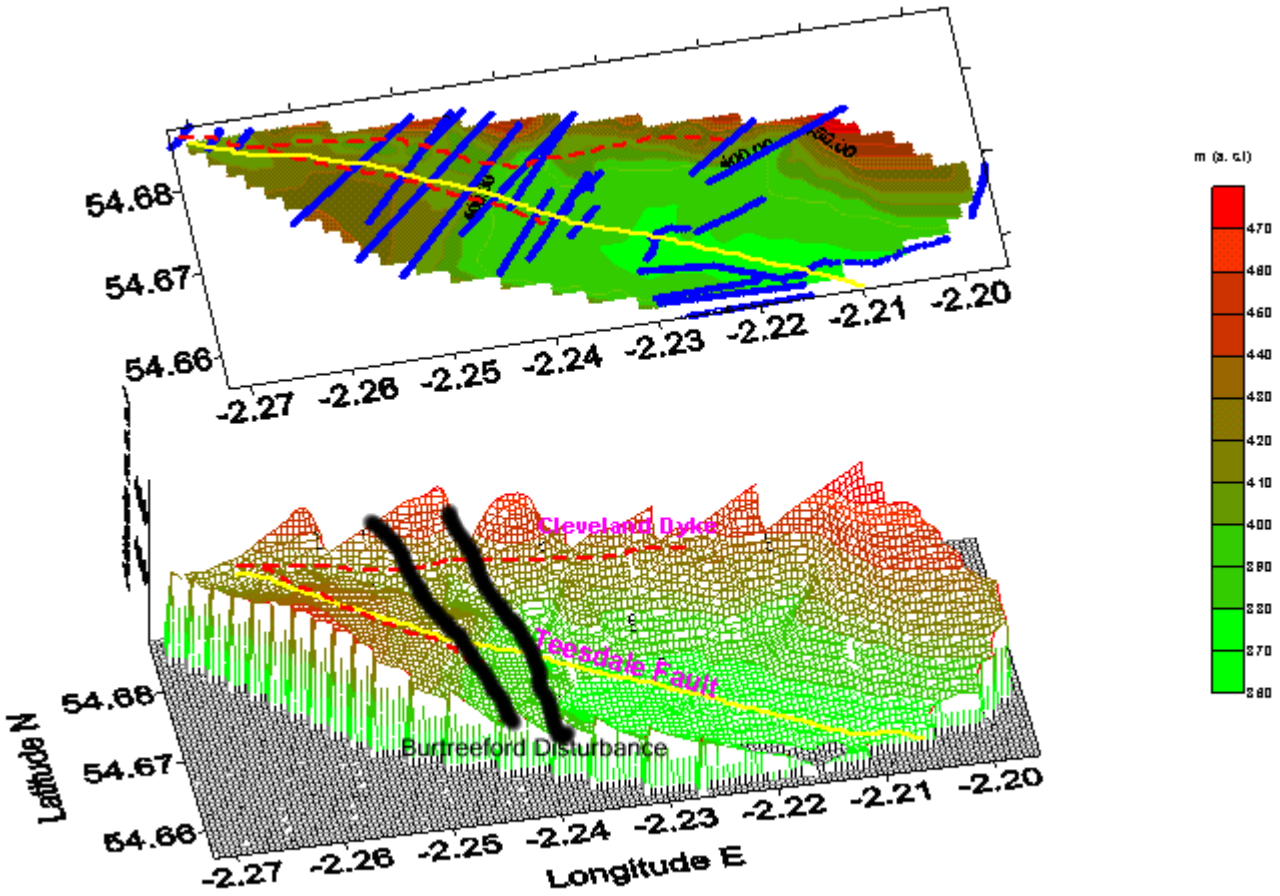

Fig.31.A 3D elevation model at Langdon Beck. The Burtreeford Disturbance, running almost NS, dominates the geological features here.

However, the individual profile anomalies clearly distinguished the Teesdale Fault as a magnetic low. Also the intersection between the main road to Alston and the Burtreeford Disturbance (see Fig.30) (2.24º W, 54.677º N) displayed a magnetic low. Magnetic modeling in the quantitative analysis (next chapter) will reveal that the inferred dyke in Langdon Beck extends and terminates at the confluence of the Tees river and Harwood Beck (2.218º W, 54.663º N) (Fig.28). Also the dyke branches off towards the east at 2.26º W and 54.68ºN (Fig. 30). It was intercepted by three magnetic profiles at different areas between Langdon Beck and Etters Gill where an outcrop can be seen at a river bed.

Figure 31 above shows the elevation of the complex geological formations at Langdon Beck. The Teesdale Fault cuts right through the valley though here, it is located further to the west from the Harwood Beck. Topographically, the Butreeford Distubance appears as an anticline running almost north-south in the survey area.

5.1.4 Etters Gill area

The map below shows the geology of Etters Gill, bounded by longitudes 2.13º and 2.20º W and latitudes 54.66º and 54.69ºN (Fig.32). The survey area (green box in fig.32) is approximately three square kilometres. The survey was extended up to this area in the south-east for purposes of confirming the nature of the exposed Cleveland dyke and if it relates to the magnetic anomalous body occupying the Teesdale fault. Traverses were surveyed very close to the dyke outcrop where it resisted erosion across the Flushlemere beck confluence with other streams. Figure 33 below displays magnetic contours surveyed here at Waterfall in Etters Gill. Four magnetic traverses were made at Etters Beck (2.175ºW, 54.662ºN) but the data could not be contoured due to an external magnetic field that was introduced to all the southern portions of the profiles by an electric fence running parallel to the dyke. This data was however successfully interpreted in the GRAVMAG program (see next chapter).

The maximum amplitude of the anomalies here is in the range of 500nT where the profile cuts the dyke some 100m from the exposed outcrop. The anomalies tend to fade with distance away from the exposure, probably due to the thickening of the overburden. The magnetic anomaly (low) in all the profiles is observed to occur where the traverse cuts the dyke.

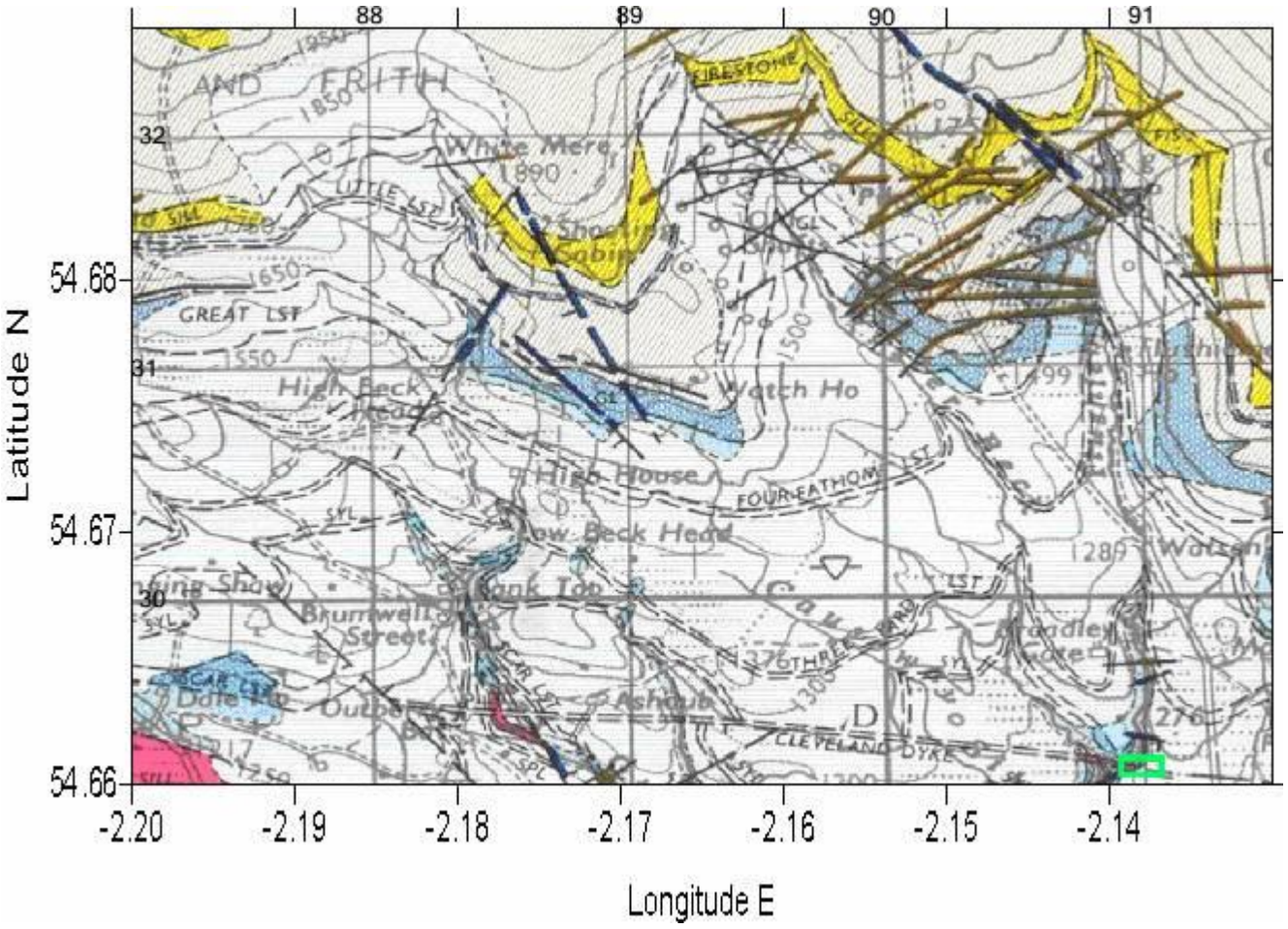

Fig.32. Geological map of Etters Gill (Dolerite intrusions in red). The box in green at the SE corner of the map represents the area of data acquisition at Waterfall.

However, the en-echelon offset of the dyke is confirmed here by closely observing the anomalies in figs. 33 & 34. There is a general shift to the south of the east-west trending anomaly at (2.1395ºW, 54.6565ºN).

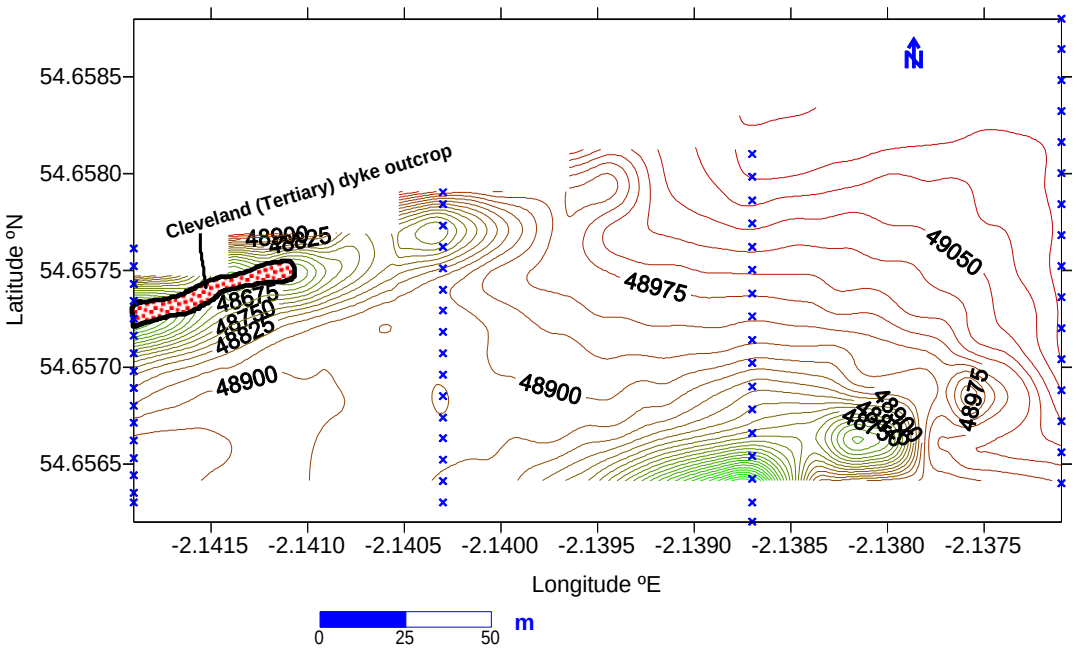

Fig.33. Magnetic contours at Etters Gill. Green contours represent 'low' magnetic levels while the red colour is the magnetic background. The blue crosses are survey stations.

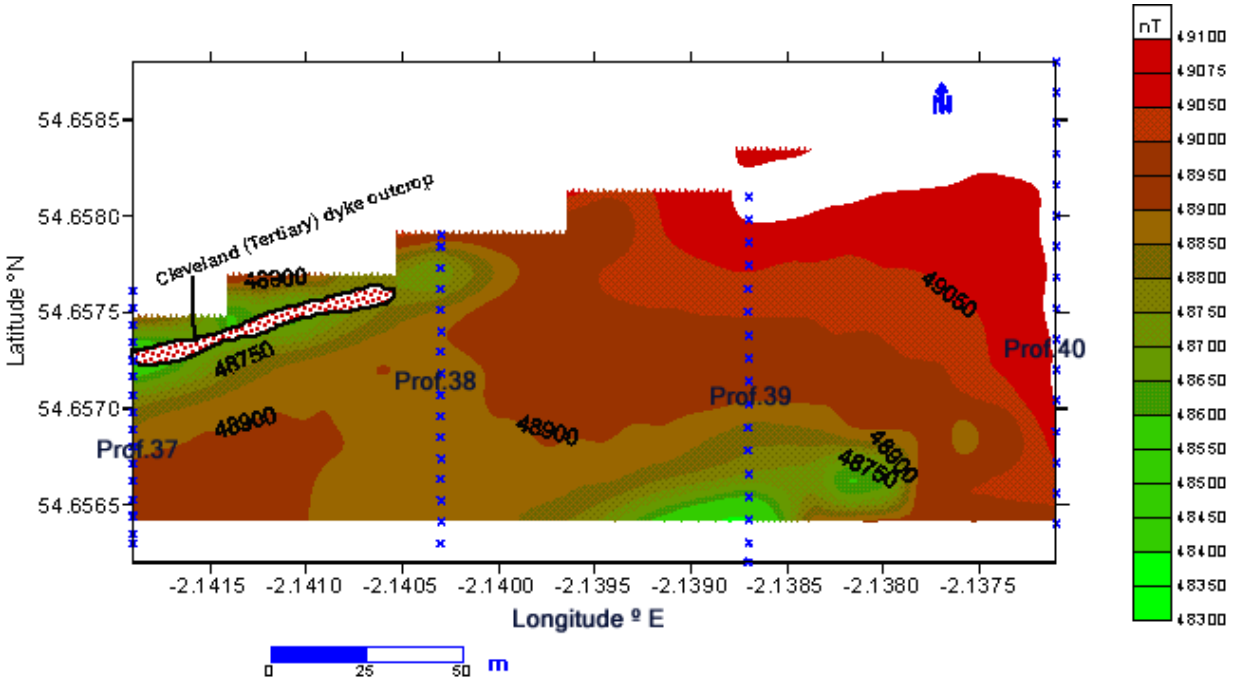

Fig.34. Magnetic anomaly map at Etters Gill. The magnetic 'lows' in green indicate a possible en-echelon trend in the east-west dyke where a displacement to the south occurs at longitude 2.14ºW. Profile numbers are inset in black (see fig.17)

Fig.35 below shows the elevation at Etters Gill with a very steep slope to the west where the Flushlemere beck has, over the years, etched a deep gorge at a confluence with another minor stream. Here the Cleveland dyke is visible on the face of the valley and has an approximate width of fifteen meters.

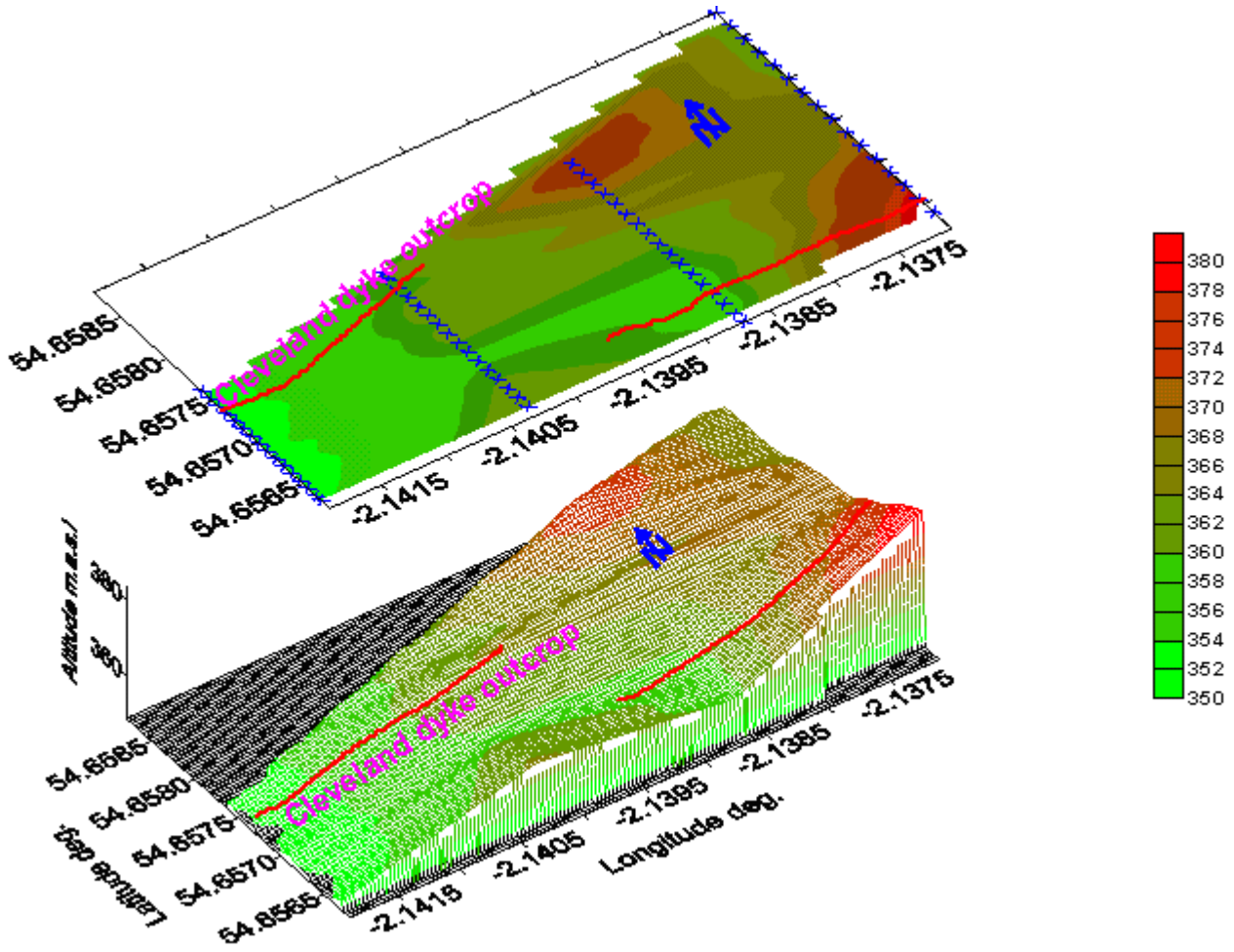

Fig.35. A 3-D elevation model at Etters Gill, tracing the probable trend of Cleveland Dyke from longitude 2.1395ºW. The dyke tracing to the east of longitude 2.14W is the actual outcrop confirmed by the magnetic anomaly (fig.33); heights are in m above sea level.

Summary

From the qualitative analysis results, it can be deduced that the Cleveland dyke, outcropping at Round Hill in the NW of Harwood and at Etters Gill in the SW, could probably be the main cause of the low magnetic anomaly encountered in the surveyed areas. The anomaly is consistently occurring along faults and with a negative value with respect to the background. This is in line with the dyke's tendency to occupy areas of weakness during intrusion.

6 QUANTITATIVE ANALYSIS

6.1 Introduction

In an attempt to quantify the nature of the source of the anomalies observed in the four different localities, the GRAVMAG program (Pedley, 1991) was used to approximate the nature of the source, depth to the top of the anomaly-causing body, depth to the bottom, width, magnetisation, magnetic susceptibility, declination and inclination.

This interpretation program works in the MICROSOFT WINDOWS domain and is interactive during the modelling process using magnetic data sets. The output is displayed on the same screen as the raw data plot and portrays the calculated magnetic profile, the surface terrain (instrument height), the anomalous bodies (called polygons) and the physical parameters of the bodies. Bodies are assumed to extend perpendicular to the profile line, but the program is '2.5D', i.e., it can apply end corrections to approximate 3Dbodies.

The data, after processing in a spreadsheet, was transferred as an X-Y-Z file in a text editor for the GRAVMAG program to recognize the parameters involved (i.e. traverse distance, magnetic value and elevation). Once in the interactive program, the operator is able to draw a possible polygon that would give rise to the anomaly on the upper part of the display. There is no limit to the number of magnetic bodies that can be drawn on the screen, though the more the bodies (or polygons), the more complicated will the interpretation be. The best technique is, however, to select the simplest model possible to generate the observed result.

Possible parameters can be entered from the draw-down menus; these play an important part in determining the accuracy of the calculated profile and a limited degree of inversion (optimization) is

available. The output, after a tedious curve matching procedure, will be displayed on the screen and can be saved as a model file or printed as a hard copy. Modelling in 2D is deemed sufficient for dyke bodies (elongated in the direction of strike) (Goulty and others, 2000) but it was found prudent to use the third dimension in the program (actually 2.5D). This was to avoid ambiguity in the calculated curve especially where dyke terminations occurred close to measured profiles. In the dyke models, the base of the dyke was always 1000m below the top.

The likely causes of the magnetic anomalies encountered in northern Teesdale could have been due to:

1. The Whin Sill, especially where it is faulted or demagnetised (Late Carboniferous/ early Permian)
2. Whin Dykes, if present (Early Permian)
3. The Cleveland dyke (Tertiary)
4. A combination of two or all the above.

Results of previous research on the Cleveland dyke, the Whin Sill and Tertiary dykes are summarized in table 4 below.

Author	**Intrusion**	**Width/ Thick-ness(m)**	**Magnetic susceptibility(SI)**	**Magnetization (A/m)**	**Remanent Declination**	**Remanent Inclination**
Giddings and others (1972)	Tertiary Dykes	5-25	0.01 to 0.03	5.0	153º	-67º
Cornwell & Evans (1986)	Whin Sill	30-74	0.025	2.7	183º	-14º
El-Harathi & Tarling (1988)	Permian Dykes	10-40	0.01	2.7	183º	-14º

Table 5. Palaeomagnetic results of the Whin Sill, Permian dykes and Tertiary Dykes in Northern England.

Many boreholes and mine shafts exist in upper Harwood. The former were drilled for scientific investigation and the latter sunk for economic mineral exploitation. Most of these sub-surface excavations were well documented though not specifically for research purposes. However, the formations encountered with depth were noteworthy and these were used, in this dissertation, to arrive at a map depicting the possible depth, to a good approximation, of the Whin Sill in the area of survey (Fig.36, table 6)

Location	Thickness (m)	Approximate Depth (m a.s.l.)	Position
Tynehead	15	515	[NY760 350]
Frog Hall	~	400	[NY 800 340]
Greenhurth	13	460	[NY 780 320]
Herdship	~	460	[NY 810 330]
Lingy Hill	~	400	[NY 820 330]
Langdon Head	~	400	[NY 840 340]
Greenhills	~	400	[NY 830 310]
Harthope Beck	~	400	[NY 860 320]
Widdybank Fell	~	460	[NY 830 300]
Cow green	73	518	[NY 800 300]
Cronkley Pasture	~	400	[NY 850 290]
High Beck Head	~	350	[NY 880 300]
Pike Law	~	350	[NY 900 310]

Table 6. Approximate depth and thickness of the Whin Sill in the survey area. Thicknesses could not be readily established in most areas. Where the Whin is exposed, it suffered erosion (i.e. Tynehead and Greenhurth)

Figure 36 below shows the Whin Sill intrusion's depth levels in the study area; from Newbeggin in the south-east to Allens Cleugh in the north-west. The depths were inferred from known outcrop sites and interpolation of mine shafts that encountered the Whin (Dunham, 1990, Burgess and Holliday, 1979). The Sill is not necessarily continuous as presented above and there are jumps and dips along the

intrusion as explained in the regional geology chapter. The level of the Whin below the surface is important in the controlling of the modelling parameters used in the GRAVMAG program. This will act as another guide in addition to the palaeomagnetic results presented above (table 4). Magnetic modelling of the survey profiles thus took into account the geology of the area as well as the magnetic parameters given by the researchers above.

The expected magnetic response on a traverse where a vertical Tertiary dyke intrudes is given on fig.37 (a). The width of the dyke, magnetization and depth to the top of the body will all contribute to the magnitude of the anomaly. Due to the narrow nature of the dyke, it tends to cool faster than other intrusions, hence the typical fine grain sized crystals that did not have enough time to grow (plate 1) producing a higher remanent magnetization. The half-width of the anomaly in this case will determine the width and/or depth of the dyke where only the dyke is the anomalous body. Fig.37 (b) shows the magnetic anomaly created by a Permian dyke.

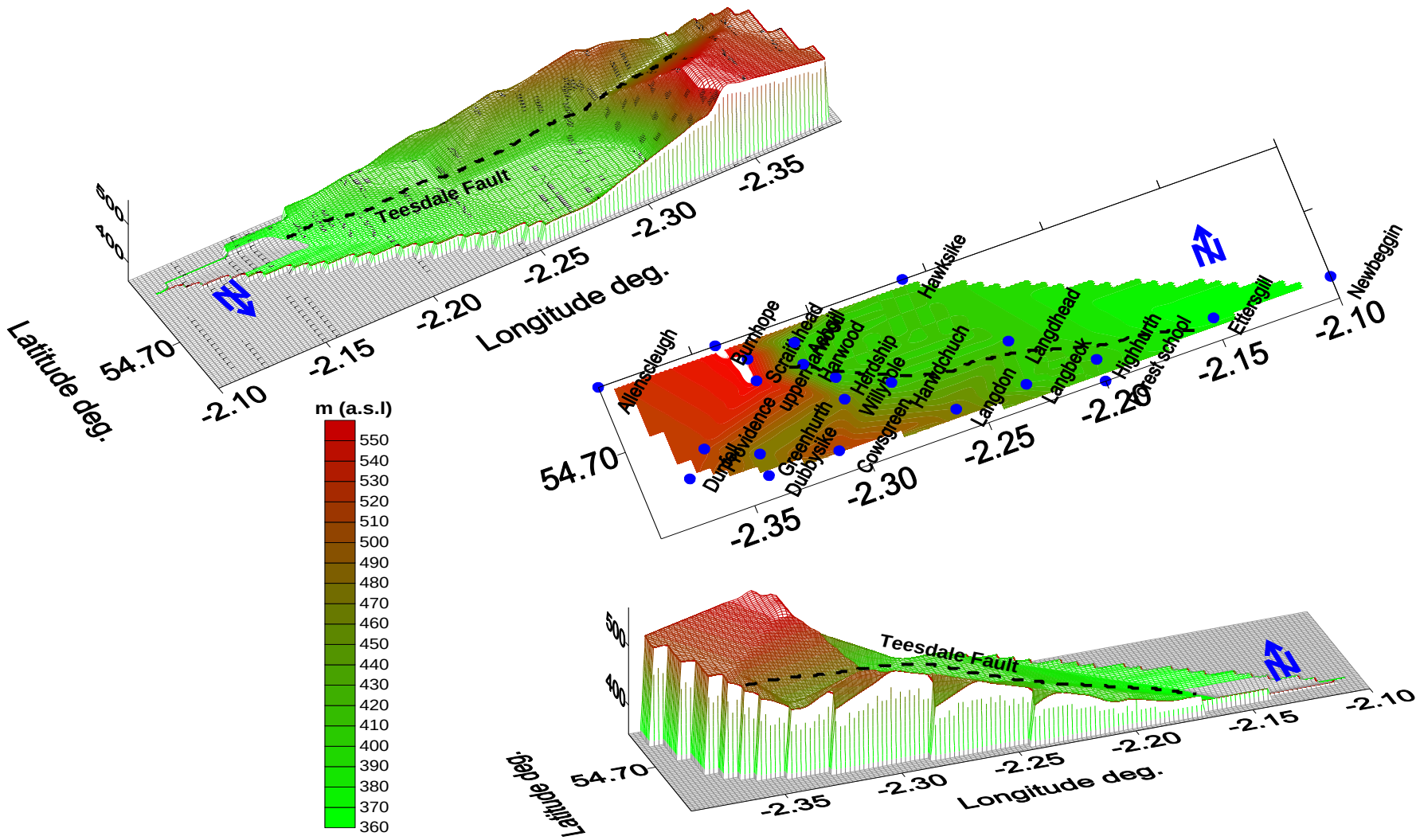

Fig.36. Whin Sill horizons deduced from outcrops, boreholes and mine shafts in Upper Teesdale. Heights are in meters above sea level.

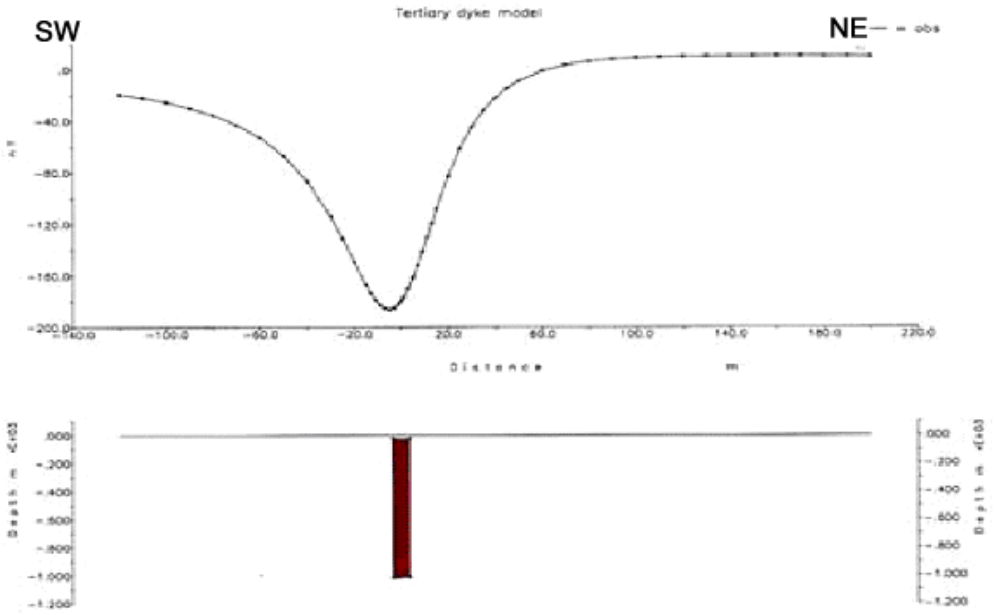

Fig.37 (a). Magnetic anomaly due to a Tertiary dyke with parameter values given by Giddings et al (1972))

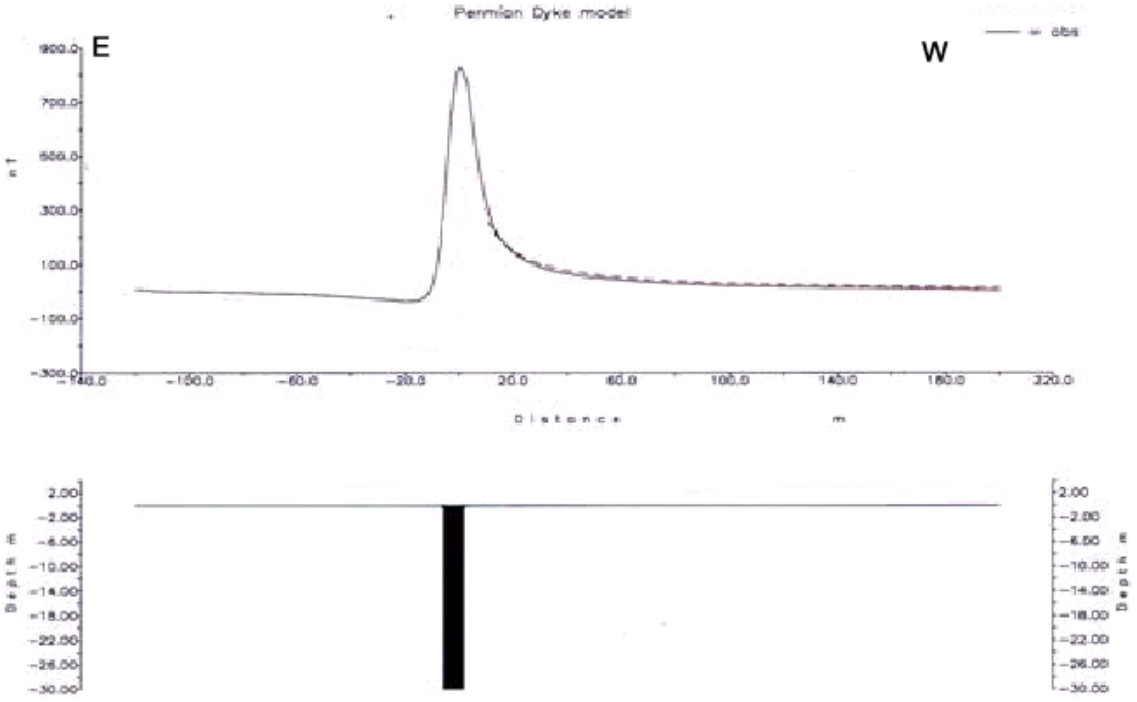

Fig.37(b). Magnetic anomaly due to a Permian dyke

A similar but inverted anomaly is observed along a traverse where a Permian dyke intrudes (Fig.37 (b)). This is due to the reversed signature of tertiary dykes. The Whin Sill, on the other hand, is observed to

'enhance' the width of the anomaly by producing a wide response (Cornwell and Evans, 1986, Bott, 1967). The Whin Sill is known to have intruded a wide area of northern Teesdale and where faults occur in it, magnetic anomalies have been observed. These anomalies vary, depending on the width of the fault and whether there is a vertical shift between the two sides of the faulted Sill.

Isostatic adjustment, after emplacement of the Sill, caused the faulted slabs of the intrusion to rise and fall at different horizons (Bott, 1967).This complicates the interpretation technique because the anomalies due to the different causative bodies cannot be separated. When a profile crosses an area where the Whin Sill is faulted, the anomaly observed depends on the magnetization at that point, the lateral shift and vertical displacement. The shape of the concave-up curve tends to have a lower shoulder on the down-thrown side. This has been observed in most of the profiles presented in this report (see fig.38).

However, if there is only demagnetization of the Whin at a particular locality across a traverse (white Whin), the anomaly will tend to be symmetrical provided that the magnetization is the same at both ends of the Whin. This has not been seen in any profile surveyed and it can be safely assumed that where the anomaly due to the Whin appeared, it was caused by faulting that was subsequently followed by uplift on one section of the Sill and/ or subsidence on the other. Fig.38 below represents models of the expected magnetic anomaly across a faulted Whin Sill.

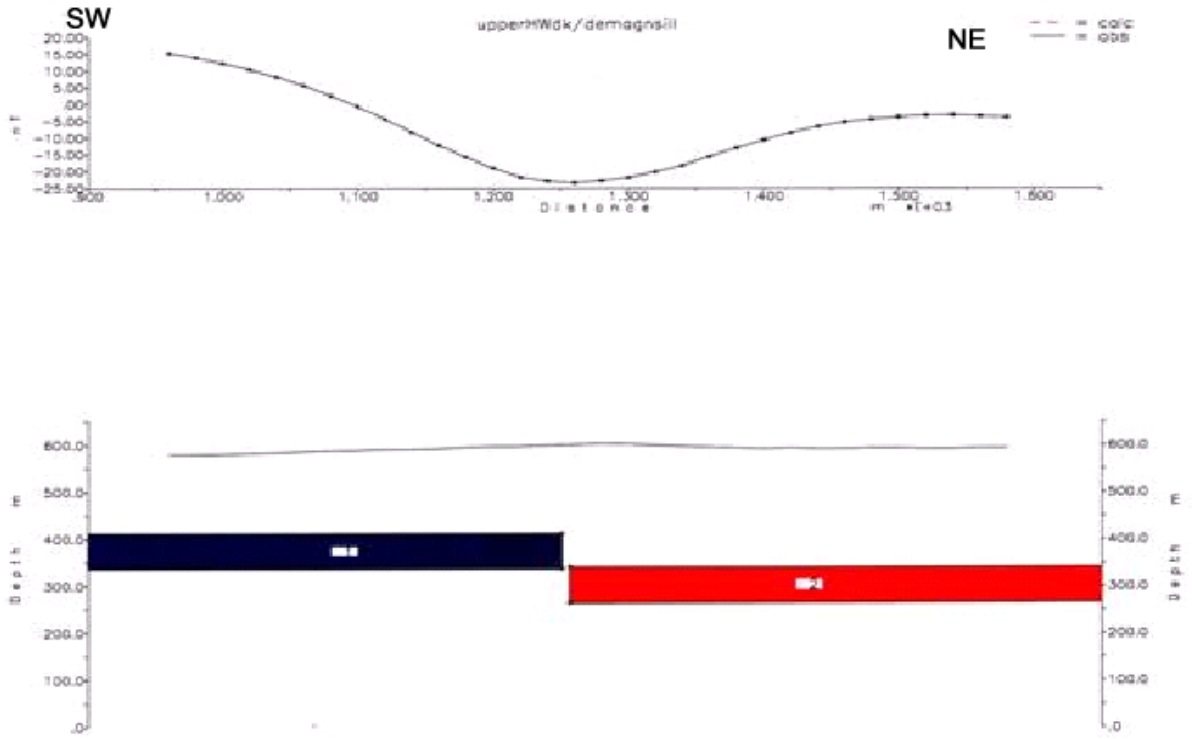

Fig.38 (a) Magnetic anomaly due to a faulted Whin Sill

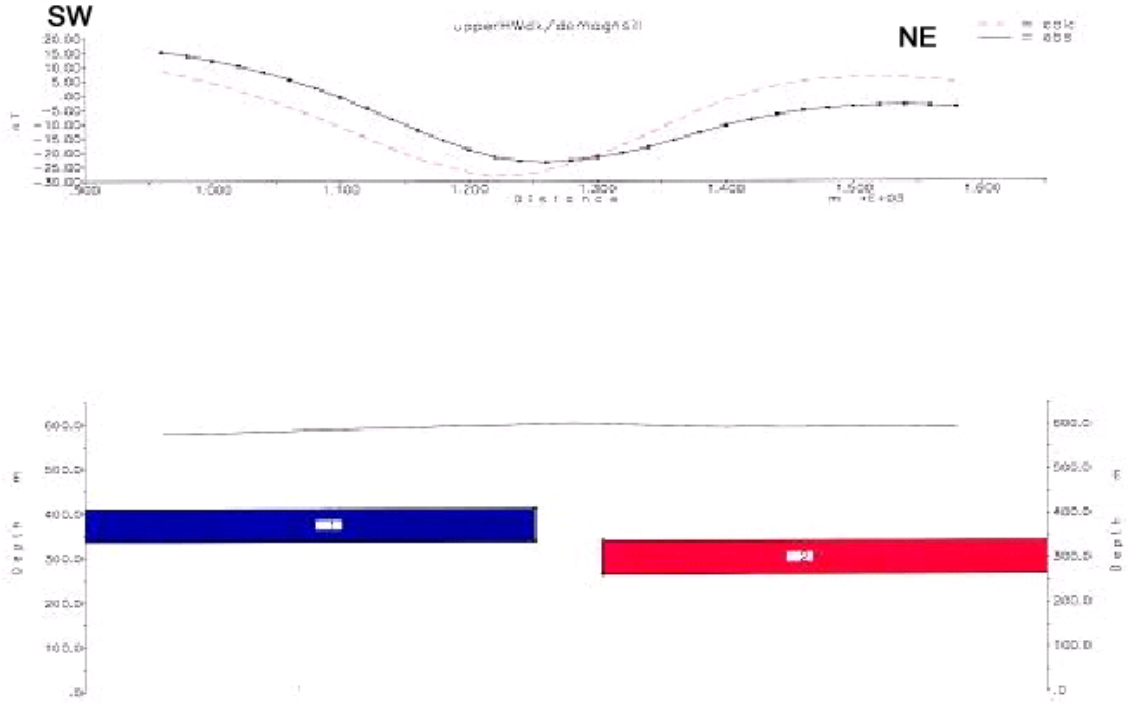

Fig.38 (b) Magnetic anomaly due to a faulted, displaced Whin Sill.

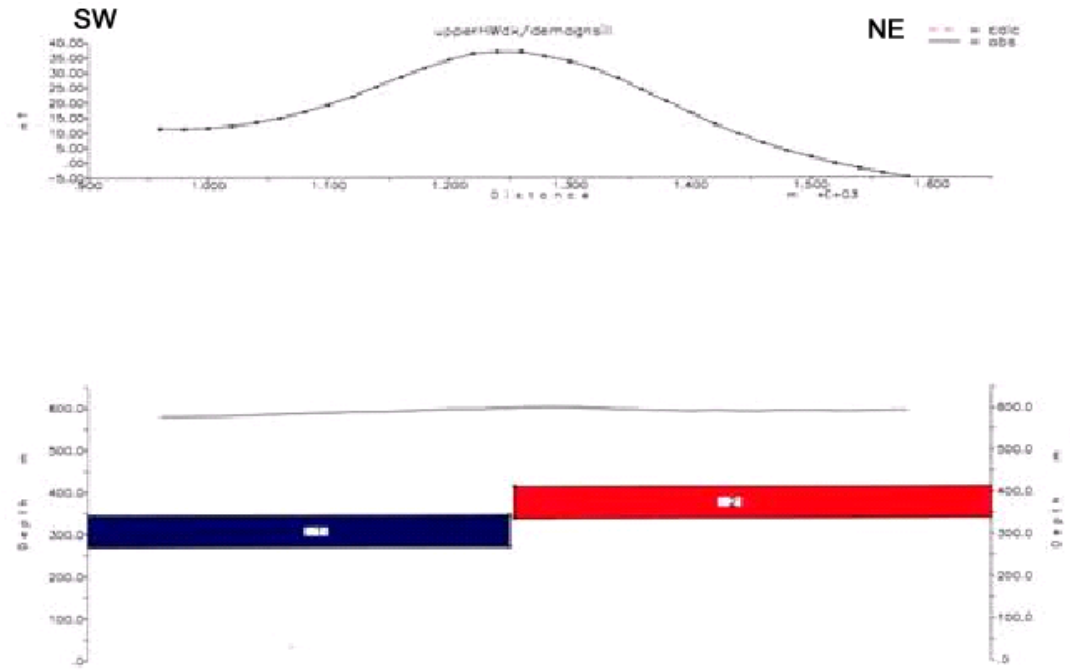

Fig.38 (c) Magnetic anomaly due to a reversely donthrown faulted Whin Sill.

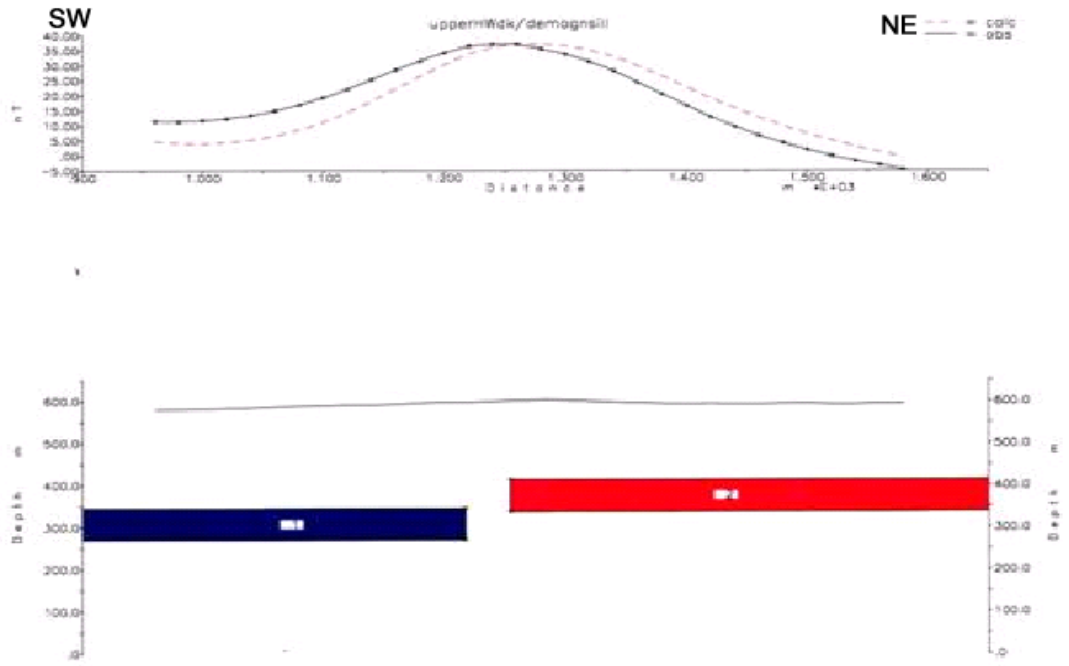

Fig.38 (d) Magnetic anomaly due to a displaced, reversely downthrown faulted Whin Sill.

Fig.38. Magnetic anomalies due to (a) Faulted Whin Sill, (b) faulted displaced Whin Sill, (c) reversely downthrown faulted Whin Sill and (d) laterally displaced reversely down-thrown faulted Whin.

6.2 Harwood area

Figure 39 below shows the various models interpreted at upper Harwood from survey profile no.6 located in figure 17. The traverse was made some 2km to the NW of Harwood valley to investigate the possible existence of a similar magnetic anomaly. The outcrop of the Cleveland dyke, 2km to the west of this area, gave a proposition that the same geological body continued in the subsurface.

The Whin Sill spreads all over the survey area at depth so the faulted Whin Sill model (fig.39 (a), and (b)) was tested as a possible cause for the anomaly encountered along this profile. While the parameters used in (a) are those experimentally arrived at by Cornwell and Evans (1986), the model does not give a match with the observed profile. The level of the Whin sill here is slightly above 500m a.s.l (fig. 36, table 6) giving it a depth-to-top of about 100m (Dunham, 1990).

When this 100m depth-to-top constraint is introduced in the model, the only likely match is obtained when the Sill is down-thrown in the reverse direction (i.e. NE, fig.39 (b)) but then a close fit could not be established. The most likely model here is a dyke. The parameters in fig.39(c) are plausible if the Tertiary dyke intruded the Allens Cleugh mineral vein/ fault, across which profile no.6 was made. The Vein is known to bear ores of Iron.

The Cleveland dyke out-crops about 2km away to the NW with a width of about 15m. The boulder clay and drift here contribute to the depth of the buried dyke; the drift has been determined to be over 50m in some areas (Burgess and Holliday, 1979). However, the presence of the Whin Sill can not be ignored and the most likely model representing this area is fig.39 (d) where both the Whin and dyke intruded. The calculated curve gives an acceptable fit and the geology agrees with this model.

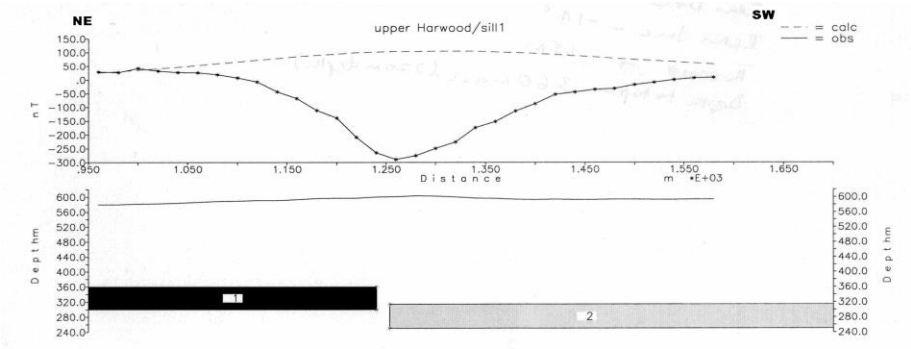

Fig.39 (a) ***Faulted Whin Sill model down- thrown to the SW. Depth-to- top: 220m, thickness: 65m, magnetic susceptibility: 0.025 (SI), remanent magnetization: 2.7 A/m, declination: 183º, remanent inclination: -14º***

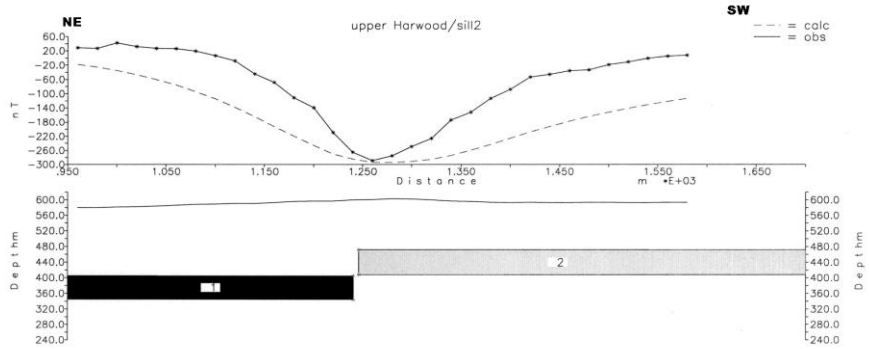

Fig.39 (b) ***Faulted Sill model down- thrown to the NE. Depth- to- top: 100m, thickness: 65m, magnetic susceptibility: 0.025 (SI), remanent magnetization: 4 A/m, declination: 183º, remanent inclination: 70º.***

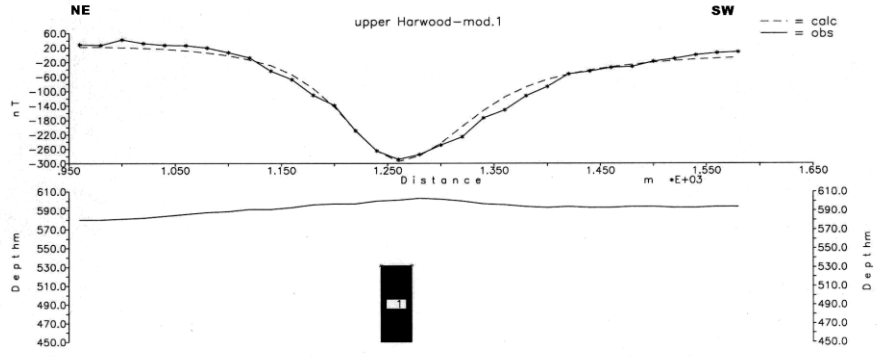

Fig.39 (c) A Dyke model. Depth-to-top: 50m, width: 20m, magnetic susceptibility: 0.02 (SI), remanent magnetization: 5A/m, declination: 153º, remanent inclination: -67º.

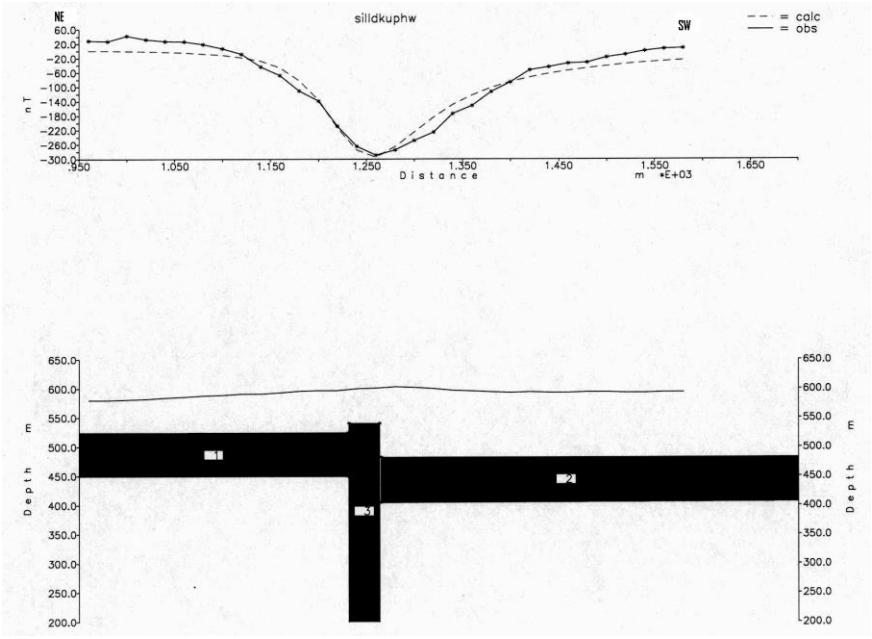

Fig.39 (d) A Dyke & Whin model. Whin:- Depth-to-top: 50m, thickness: 70m, magnetic susceptibility: 0.025 (SI), remanent magnetization: 2.7A/m, declination: 183º, remanent inclination: -14º. Dyke:- Depth-to-top: 30m, width: 25m, magnetic susceptibility: 0.02 (SI), remanent magnetization: 5A/m, declination: 153º, remanent inclination: -67º

Fig.39. 2.5D Magnetic modelling of profile no. 6 located in figure 17 at upper Harwood. Depth is in meters above sea level and the Sill in (a) & (b) extends to 1000m horizontally while the dyke in (c) and (d) extends to 1000m below the surface (assumed to be infinity).

About 2km south-east of profile 6 lies the Harwood valley where the magnetic survey was most intense. Several profiles are discussed below (fig.40). In these models it was assumed that the Whin extended to infinity horizontally while the Dyke dipped vertically to infinity with respect to the survey's dimensions.

The faulted Whin Sill model (fig.40 (a)) could not fit the observed curve even when the correct down-thrown side (fig.36), as well as the depth of the Sill, are used. The height above sea level of the Whin

here is about 350m (fig.36). Variations of the parameters, e.g. increasing or decreasing the magnetization and trading off with depth and/ or thickness could not match the calculated response with the observed curve. The calculated profile would either widen at the shoulders, or overshoot the base of the observed anomaly.

As seen in figure 40 (b) the dyke model here once again gives a matching calculated curve. The parameters given by Giddings and others (1972) require the dyke body to have a depth-to-the-top of 30m and a width of 15m (fig.40 (b)).

Figure 40 (c) gives a model of both the Whin and dyke intruding the Carboniferous sediments. The depth-to-top of the dyke at 30m seems agreeable with the geology. So does the Whin elevation at 350m above sea level. To the right, the surface geology confirms that the Whin Sill has been eroded over the years since intrusion.

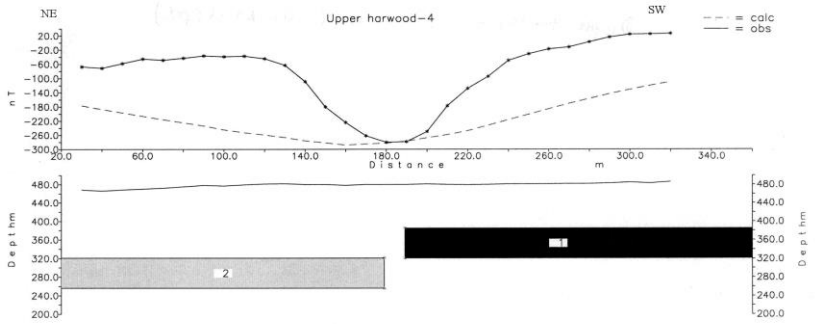

Fig.40 (a) Faulted Sill model down- thrown to the NE. Depth-to-top: 100m, thickness: 65m, magnetic susceptibility: 0.025 (SI), remanent magnetization: 2.7 A/m, declination: 183º, remanent inclination: -14º

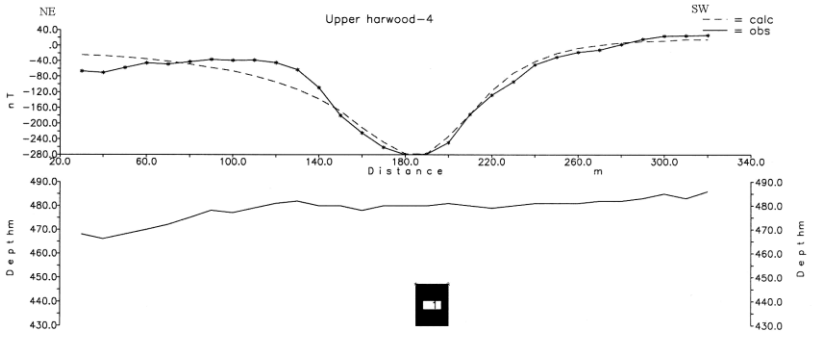

Fifg.40 (b) A Dyke model. Depth-to-top: 30m, width: 15m, magnetic susceptibility: 0.02 (SI), remanent Magnetization: 5A/m, declination: 153º, remanent inclination: -67º.

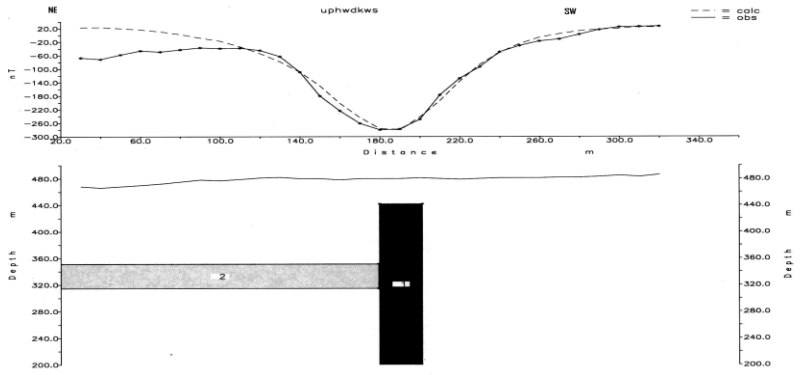

Fig.40 (c) A Dyke & Whin model. Whin Depth-to-top: 120m, thickness: 40m, magnetic susceptibility: 0.025 (SI), remanent Magnetization: 2.7A/m, declination: 183º, remanent inclination: -14º. Dyke Depth-to-top: 30m, width: 25m, magnetic susceptibility: 0.02 (SI), remanent Magnetization: 5A/m, declination: 153º, remanent inclination: -67º.

Fig.40. 2.5D Magnetic modelling at Harwood. The model is of profile no. 11 in fig. 17. The Whin is assumed to extend to infinity while the same applies to the dyke in (b) & (c) at depth. The Sill appears to have undergone erosion on the SW portion (right of part (c)).

Fig.41 below shows more modelling at Harwood valley. The models are from magnetic profile no. 14 located in fig.17, about 800m from profile 11 above. The faulted Whin here is considered in both (a) and (b) to bear the same magnetic parameters and only the depth of the intrusion is varied. As the Sill gets shallower, the calculated curve gets more distorted. Trading off values of magnetization, thickness

and susceptibility always led to a non-conforming calculated plot, leading to a conclusion that the Whin Sill is not the only likely cause of the anomaly encountered along this profile in the Harwood valley.

A dyke model was tried and the parameters presented by Giddings and others (1972) gave an almost perfect match, save for a few spikes due to subsurface variations in the observed plot (Fig.41 (c)). The depth to the top of the dyke (35m) was very close to that calculated in a nearby profile and the width of 12m obtained here agrees with the records from the old mining plans.

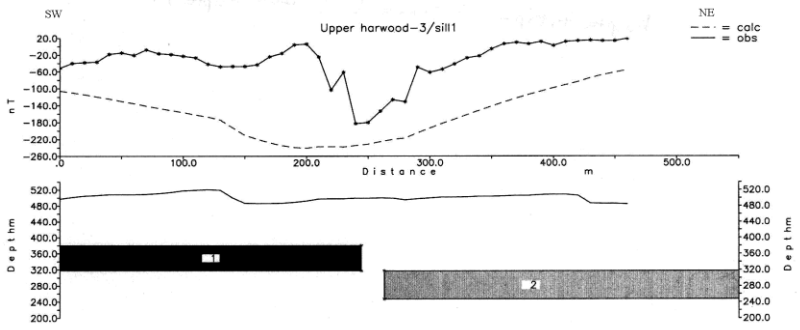

Fig.41 (a) Faulted Sill model with a NE downthrow. Depth-to-top:160m, thickness: 65m, magnetic susceptibility: 0.025 (SI), remanent magnetization: 2.7 A/m, declination: 183º, remanent inclination: -14º

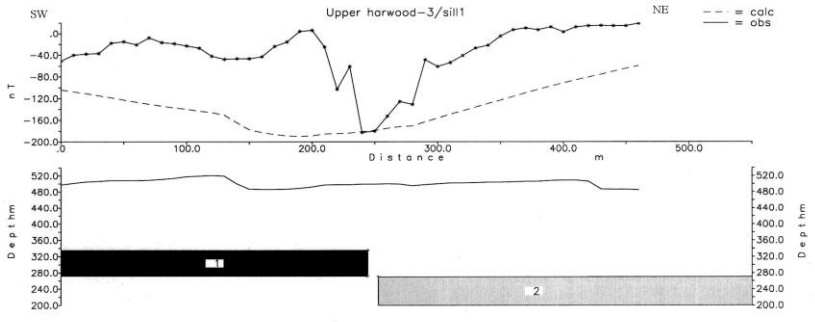

Fig.41 (b) Same model as (a) above but at a deeper Whin level. Depth-to-top: 140m, thickness: 65m, magnetic susceptibility: 0.025 (SI), remanent magnetization: 2.7 A/m, declination: 183º, remanent inclination: -14º

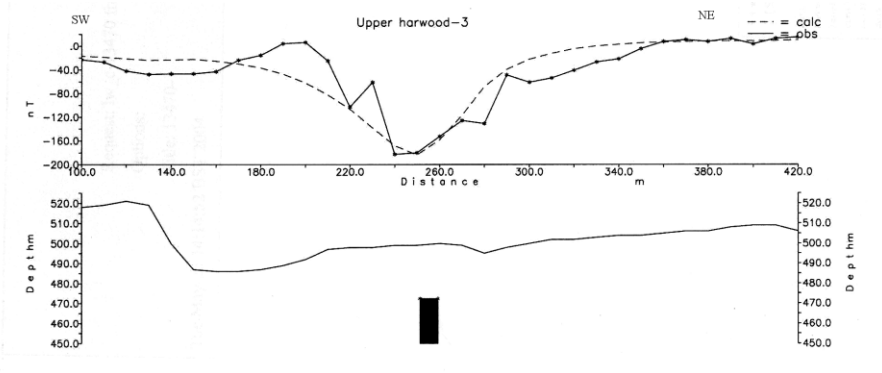

Fig.41 (c) Dyke model across the Harwood valley. Depth-to-top: 35m, width: 12m, magnetic susceptibility: 0.02 (SI), remanent magnetization: 5A/m, declination: 153º, remanent inclination: -67º

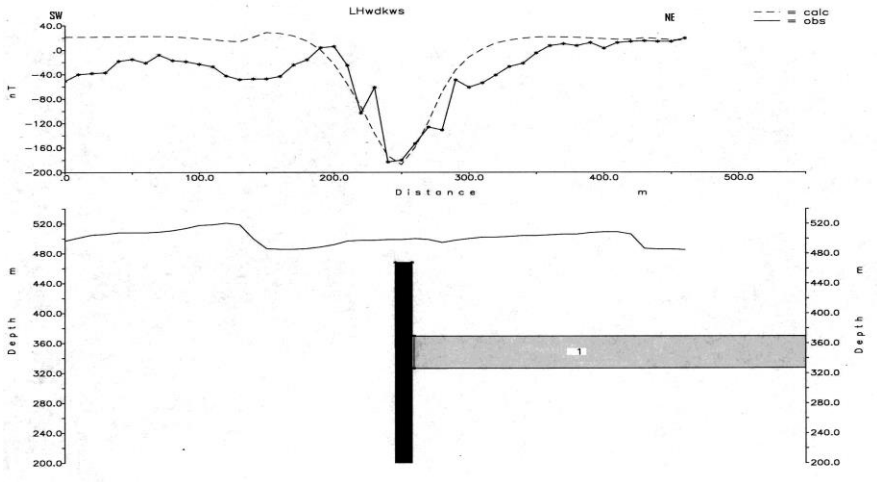

Fig.41 (d) Dyke & Whin model across the Harwood valley. Whin Depth-to-top: 120m, thickness: 40m, magnetic susceptibility: 0.025 (SI), remanent magnetization: 2.7A/m, declination: 183º, remanent inclination: -14º. Dyke Depth-to-top: 25m, width: 15m, magnetic susceptibility: 0.02 (SI), remanent magnetization: 5A/m, declination: 153º, remanent inclination: -67º.

Fig.41. Magnetic modelling of profile no. 14 located in fig.17 at upper Harwood. Extent of the Whin and Dyke are assumed to be to infinity with respect to the survey dimensions. The Whin is eroded on the left hand side (SW)

Fig.41 (d) shows a combination of both the Whin Sill and dyke in the model. The magnetic parameters mentioned earlier were used and the calculated curve gave a good match. The model is more realistic as the Whin is known to exist in the subsurface and the dyke model alone will not geologically hold. Depth to the top of the Whin at 350m above sea level here (as in figure 40 (c)) agrees with the geology

while the dyke buried depth of about 25m and thickness of 15m is consistent with neighbouring profile models.

Mine plans obtained from old records at the Raby Castle in Middleton-In-Teesdale indicate that the miners encountered a 'Whin Rock' at a depth of about sixteen 'fathoms' (~ 30m) from the surface at Lady's rake mine. They apparently circumnavigated above the rock and gave it an approximate thickness of 12m (fig. 42). This 'hard' rock is interpreted as a dyke in the next chapter.

Fig.42. Mine drawing showing a 12m wide intrusive 'hard' rock encountered by 19th century miners near Lady's Rake mine

Figure 43 below illustrates magnetic modelling of profile 15 (fig.17) at lower Harwood. When the magnetic parameters given by Cornwell and Evans (1986) were used for the faulted Whin in (a), the

calculated response was inverted with respect to the observed curve. For the calculated and observed curves to match, an attempt was made to alter the inclination and depth of intrusion (Fig.43 (b)).

This did not yield the desired effect even after laborious manipulation of other significant parameters. The dyke model in fig.43 (c), however, gave a near- perfect overlap, again where the width of the dyke was introduced as 12m at a depth of 40m.

On introducing both the Whin and the tertiary dyke as models causing the anomaly, a balance is struck where the depth to the top of the Whin is about 395m with a 40m width. The dyke, on the other hand, has a thickness of about 10m and its depth is at about 25m below the surface.

All the dyke parameters in Harwood seem to agree with the results of sampled specimens obtained in the Upper Teesdale by Giddings and others (1972). The depth to the top of the body can be explained by the cover of boulder clay and drift that was deposited during the Ice Age when moraine debris swept down the Harwood valley.

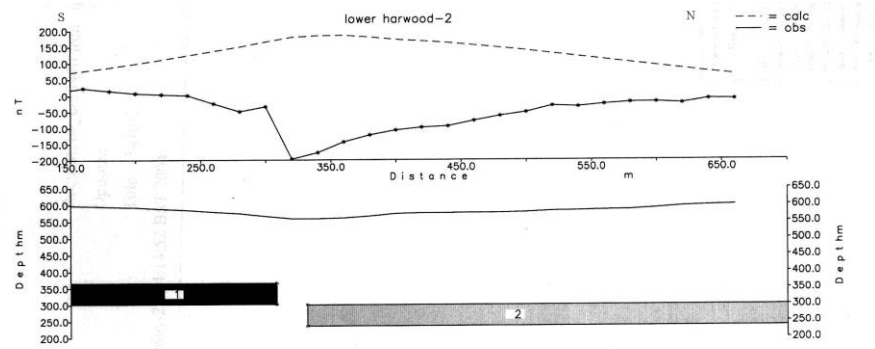

Fig.43 (a) A Faulted Whin Sill model at lower Harwood. Depth-to-top: 220m, thickness: 65m, magnetic susceptibility: 0.025(SI), remanent magnetization: 2.7 A/m, declination: 183º, remanent inclination: -14º

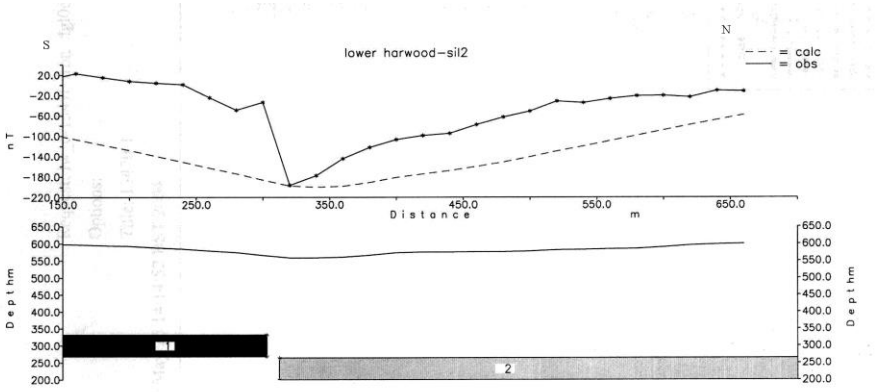

Fig.43 (b) Faulted Sill. Depth-to-top: 240m, thickness: 65m, magnetic susceptibility: 0.025 (SI), remanent magnetization: 2.7 A/m, declination: 183º, remanent inclination: 70º

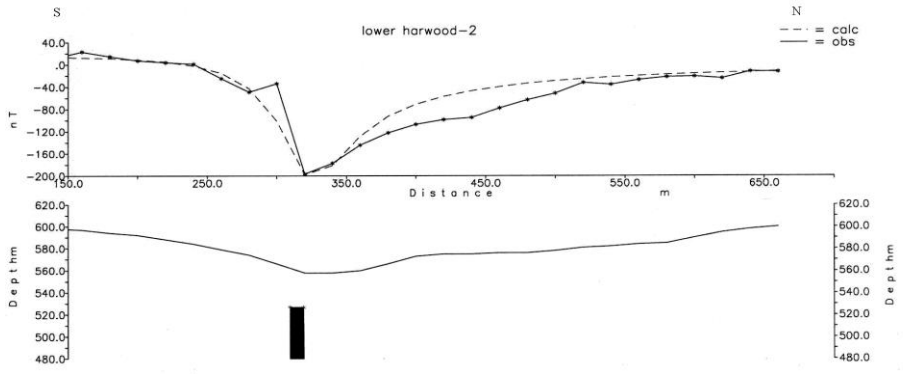

Fig.43(c) Dyke model at lower Harwood. Depth-to-top: 40m, width: 12m, magnetic susceptibility: 0.02 (SI), remanent magnetization: 5A/m, declination: 153º, inclination: -67º.

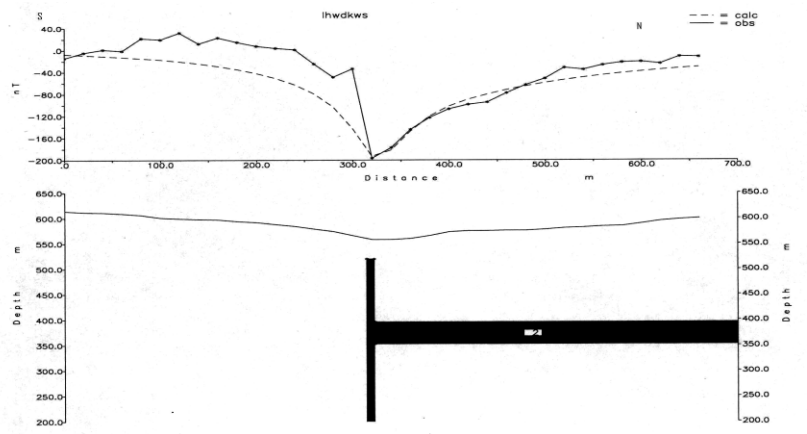

Fig.43 (d) Dyke & Whin Sill model at lower Harwood.Whin depth-to-top: 170m, thickness: 40m, magnetic susceptibility: 0.025 (SI), remanent magnetization: 2.7A/m, declination: 183º, inclination: -14º. Dyke depth-to-top: 25m, width: 10m, magnetic susceptibility: 0.02 (SI), remanent magnetization: 5A/m, declination: 153º, inclination: -67º

Fig.43. Magnetic modelling of profile no.15 (fig.17) at Lower Harwood. The dyke model extends to infinity downwards. The Whin suffered erosion to the south of the profile (left of fig.43 (d))

6.3 Langdon Beck area

This survey area is located at a very geologically complex zone and the modelling in the GRAVMAG program required much human intervention. The profiles featured here were acquired from zones of varying topography and geological formations, i.e. some of the traverses were surveyed across the Teesdale fault, others across both the Burtreeford disturbance and the Teesdale fault while other profiles were surveyed away from both features.

Figure 44 below displays modelling of profile no.16 (see fig.17) from the same zone as profile 15 above but located some 800m to the SE.

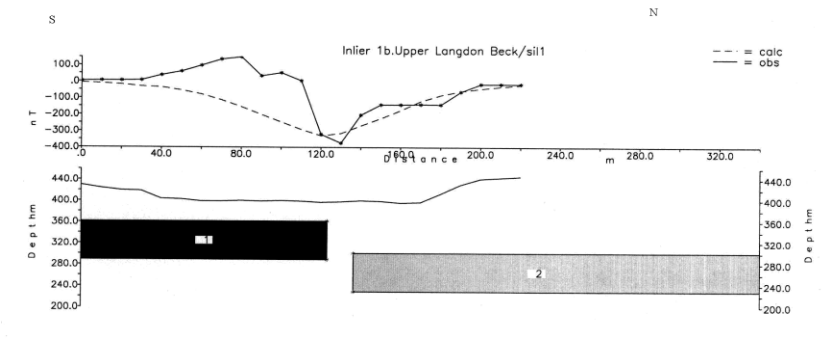

Fig.44 (a) Faulted Whin Sill. Depth-to-top: 40m, thickness: 65m, magnetic susceptibility: 0.025 (SI), remanent magnetization:2.7 A/m, declination: 183º, remanent inclination: -14º

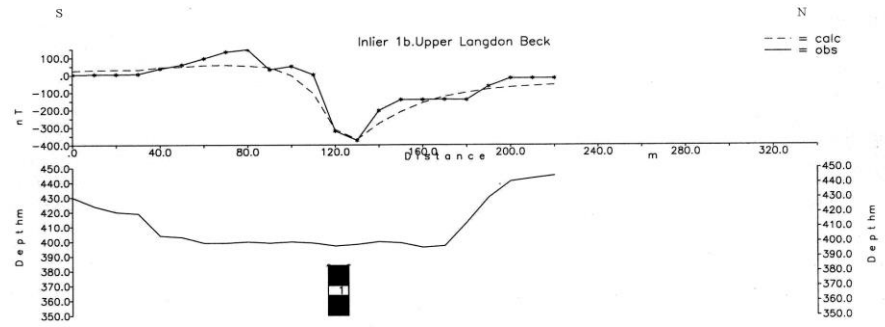

Fig.44 (b) Dyke model. Depth-to-top: 15m, width: 12m, magnetic susceptibility: 0.02 (SI), remanent magnetization: 5A/m, declination: 153º, remanent inclination: -67º.

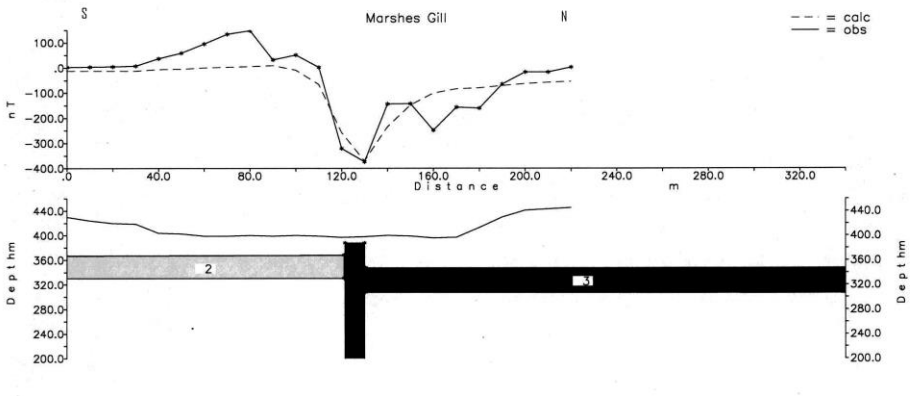

Fig.44 (c) Dyke & Whin model. Whin Depth-to-top: 50m, thickness: 40m, magnetic susceptibility: 0.025 (SI), remanent magnetization: 2.7A/m, declination: 183º, remanent inclination: -14º. Dyke Depth-to-top: 10m, width: 12m, magnetic susceptibility: 0.02 (SI), remanent magnetization: 5A/m, declination: 153º, remanent inclination: -67º.

Fig.44. 2.5D magnetic modelling of profile no.16 (see fig.17) at Upper Langdon Beck. Both the tertiary dyke and the Whin Sill extend to infinity in depth and laterally respectively.

The faulted Whin Sill Model in fig.44 (a) above gave a typical response in the calculated curve. This is the general anomaly curve expected due to a faulted Whin (Cornwell and Evans, 1986). There is a known Whin outcrop slightly to the south-east of this profile (2.25ºW, 54.64ºN) at about 400m above sea level (see fig.36). Nevertheless the calculated curve could not fit the observed plot.

The dyke model, on the other hand, gave a more likely match to the observed plot, using the parameters given by Giddings et al (1972). Depth to the top of dyke was approximately 15m, the width being 12m. But the satisfactory model was obtained when both the Whin and dyke were introduced together in fig.44 (c), still using the parameters by Cornwell and Evans (1986) and Giddings et al (1972).

Figure 45 below illustrates further modelling undertaken at Langdon Beck. The modelling is that of profile no. 17 in fig.17. The general topography beyond the profile dimension here appears to match the geological controls, giving the up-thrown side of the faulted Whin Sill a higher elevation, contrary

to some southern sections where drift has, over the years, filled up the down-thrown slab to the level of the other.

The profile considered here is one of the three that were surveyed three hundred meters from each other at upper Langdon Beck. They all gave a similar magnetic response with respect to intensity, position and magnitude. The Sill model considered in fig.45 (a) could not fit the calculated curve on the observed data when the parameters given by Cornwell and Evans (1986) were used. A vertical off-set for the Whin is achieved by using the available structural geological information. A variation of the inclination parameter in (b) was necessary to return a closer fit for the calculated curve from its reverse state. However, this could not raise the curve higher towards the SW shoulder as required. Efforts to balance all the other constraints like depth of the Whin Sill, thickness and declination were frustrated by the inability of the calculated response to match the observed data.

The dyke model in (c) gave a good indicator on the first trial, using the values given by Giddings and others (1972). When both the Whin and dyke were modelled, a more realistic response was observed (fig. 45(d)). Though the NE side could not be fitted accurately with the observed curve, this appeared to represent the expected subsurface. The model, for the sake of simplicity, depicts both faulted slabs of the Whin as having the same thickness. Lee (1978, unpublished) reports a lot of erosion of the Whin boulders found in this area

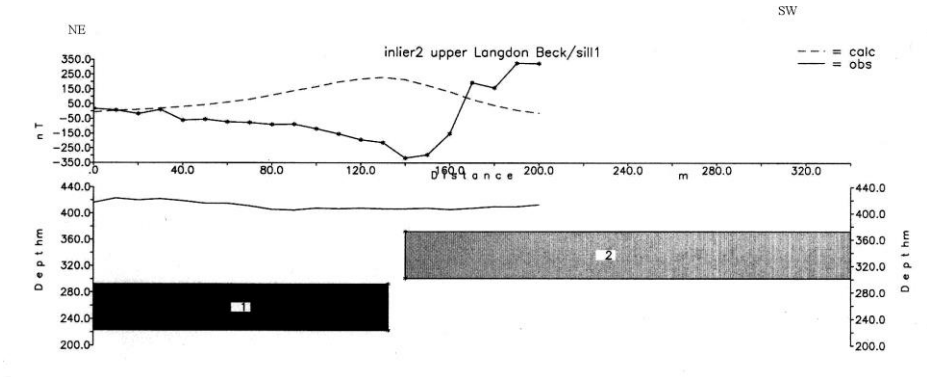

Fig.45 (a) Whin model at upper Langdon Beck. Depth-to-top: 30m, thickness: 65m, magnetic susceptibility: 0.025 (SI), remanent magnetization: 2.7 A/m, declination: 183º, remanent inclination: -14º

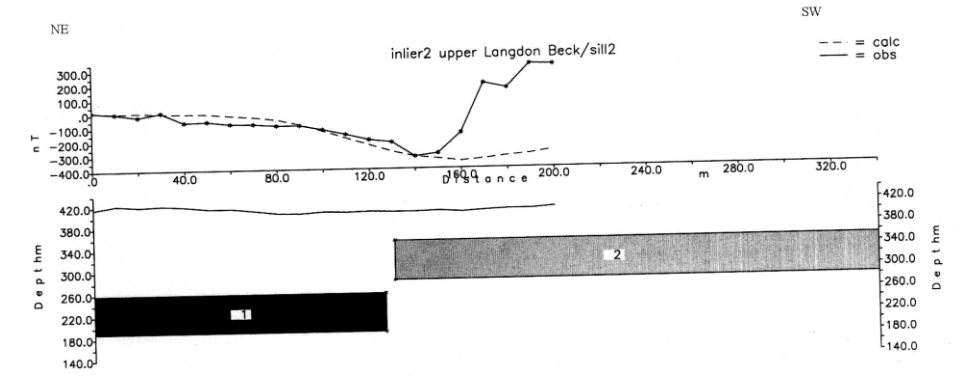

Fig.45 (b) Faulted Sill. Depth-to-top: 65m, thickness: 65m, magnetic susceptibility: 0.025 (SI), remanent magnetization: 2.7 A/m, declination: 183º , remanent inclination: 110º.

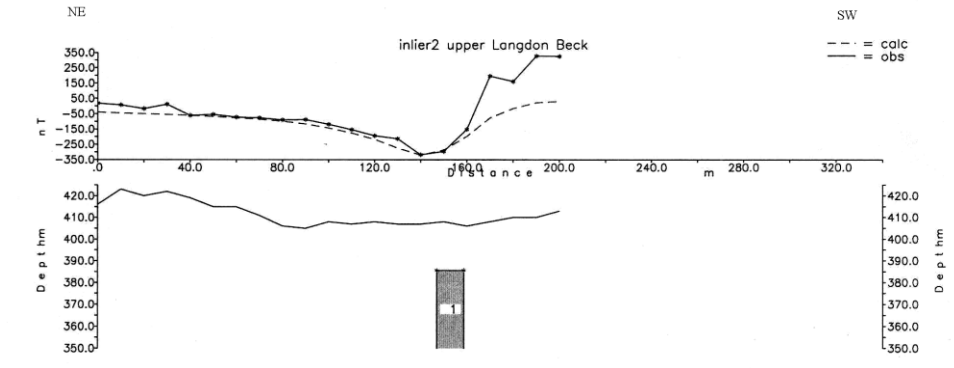

Fig.45 (c) Dyke model at upper Langdon Beck. Depth-to-top: 20m, width: 15m, magnetic susceptibility: 0.02 (SI), remanent magnetization: 5A/m, declination: 153º, remanent inclination: -67º.

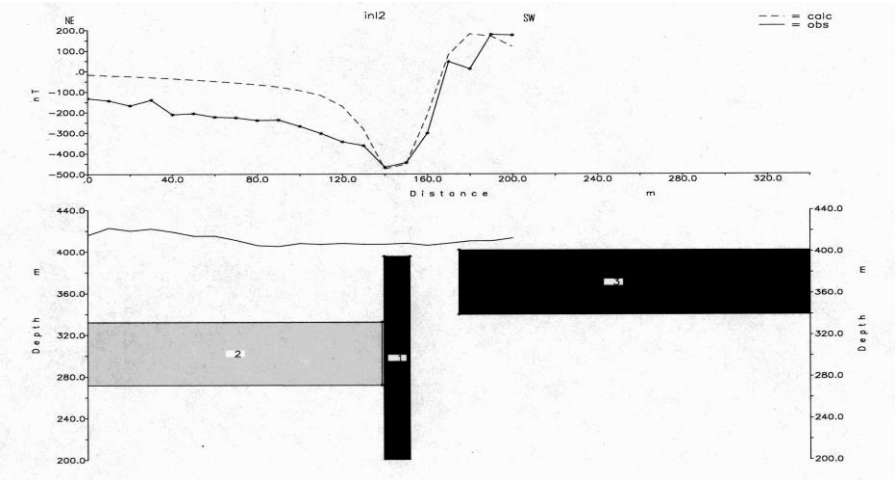

Fig.45 (d) Dyke & Whin model at upper Langdon Beck. Whin Depth-to-top: 14m, thickness: 60m, magnetic susceptibility: 0.025 (SI), remanent magnetization: 2.7A/m, declination: 183º, remanent inclination: -14º. Dyke Depth-to-top: 15m, width: 15m, magnetic susceptibility: 0.02 (SI), remanent magnetization: 5A/m, declination: 153º, remanent inclination: -67º.

Fig.45. 2.5D Magnetic of profile no. 17 in fig. 17 modelling at upper Langdon Beck. The modelled bodies extend to infinity laterally and downwards.

Fig.46 below displays modelling of profile no. 23 (fig.17) at Langdon Beck. This is one of the longest traverses surveyed in this area. It starts at the top of the 'fold' axis just beyond the road junction to Weardale and cuts across the Burtreeford disturbance before crossing the Teesdale fault. For the sake of simplifying the modelling, only a section of the profile is considered in preliminary figures though the whole traverse is presented in the last model.

The calculated curve of the faulted Whin Sill Model in (a) appears reversed in comparison with the observed data. When the inclination and depth to the top is altered in (b), the calculated response changes signature at some point but does not fit the observed profile well. Variations in inclination angle only managed to raise one 'shoulder' above the other. The nature of the magnetic anomaly here differs from profiles made in other zones due to the presence of the Burtreeford disturbance. However,

the anomaly size and signature was still maintained as in other areas, suggesting that the causative event could have been post Permian. The dyke model in (c) gave a better fit to the observed data with a depth to the top of 30m and a 15m width; though again the magnetic high to the SW end of the plot introduced another complication.

In fig.46 (d) the entire profile is modelled using several bodies that could possibly give rise to the observed anomalies. Here there is a possibility that the Tertiary dike forms a branch to the East and at the same time continues southwards along the Teesdale fault (see fig.30). The survey station at 650m (fig.46 (d)) indicates a clear reversed anomaly. Another similar anomaly is also seen at station 900m and yet another one at 1350. It is not difficult to distinguish the first and last anomaly as possibly belonging to the same type of dyke but may be at different depth and/or thickness.

On the other hand, the 'wider' anomaly at station 900m is most likely due to a faulted Whin down-thrown to the NE. Due to the presence of the Burtreeford disturbance here, it is difficult to impose more bodies just for the purpose of fitting the middle section of the calculated response. All the same, the Burtreeford Disturbance itself clearly appears as a magnetic high in some sections.

Fig. 47 below displays modelling of profile no. 28 (fig.17). The faulted Sill model in (a) could not fit the observed curve after a series of parameter variations. The nearest fit was obtained when the Whin was assumed to be at a depth of 180m with a remanent inclination of -160º. The Sill, however, outcrops in the SW part of the traverse and this remanent inclination is unrealistic. The dyke model in (b) tends to match the observed data. The parameters used to arrive at this model were agreeable with the

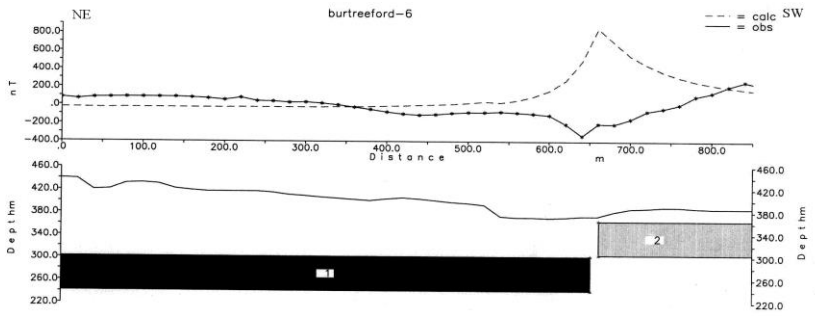

Fig.46 (a) Faulted Whin Sill. Depth-to-top: 0m (exposed), thickness: 65m, magnetic susceptibility: 0.025 (SI), remanent magnetization: 2.7 A/m, declination: 183º, remanent inclination: -14º

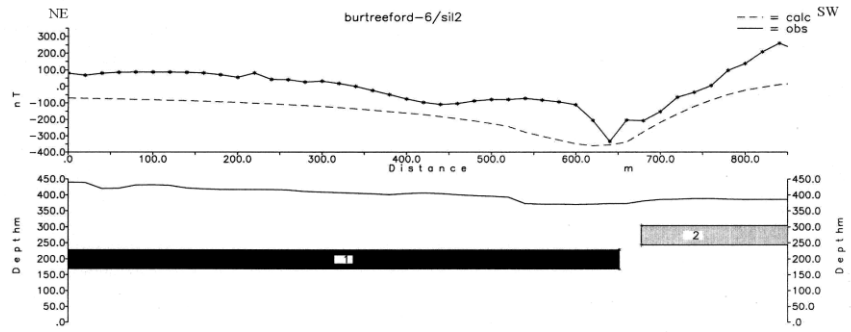

Fig.46 (b) Faulted Sill, depth-to-top: 80m, thickness: 65m, magnetic susceptibility: 0.025 (SI), remanent magnetization: 2.7 A/m, declination: 183º, remanent inclination: 0º.

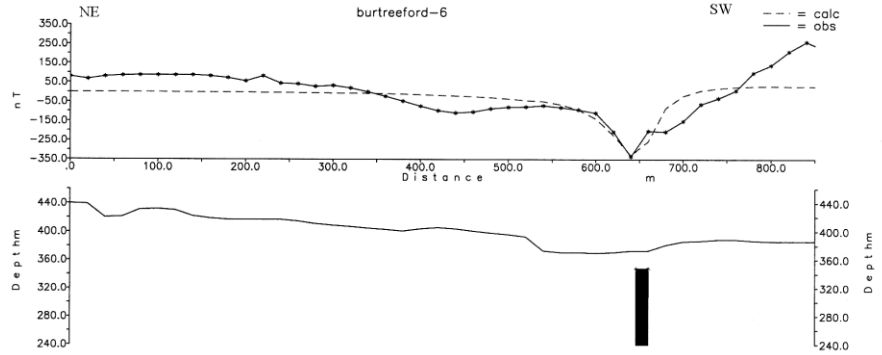

Fig.46 (c) Dyke model; depth-to- top: 30m, width: 15m, magnetic susceptibility: 0.02 (SI), remanent magnetization: 5A/m, declination: 153º, remanent inclination: -67º.

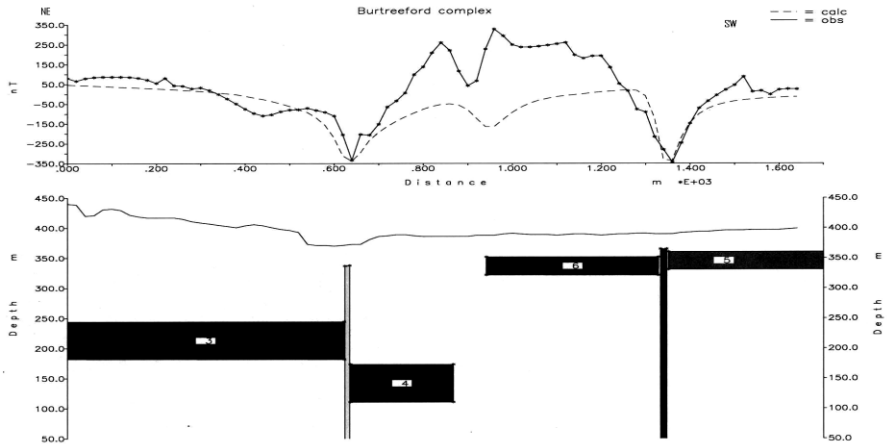

Fig.46 (d) Dyke & Whin model. Whin depth-to- top: 35m, thickness:30m, magnetic susceptibility: 0.025 (SI), remanent magnetization: 2.7A/m, declination: 183º, remanent inclination:-14º. Dyke depth-to-top: 30m, width:20m, magnetic susceptibility: 0.02 (SI), remanent magnetization: 5A/m, declination: 153º, remanent inclination:-67º.

Fig.46. 2.5D magnetic modelling of profile no. 23 (fig.17) at Langdon Beck. As in previous models, the anomaly causative 'bodies' are assumed to extend to infinity. Part (d) represents the whole traverse and the possible sub-surface formations.

geology of the area though the depth and width of the dyke seem to be slightly more than expected. The last figure (c) gives a better explanation of the anomaly occurring here. The tertiary dyke still plays a major role in fitting the calculated curve even though it appears to be deeper here than anywhere else surveyed. A narrower and shallower dyke model produced a distorted calculated curve when tried. The level of the Whin here agrees with the expected intrusion level, giving this model the best fit compared to the previous two (i.e. (a) & (b)).

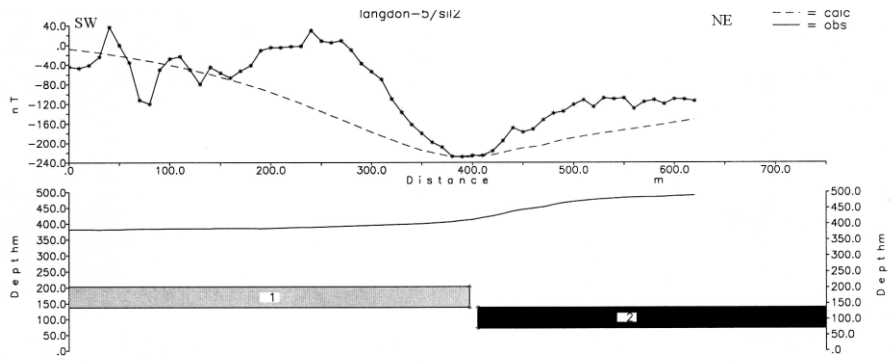

Fig.47 (a) Faulted Whin Sill at a depth-to-top: 180m, thickness: 65m, magnetic susceptibility: 0.025 (SI), remanent magnetization: 2.7 A/m, declination: 183º, remanent inclination: 70º.

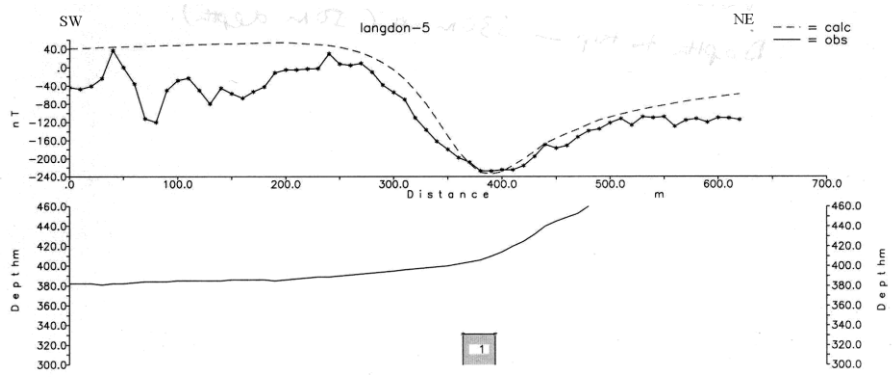

Fig.47 (b) A Dyke model at depth-to-top: 50m, width: 25m, magnetic susceptibility: 0.02 (SI), remanent magnetization: 5A/m, declination: 153º, remanent inclination: -67º.

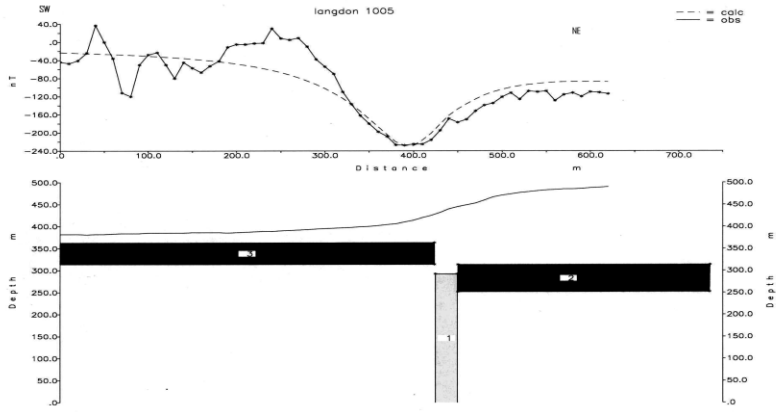

Fig.47 (c) A Dyke & Whin model. Whin model at depth-to-top: 20m, width: 50m, magnetic susceptibility: 0.025 (SI), remanent magnetization: 2.7A/m, declination: 183º, remanent inclination: -14º. Dyke model at depth-to-top: 100m, width: 20m, magnetic susceptibility: 0.02 (SI), remanent magnetization: 5A/m, declination: 153º, remanent inclination: -67º

Fig.47. 2.5D magnetic modelling of profile no. 28 (fig.17) at lower Langdon Beck. The dyke and Whin model give a more geologically acceptable interpretation with both bodies extending to infinity.

6.4 Etters Gill area

Five traverses were surveyed at Ettersgill but only two profiles will be considered here. At this particular site, the Whin Sill is known to be cut by the Cleveland dyke (Giddings and others, 1972, Burgess and Holliday, 1979, Dunham, 1990) at a river bed (long. 2.178º W, lat. 54.664º N). The geological map (fig.32) shows a narrow outcrop of the Whin cut at right angles by the Cleveland dyke. Thin sections of both the rocks from this site were viewed under the microscope (see next chapter) and there exists a marked difference in the grain size between them (Dunham, 1990).

Figure 48 below represents three models of profile no.34 (fig.17); one (a) for the faulted Whin Sill another (b) for the Cleveland dyke and the third model (c) representing both the Whin and dyke in contact. As presented in the geology (chapter 2), the Whin Sill intruded earlier (Permian) than the Cleveland dyke (Tertiary). In this locality, the dyke intruded a fault that separated the Whin in to north

and south sections. In Model (b) the dyke is assumed to have heated the Whin to levels beyond the curie temperature of magnetite (580-590ºC) during intrusion and, while cooling, the Whin acquired the dyke's magnetic properties, degrading with distance away from contact. The faulted Sill model in (a) could not fit the observed curve, given that the thickness of the Sill here (69m) and the depth to top (340m a.s.l) are known (Burgess and Holliday, 1979). The laboratory obtained parameters from Cornwell and Evans (1986) acted as controls in addition to the known geology and the acceptable dyke model in (b) gave a depth to the top of 15m and a thickness of 15m.

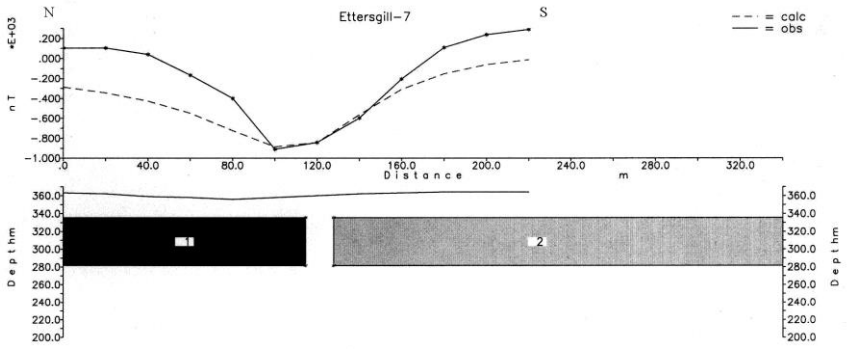

Fig.48 (a) Faulted Whin Sill. Depth-to-top: 25m, thickness: 65m, magnetic susceptibility: 0.025 (SI), remanent magnetization: 2.7 A/m, declination: 183º, remanent inclination: -14º.

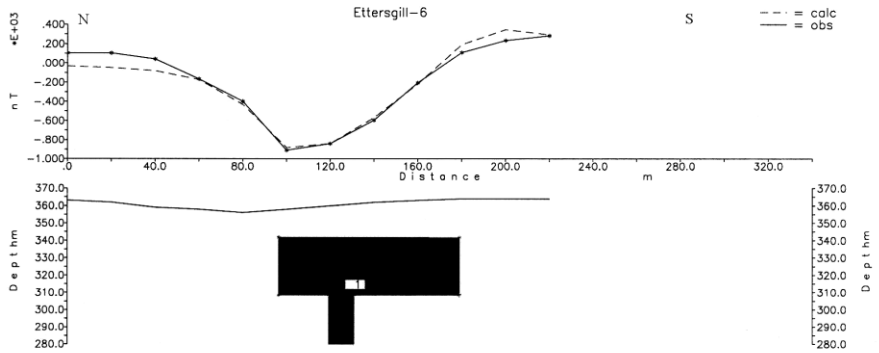

Fig.48 (b) Dyke model at a depth-to-top: 15m, width: 15m, magnetic susceptibility: 0.02 (SI), remanent magnetization: 5A/m, declination: 153º, remanent inclination: -67º.

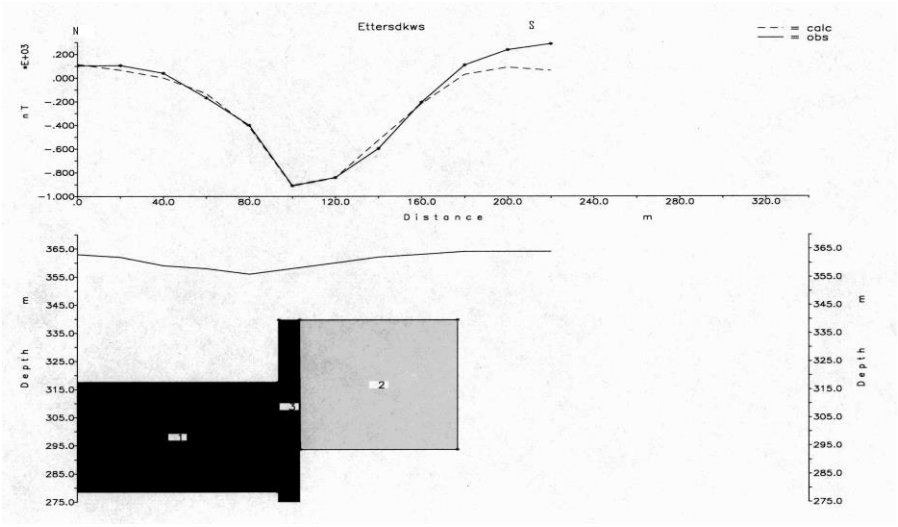

Fig.48 (c) Dyke & Whin model. Whin depth-to-top: 15m, thickness: 40m, magnetic susceptibility: 0.025 (SI), remanent magnetization: 2.7A/m, declination: 183º, remanent inclination: -14º. Dyke depth-to-top: 15m, width: 12m, magnetic susceptibility: 0.02 (SI), remanent magnetization: 5A/m, declination: 153º, remanent inclination: -67º.

Fig.48. 2.5D magnetic modelling of profile no.34 (fig.17) at Etters Gill. As in most of the area surveyed, the Whin contributes to the observed anomaly but is seen here to have been in direct contact with the intruding dyke, giving a more interesting interpretation challenge. The southern slab of the Whin in (c) does not extend to infinity as the northern section or the dyke. It is probably off-set due to isostatic uplift.

However, model (c) of both the dyke and Whin depicts the latter with a thickness of 40m and a northern down-throw of about 20m. This model offers the best interpretation of the profile since the northern Whin slab can be explained by erosion, and the calculated curve gives a good fit; especially in the northern side.

Figure 49 below displays modelling of profile no.35 (fig.17) at Etters Gill. This profile was made a distance of about 100m to the east of traverse no.34 at a slightly higher altitude. Parameters for the

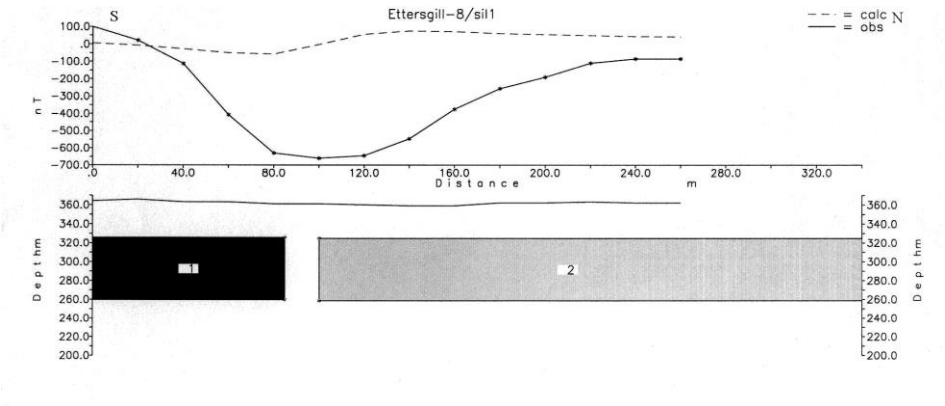

Fig.49 (a) Faulted Whin Sill. Depth-to-top: 35m, thickness: 65m, magnetic susceptibility: 0.025 (SI), remanent magnetization: 2.7 A/m, declination: 183º, remanent inclination: -14º.

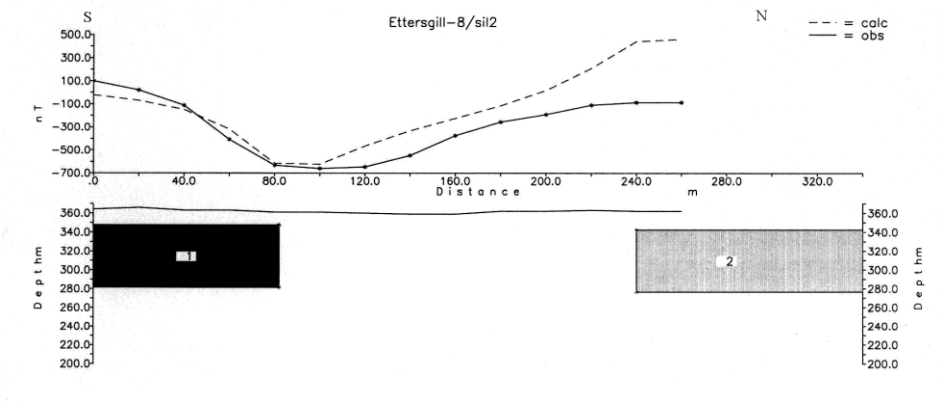

Fig.49 (b) Faulted Whin Sill, depth-to-top: 10m, thickness: 65m, magnetic susceptibility: 0.025 (SI), remanent magnetization: 2.7 A/m, declination: 183º, remanent inclination: -14º.

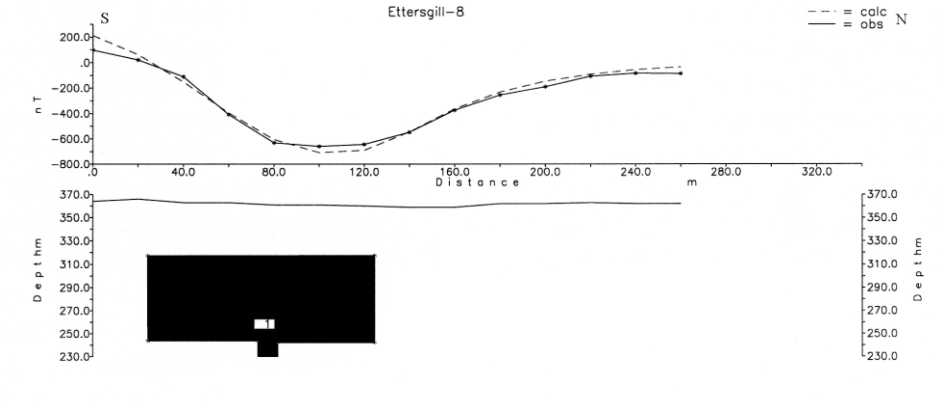

Fig.49 (c) Dyke model with re-magnetized Whin, depth-to-top: 40m, width: 12m, magnetic susceptibility: 0.02 (SI), remanent magnetization: 5A/m, declination: 153º, remanent inclination: -67º.

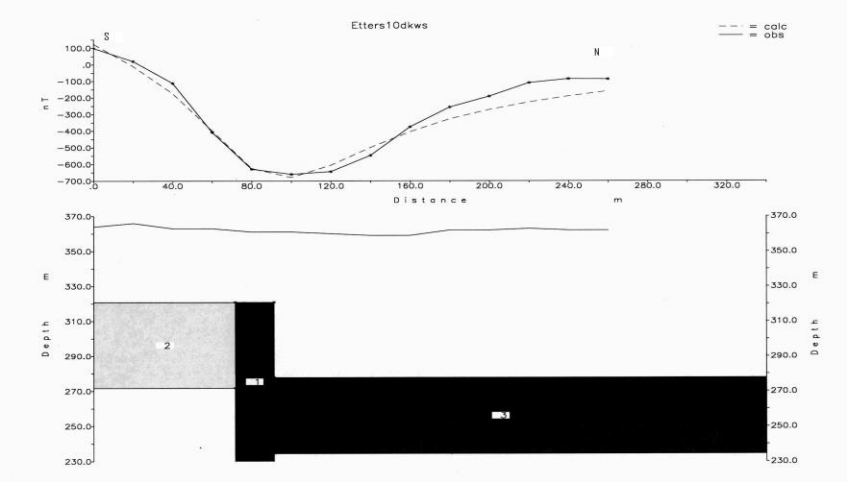

Fig.49 (d) Dyke & Whin model. Whin depth-to-top: 40m,thickness: 50m, magnetic susceptibility: 0.025 (SI), remanent magnetization: 2.7A/m, declination: 183º, remanent inclination: -14º. Dyke depth-to-top: 40m, width: 18m, magnetic susceptibility: 0.02 (SI), remanent magnetization: 5A/m, declination: 153º, remanent inclination: -67º.

Fig.49. 2.5D magnetic modelling of profile 35 (fig.17) at Etters Gill. The magnetic bodies extend to infinity both laterally and in depth, but the southern slab of the Whin extends to only 180m from the dyke contact.

faulted Whin were varied in order to match the observed curve without success. Although a close match could be realized when the demagnetized zone was exaggerated to 160m (Fig.49 (b)), this was not practical given the known geology of the area. The Whin (fig.31) is known to be in contact with the Cleveland dyke and the assumption of such a large de-magnetization area is inconsistent with the fact that the dyke here has a width of only 14m (Dunham, 1990). At the same time there was no better fit for the calculated curve after varying the depth, width and displacement of the Whin slabs.

The model in Fig.49 (c) gave a better fit by considering, as in figure 48, that the dyke re-magnetized the Whin during intrusion with its reversed magnetization with respect to the present earth's magnetic field. (See fig.50).

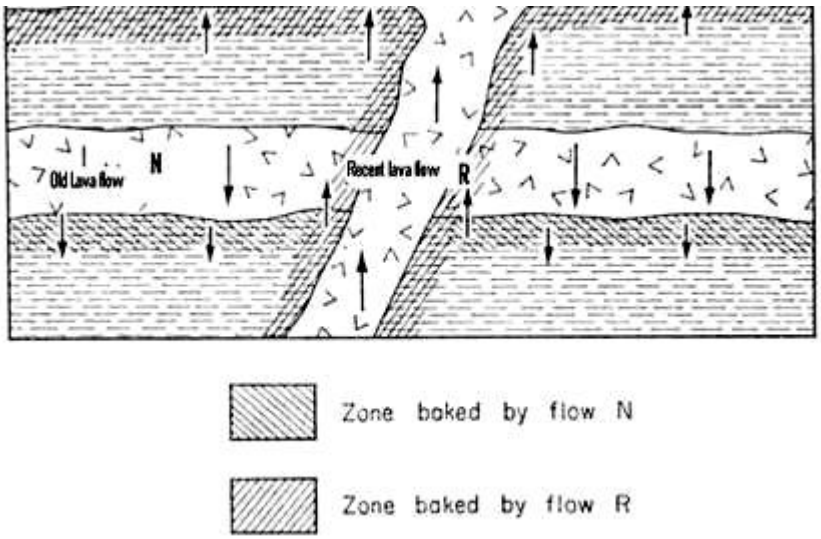

Fig.50. Magnetized lava flows cross sedimentary layers and older intrusions (from Jacobs, 1967)

The observed magnetic values across this magnetic body will thus resemble those of a much wider dyke due to the Whin Sill's (albeit reversed) contribution. At the same time the faulted Whin will contribute an anomaly with a lower 'shoulder' on the down-thrown side (Cornwell and Evans, 1986). Fig. 49(d) gives a more realistic approach to the curve-matching having the Whin with a 50m thickness and depth–to-top of 40m, which is quite acceptable here. Also the Tertiary Cleveland Dyke, having a thickness of about 18m and depth-to-top of 40m, fits the geology on the ground.

There have been many cases where magnetized lava flows cross sedimentary layers and other previous intrusions. Where the sediments or older intrusions were baked by the heat of the cooling lava flow, they were also found to be strongly magnetized in the same direction as the flow (Jacobs, 1967). In fact in all the reported cases the direction of magnetization of the older material is the same as that of the dyke or lava that heated it, whether normal or reversed (fig.50).

Summary

As observed in the qualitative analysis (previous chapter), the low magnetic anomaly tends to occur parallel to the Teesdale Fault and along the known Cleveland dyke outcrops. The Depth to the top and thickness of the Whin Sill has been estimated at different localities in the survey area as well as the width and depth (from the surface) of the dyke.

Where the Burtreeford disturbance intersects the Teesdale Fault, quantification of the dimensions of the magnetic anomaly-causing bodies became more complex. This led to individual resolution of each anomalous body, followed by a combination of all the magnetic bodies in the particular profile. However, it was not practically possible to separate the individual anomalies since the causative bodies appeared to be fused together.

7 DISCUSSION

From the above analyses, it is evident that a magnetic dyke-like body exists at shallow depths in Harwood valley and along the Teesdale fault. The parameters used in modelling the body were those obtained by Giddings and others (1972) in their paper, 'Palaeomagnetism of the Cleveland-Armathwaite Dyke, Northern England'; representative of Tertiary magnetization.

In upper Harwood, the dyke departs from its path along the Teesdale fault and occupies the Allens Cleugh mineral vein/ fault. Here the dyke seems to be much wider and deeper but this could be due to the contribution of the mineralization in the vein. Ores of iron could have been magnetized by the dyke as it cooled, causing the whole ore body to behave like a huge dyke. An outcrop of the Cleveland dyke is visible some three kilometres to the north-west of this site. The mine drawings from the late 19th century, depicting a 12m dyke parallel to Teesdale Fault at Harwood valley, act as controls to the near-surface geology and the accompanying descriptions at Lower Harwood agree with the results. The 'dyke' was encountered at a depth slightly beyond 30m and the samples collected from the ore dumps in Cadger Well confirmed dolerite rock with very fine grain without the quartz which is common in the Whin Sill.

Fig. 51 below shows the locations of two geological cross-sections done in upper and lower Harwood. The geological cross section at Tynehead Fell (fig.52) reveals the possible subsurface formations when all the geology (e.g. Burgess and Holliday, 1979, Dunham, 1990) and the magnetic interpretations are put into perspective. This cross section was undertaken to compare the magnetic profile no. 6 with the structural detail as researched in this survey. The section (see fig.52) was made from SW to NE and the magnetic result of profile no.6 tends to support the subsurface formations reproduced here. The Allens Cleugh Fault & Vein apparently downthrows the Whin Sill to the SW, opposite to the orientation at

Lower Harwood where the Teesdale fault downthrows the Sill to the NE. The boulder clay cover here is quite extensive and there is no outcrop of either the Whin or dyke.

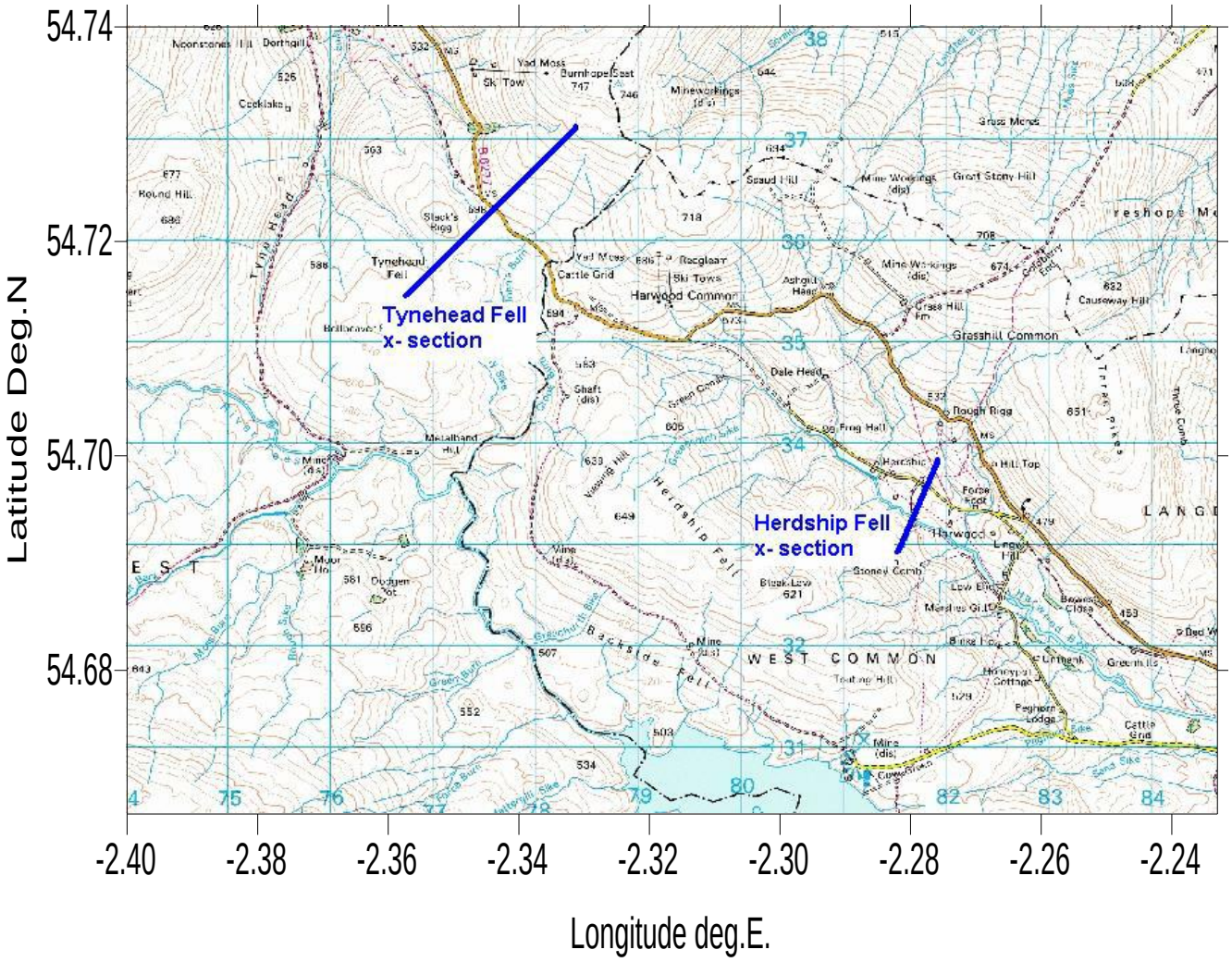

Fig.51. Location map of cross section traverses in Figs. 52 & 53.

At Herdship Fell in lower Harwood (fig.53) the sub-surface formations is somewhat similar to that at Tynehead but here the Teesdale fault dominates the structural geology; down-throwing the Whin Sill to the NE at more that 50m in some places. Some parts of the Whin to the SW can not be seen due to the boulder clay cover and, apparently, erosion thinned out part of the Whin during the glacial age (fig.53)

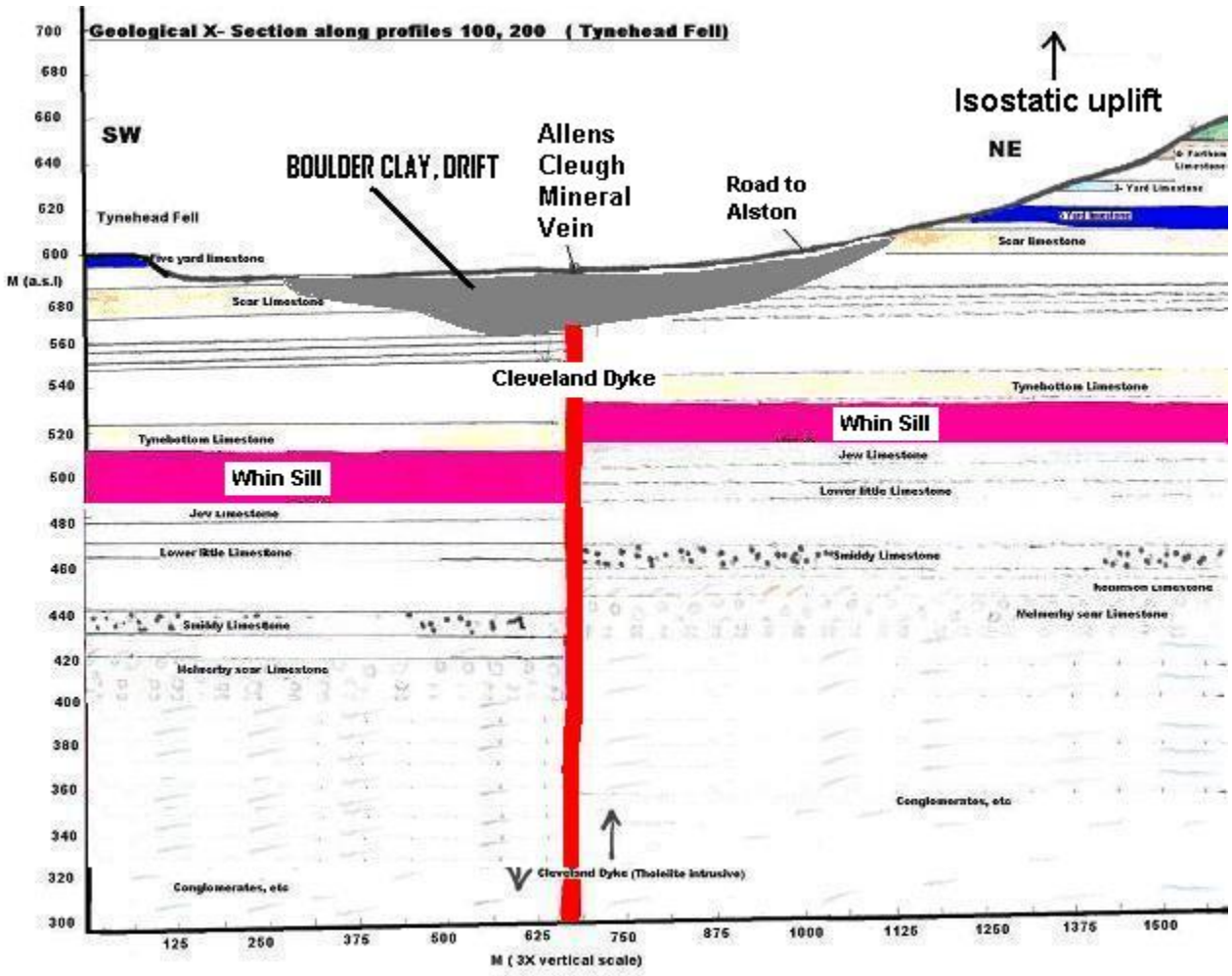

Fig.52. Geological cross section at Tynehead Fell. The horizontal scale is three times the vertical. Here the Whin Sill intrudes just below the Tynebottom limestone and above the Jew Limestone while the Cleveland (Tertiary) dyke intrudes the Allens Cleugh mineral Vein/fault.

At Tynehead Fell the Whin intruded above the Jew Limestone while it intruded above the Robinson Limestone at Herdship Fell and probably below the Peghorn Limestone. The main difference in its elevation at the two areas is attributed to isostatic adjustment. There is an elevation difference of about 100m between the Whin Sill at Herdship and at Tynehead. The distance between the two cross-sections is about 3km and the change in horizon of the When Sill confirms earlier predictions that the Whin rises towards the west, i.e. from above the Melmerby Scar Limestone at Cow Green to Robinson Limestone at Herdship and finally to Jew Limestone at Tynehead Fell. However, this change in horizon of the Whin is not confined to this area alone (Dunham, 1990). The level of intrusion also determines

the temperatures in which the Whin intrudes. The Whin level of intrusion at cow Green is the lowest known in Upper Teesdale. It is found to be thickest here (69m) as well. As it intrudes at higher levels, the temperatures are bound to decrease; hence the reason for widespread metamorphism only in Cow Green and nearby areas.

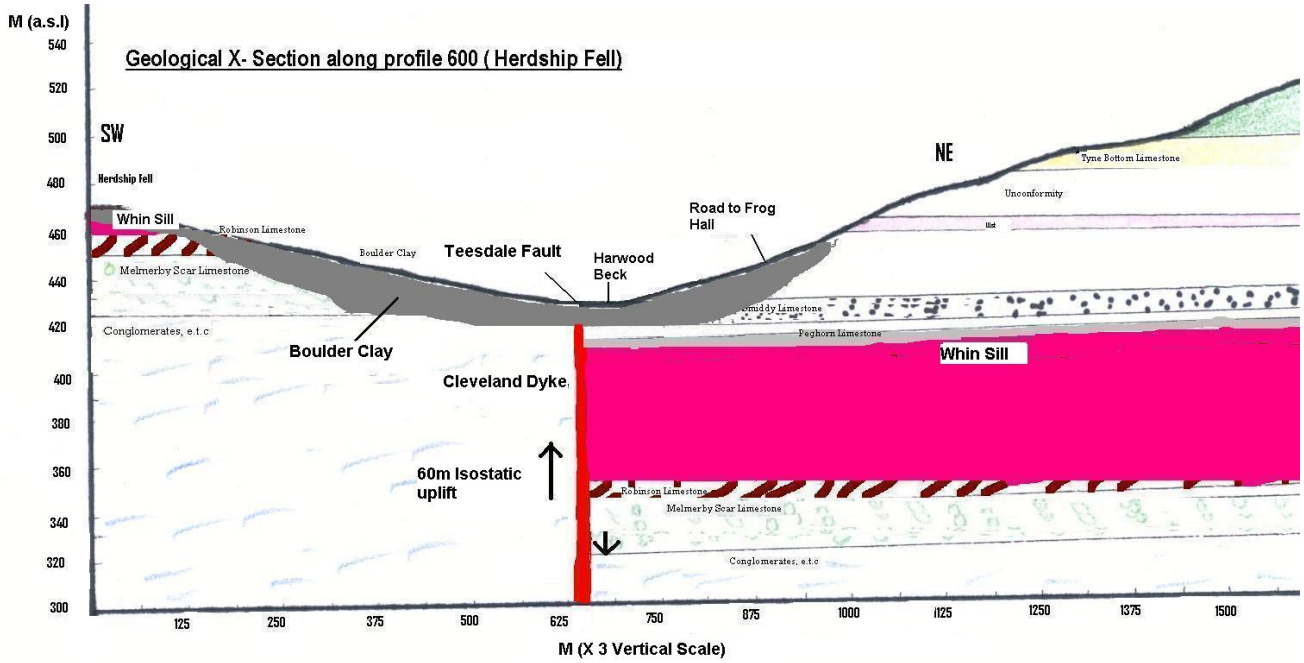

Fig.53. Geological cross- section at Herdship Fell. Note the vertical exaggeration.

At Langdon Beck, the Burtreeford disturbance complicates the interpretation process even farther due to the nature of the folding and faulting that was a result of compressional forces in the NE-SW direction even after the emplacement of the Whin Sill (Dunham, 1932). Here the Sill is exposed at some locations and there is evidence, from the interpreted profiles, and geology that the intruding dyke deviated from its path along the Teesdale fault and occupied one of the many faults running NW-SE at depth to outcrop at Etters Gill (Fig.54).

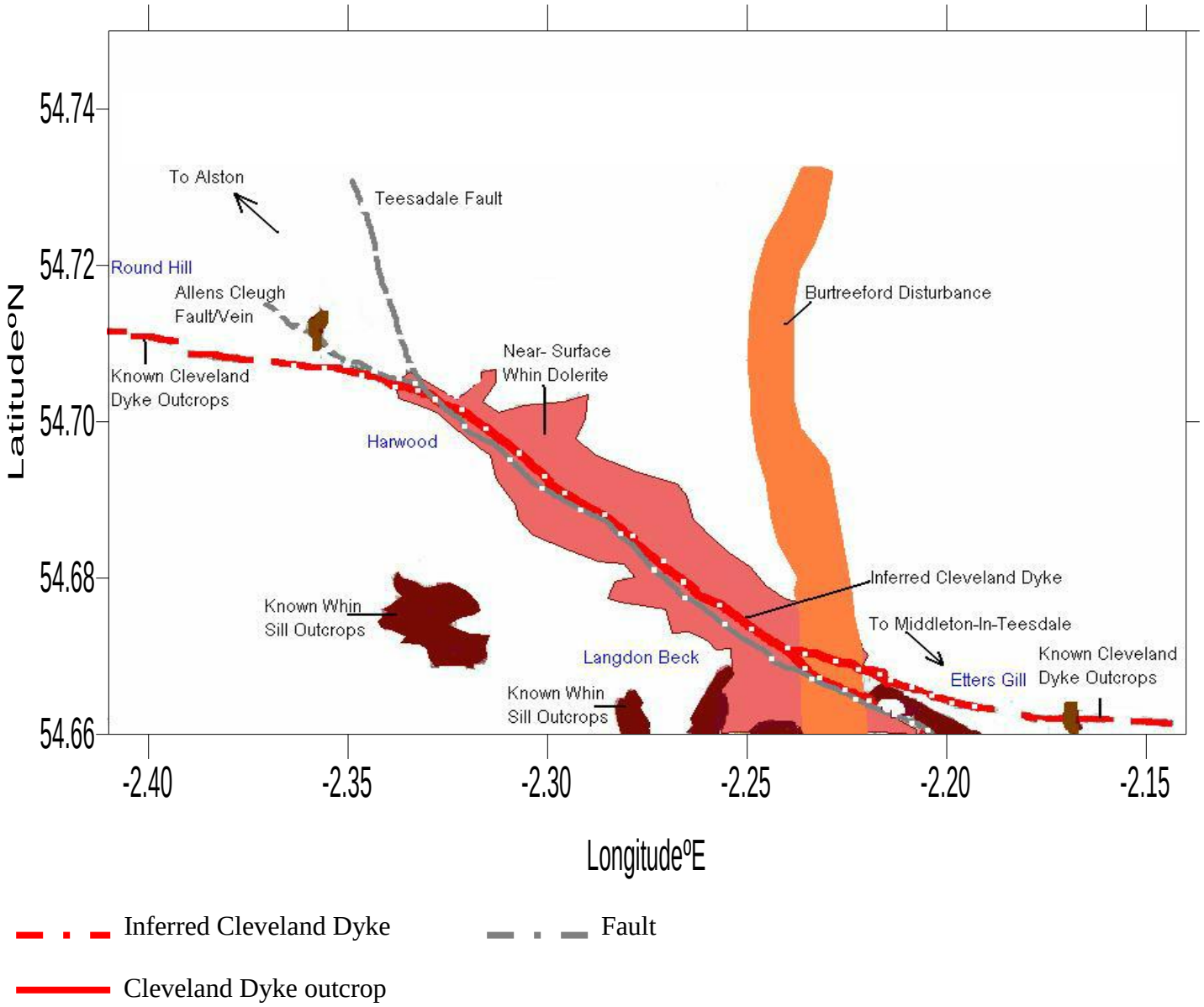

Fig.54. The inferred location of the NW-SE trending Cleveland Dyke in Upper Teesdale. The Whin outcrops are in deep brown while the near-surface sill is shaded pink. The Burtreeford Disturbance is coloured orange running approximately N-S.

Several magnetic traverses were surveyed with the sole intention of intercepting the assumed buried dyke (e.g. profiles 23, 27, 28 and 33 in fig. 16). All these profiles portrayed a similar anomaly, relating with the Cleveland dyke. The branching off the dyke at lower Langdon beck (shown below in fig.55)

Fig.55. Location of recently sighted Cleveland dyke outcrop in Langdon Beck at the confluence of the Tees and Harwood rivers (see fig.1). The Sill outcrop can be seen in the background to the west while the dyke juts into the river from the bottom right side of the picture (under the left hand).

could be explained by the Dyke's nature of intruding formations offering least resistance (e.g. the Teesdale Fault). There is a low magnetic anomaly stretching from the road to Cow Green [NY 830 310] to the confluence of the Tees and Harwood rivers [NY 860 290]. An outcrop of an intrusive rock whose samples were found to match those found at the known dyke outcrops was recently sighted by the author at the confluence of the Tees and Harwood rivers [NY 860 290] (Fig.55). An attempt to find the similarity between the specimens of the Tholeiite Dyke intrusion rock obtained at various outcrop sites (i.e. Round Hill, Harwood, Langdon Beck and Etters Gill) gave positive results when they were studied under the microscope (fig.56).

Fig.56 below is a photograph of thin sections of outcrops of both the Dyke and the Whin Sill from three different survey areas. The obvious difference between the two intrusive bodies is the grain size. The dyke tends to appear 'smoother' in comparison due to its smaller formation crystals. This is theoretically due to a faster cooling period after intrusion. The Whin on the other hand has a peculiar greenish pigment inherent from its high iron (III) compounds. This is more magnified when the slides were viewed under the microscope. The Whin rock is easily attracted to a hand bar-magnet in the field. When exposed, the green compounds oxidise to the common brown iron (II) compounds seen as 'rust' on the surface in many Whin outcrops.

At Newbeggin, the dyke outcrops again at the confluence of two streams that form a miniature waterfall that is due to its resistance to erosion (2.18ºW, 54.66ºN). Here, the dyke, 14m wide, is seen in Smithy sike [NY 892 296] and again in Bow Lee Beck [NY 908 292] near Mirk Holm (fig.1) where it is split into two parts and includes a screen of baked sediments belonging to the Upper Alston Group (Burgess and Holliday, 1979).

Figure 57 below gives a summary of the result of this study. The Cleveland Dyke intruded the Harwood valley in the Tertiary period along the Teesdale Fault because the Fault offered little resistance in the NW-SE direction. Though the Whin Sill exists in the sub-surface in upper Teesdale, the extent of metamorphism is determined by the horizon in which the Whin intruded, the lowest being the Melmerby Scar Limestone at Cow Green [NY 800 300]. The low magnetic anomaly observed along the four different localities is mainly due to the intruding Dyke even though the faulted, displaced Whin Sill contributed to the magnetic anomaly wavelength by amplifying the width of the observed anomaly. Fig. 58 below portrays the regional magnetic contours super-imposed on the geology, indicating a magnetic low along the Teesdale fault and the Cleveland dyke.

The cause of the unique mineralization observed at Harwood valley can therefore be connected to the intrusion of the Cleveland dyke. The intrusion temperature of the dyke in the area must have affected the mineralization more than that of the Whin Sill. Though the Sill spreads all over the sub-surface, its intrusion in Harwood above the Tyne Bottom Limestone indicates contact temperatures lower than at Cow green where it intruded at its lowest horizon. Niccolite mineralization observed at Harwood would require temperatures above 550ºC but the Whin intrusion here would create mineralization at temperatures below 250ºC (the temperature at Cow Green). In fact the metasomatism at Harwood could possibly be a confirmation that it was not the Whin Sill that was involved in the heating process.

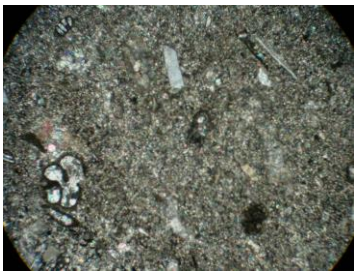

Dyke **ETTERS GILL** Whin sill

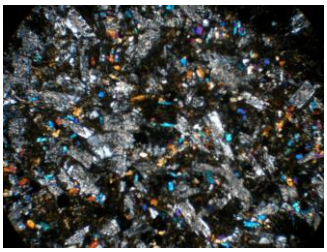

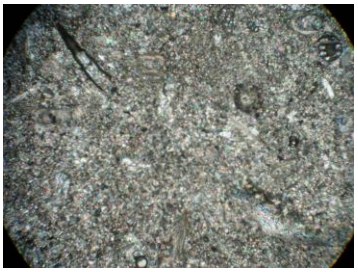

Dyke **LANGDON BECK** Whin Sill

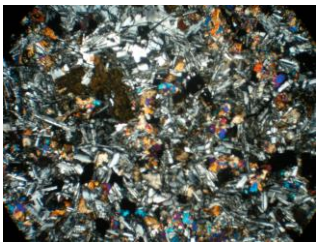

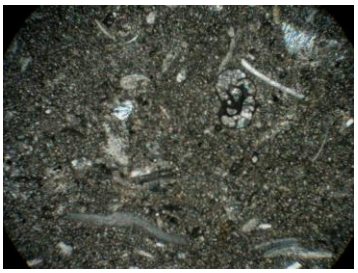

Dyke **HARWOOD** Whin Sill

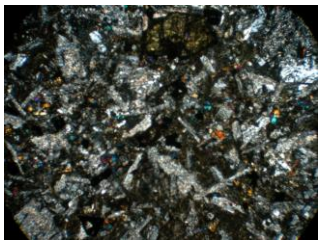

Fig.56. Photographs of thin section samples of both the Whin quartz Dolerite and the Cleveland tholeiite Dolerite obtained from three different localities; at Harwood, Langdon Beck and Etters Gill. The dolerite intruded the Alston Limestone group in Upper Teesdale, Northern England.

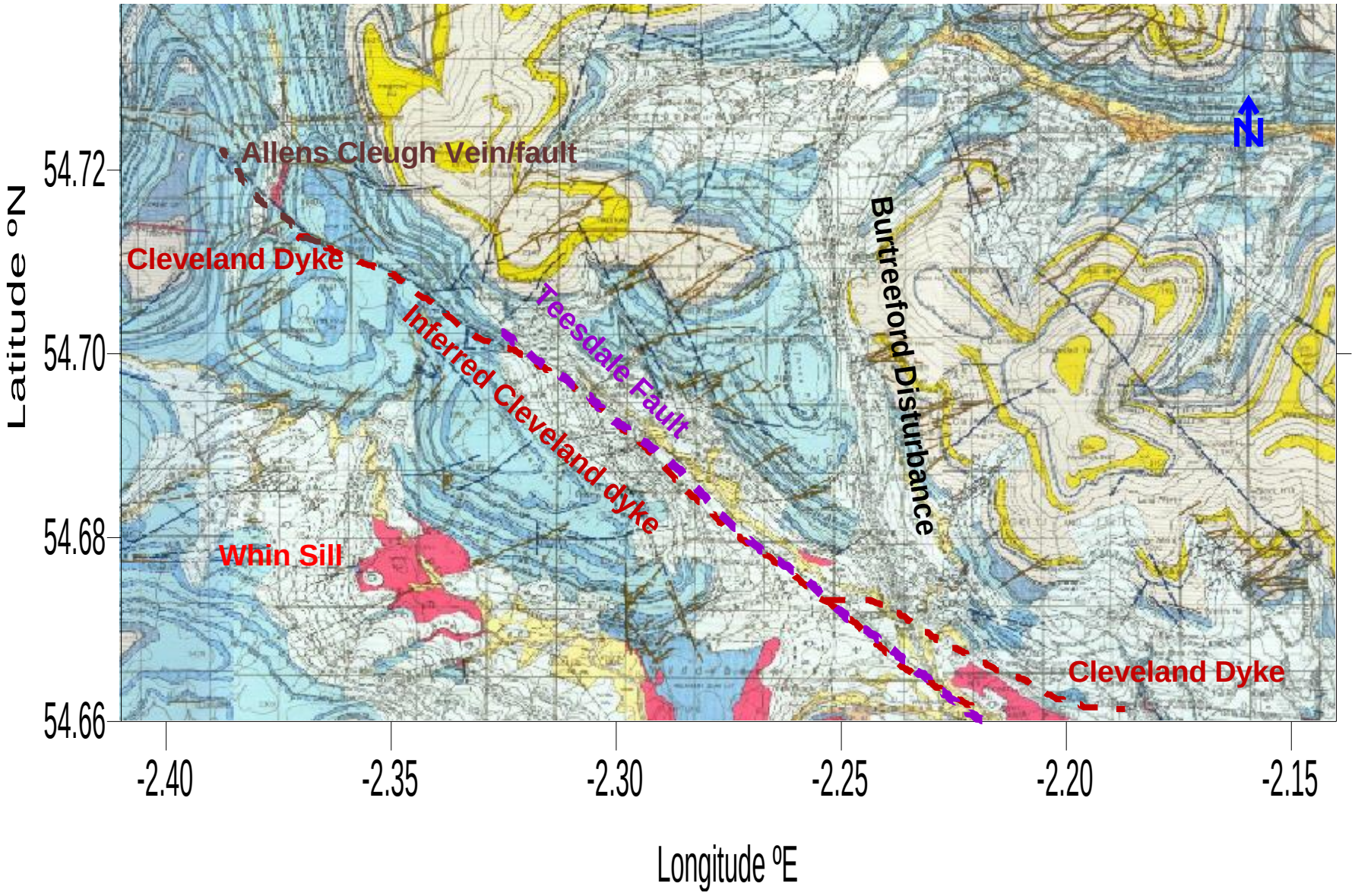

Fig.57. Geological interpretation in Upper Teesdale. The inferred Cleveland (Tertiary) dyke occupies the Teesdale Fault between Harwood and Langdon Beck.

Fig.58. Regional magnetic contours superimposed on geology in Upper Teesdale, northern England (Adopted from sheet 54N 02W, 1:250,000, Institute of geological Sciences London, 1977)

8 CONCLUSIONS

The objective of the magnetic survey in Teesdale was realized, as the cause of the low magnetic anomaly in Harwood Valley was found to be most likely due to the Cleveland dyke intruding the Teesdale fault. The dyke appears to occupy the Teesdale fault between Harwood and Langdon Beck. Beyond upper Harwood, the dyke intrudes the Allens Cleugh mineral vein/fault for about a kilometer before changing direction towards the west where it outcrops at Round Hill. Beyond Langdon Beck in the SE of Harwood, the dyke departs from occupying the Teesdale Fault and changes direction towards the east, outcropping at Etters Gill.

The Cleveland dyke is approximately 12m wide at Harwood and lies at a depth of about 30m under the boulder clay and drift. At Newbeggin, it is about 14m wide and outcrops at a riverbed. An outcrop, about 5m wide, was recently sighted by the author at Lower Langdon Beck at the confluence of the Tees and Harwood rivers.

The Whin Sill on the other hand is confirmed to have been faulted, displaced and grossly eroded along the Teesdale fault. The magnetic technique proved instrumental in easily identifying the down-thrown side of the Whin Sill and confirming that the Whin intrudes at varying depths above sea level.

9 REFERENCES

Astle J. M. 1978. A magnetic and electromagnetic survey of the Burtreeford disturbance, upper Teesdale. *(Dissertation, unpublished). Durham University,* pp. 64

Bott, M. H. P. 1961. Geological interpretation of magnetic anomalies on the Askrigg Block. *Journal of the Geological Society, Vol.* 117, pp. 481- 495.

Bott, M. H. P. 1967. Geophysical investigations of the northern Pennine basement rocks. *Proceedings of the Yorkshire Geological Society, Vol.* 36, pp. 139- 168.

Bruckshaw, J. McG and Robertson, E. I. 1949. The magnetic properties of tholeiite dykes of north England. *Mon. Not. R. Astronom. Soc., Geophys. Suppl.,* Vol. 5, pp. 308- 320

Burgess, I. C and Holliday, D. W. 1979.Geology of the County around Brough- Under- Stainmore. Mem. *Geol. Surv. G.B., Sheet 31*, pp. 131

Cornwell, J. D. and Evans A. D. 1986. Magnetic surveys and structures in the Whin Sill, northern England. In: *Geology in the Real World -The Kingsley Dunham Volume.* Ed. R. W. Nesbitt and I. Nichol, Publ. Institution of Mining and Metallurgy.

Dunham, A. C 1934. The genesis of the North Pennine ore deposits. Q. *J. Geol. Soc. London,* Vol. 90, pp. 689- 720

Dunham, A. C and Kaye, M. J. L. 1965. The petrology of the Little Whin Sill, County Durham. *Proc. Yorkshire Geol. Soc.,* Vo1.35, pp. 229- 276.

Dunham, A. C. 1990. Geology of the Nothern Pennine Orefield. Vol. l, Tyne to Stainmore. Economic *Mem.of the Brit. Geol. Surv.* 300 pp.

Dunham, A. C. 1990. Geology of the Northern Pennine Orefield. *Economic memoir of the British Geological Survey*. Vol 1, pp.299

EI- Harathi, R. M. and Tarling D. H.. 1988. A magnetic study of the Holy Island en echelon dyke system, Northumberland. *Transactions of the Natural History Society of Northumbria*, Vol. 55, 12- 19.

Evans, A. D. 1984. Some new data on the magnetic properties of the Whin Sill intrusion, Northumberland. *Geophysical Journal of the Royal Astronomical Society, Vol.* 77, pp. 313.

Evans, A. L., Fitch, F. and Miller, A. 1973. Potassium-argon age determinations on some British Tertiary igneous rocks. *J. Geol. Soc. London,* Vol. 129, pp. 4 I 9- 443.

Giddings, J. W., D. H. Tarling, et al. 1972. The palaeomagnetism of the Cleveland Armathwaite dyke, northern England. *Transactions of the Natural History Society of Northumbria, Vol.* 41, pp. 220.

Goulty, N. R., C. Pierce, T. D. Flatman, M. Home and J. H. Richardson. 2000. Magnetic survey of the Holy Island Dyke on Holy Island, Northumberland. *Proceedings of the Yorkshire geological society*, Vol. 53, part 2, pp. 111- 118.

Jacobs J. A., 1967. The Earth's core and geomagnetism. *Pergamon Press Ltd. Pp. 137.*

Johnson, G. A. L. and K. Dunham 2001. Emplacement of the Great Whin Dolerite Complex and the Little Whin Sill in relation to the structure of northern England. *Proceedings of the Yorkshire Geological Society, Vol.* 53(3), pp. 177-186.

Ledigo M., 1978. Geophysical investigation of the Teesdale inlier, upper Teesdale. *(Dissertation, unpublished). Durham university*, pp.78

Lee T. D., 1978. A geomagnetic investigation of Harwood beck, upper Teesdale. *(Dissertation, unpublished). Durham University*, pp.132

Pedley R C, 1991. Interactive 2.5D Gravity and Magnetic modelling program. British Geological Survey. Manual.

Robinson, D. 1970. Metamorphic rocks. In Geology of Durham County. Hickling, G. (Editor). *Trans. Nat. Hist. Soc. Northumberland*, Vol. 4l, No. 1 Pp. 119- 123

Robson, D.A. 1964. The Acklington Dyke- a proton magnetometer survey. Proc.Yorkshire Geol.Soc., Vol. 34, pp. 293-308.

Telford W. M., and others, 1995. Applied Geophysics. Cambridge University Press. Pp. 770

Young, B., M. T. Styles, et al. 1985. Niccolite-magnetite mineralization from Upper Teesdale, North Pennines. *Mineralogical Magazine, Vol.* 49, pp. 555- 559.

APPENDIX 1 EQUIPMENT USED

Magnetometer:

EG & G Geometrics Model: G-856AX Serial no. 277011 12VDC, 1AMP

Sensitivity – 1 gamma (1nT)

Operation Temp. -5 to 60 deg.Celcius

GPS (Geographical Positioning System):

GBX-PRO

1. 12 channel all- in- view GPS satellite tracking
2. 5Hz NMEA position update rates
3. Dual channel beacon receiver
4. 2- line by 16 character LCD display and 3- switch keypad
5. Automatic and manual beacon modes
6. <1 m horizontal differential accuracy (95%), 5m vertical accuracy
7. <1 minute cold start time
8. -30 to 70 deg.C operating temperature
9. 9-40 V DC, 4.8 W
10. 10V DC antenna voltage output
11. 1.75lb weight

Persona Digital Assistant (PDA):

Compaq Bluetooth Ipaq series pocket PC

model: 3870

1. 5V DC, 2Amps
2. Li- Ion rechargeable battery
3. Microsoft Windows powered, MS- Outlook 2002, MS- Word 2002, MS- Excel 2002

APPENDIX II MAGNETIC DATA

The data presented here includes all the work done by the author as well as that integrated from other previous surveys in Upper Teesdale. A table summarising which profile each surveyor traversed is also included below. The first column of the Data table represents the number of the profile; the second column is for station numbers while the third represents the reduced magnetic value. The fourth, fifth and sixth columns represent the longitude, latitude and altitude respectively.

Surveyor	Profile no.
J.M. Astle	26, 30, 32
T.D. Lee	20, 21, 23
R.C. Searle	11, 12, 13, 14
E. Mwandoe	1, 2, 3, 4, 5, 6, 7, 8, 9, 10, 15, 16, 17, 18, 19, 22, 24, 25, 27, 28, 29, 31, 33, 34, 35, 36, 37, 38, 39, 40

Profile no.	ROUND HILL				
	Stn. No.	Mag.anomaly.nT	long deg.E	lat deg.N	alt.m
1	76	49079	-2.4077	54.7239	650
	77	49052	-2.4076	54.7240	649
	78	49002	-2.4077	54.7242	646
	79	48940	-2.4079	54.7243	647
	80	48671	-2.4080	54.7245	646
	81	48764	-2.4081	54.7246	644
	82	49176	-2.4082	54.7248	638
	83	49174	-2.4083	54.7249	635
	84	49126	-2.4085	54.7250	632
2	85	49175	-2.4071	54.7249	644
	86	49171	-2.4070	54.7248	648
	87	49155	-2.4069	54.7247	648
	88	49142	-2.4068	54.7245	655
	89	48197	-2.4067	54.7244	658
	90	48285	-2.4066	54.7244	661
	91	48836	-2.4065	54.7242	659
	92	48949	-2.4064	54.7240	661

	93	49010	-2.4063	54.7239	660
	94	49046	-2.4061	54.7238	662
	95	49074	-2.4057	54.7236	664
	96	49055	-2.4040	54.7241	671
3	97	49026	-2.4041	54.7241	669
	98	48939	-2.4040	54.7243	667
	99	48599	-2.4040	54.7244	667
	100	48816	-2.4040	54.7246	663
	101	49169	-2.4038	54.7247	660
	102	49195	-2.4038	54.7249	660
HARWOOD					
	stn	magred.nT	long deg.	lat deg.	alt.m
6	309	48972	-2.3024	54.6988	473
	310	48971	-2.3025	54.6988	468
	311	48993	-2.3027	54.6987	469
	312	48983	-2.3028	54.6987	468
	313	48979	-2.3030	54.6986	466
	314	48992	-2.3031	54.6986	468
	315	48976	-2.3033	54.6985	470
	316	48982	-2.3034	54.6985	472
	317	48973	-2.3036	54.6984	475
	318	48989	-2.3037	54.6984	478
	319	48999	-2.3039	54.6983	477
	320	48988	-2.3040	54.6983	479
	321	48993	-2.3042	54.6982	481
	322	48987	-2.3043	54.6982	482
	323	48941	-2.3045	54.6981	480
	324	48870	-2.3046	54.6981	480
	325	48826	-2.3049	54.6980	478
	326	48789	-2.3048	54.6980	480
	327	48770	-2.3052	54.6979	480
	328	48772	-2.3057	54.6978	480
	329	48801	-2.3055	54.6978	481
7	330	48873	-2.3073	54.6977	480
	331	48922	-2.3061	54.6977	479
	332	48956	-2.3074	54.6975	480
	333	49000	-2.3078	54.6974	481
	334	49019	-2.3078	54.6973	481
	335	49032	-2.3084	54.6971	481
	336	49038	-2.3087	54.6970	482
	337	49032	-2.3092	54.6968	482
	338	49036	-2.3097	54.6966	483
	339	49044	-2.3101	54.6964	485
	340	49045	-2.3106	54.6962	483
	341	49036	-2.3110	54.6960	486
	342	49049	-2.3115	54.6958	492

9	186	48922	-2.3027	54.7031	477
	187	48999	-2.3030	54.7030	481
	188	49010	-2.3032	54.7029	485
	189	49012	-2.3033	54.7029	486
	190	49013	-2.3035	54.7028	488
	191	49032	-2.3036	54.7028	488
	192	49035	-2.3038	54.7027	488
	193	49029	-2.3039	54.7027	489
	194	49042	-2.3041	54.7026	491
	195	49033	-2.3042	54.7026	494
	196	49031	-2.3044	54.7025	498
	197	49027	-2.3045	54.7025	499
	198	49023	-2.3047	54.7024	501
	199	49008	-2.3048	54.7024	467
	200	49003	-2.3050	54.7023	466
	201	49007	-2.3051	54.7023	466
	202	49026	-2.3053	54.7022	467
	203	49034	-2.3054	54.7022	469
	204	49034	-2.3056	54.7021	472
	205	49026	-2.3057	54.7021	477
	206	49025	-2.3059	54.7020	478
	207	48947	-2.3060	54.7020	478
	208	48989	-2.3063	54.7019	479
	209	48867	-2.3066	54.7018	479
	210	48870	-2.3068	54.7018	480
	211	48897	-2.3072	54.7017	479
10	212	48924	-2.3084	54.7017	475
	213	48919	-2.3085	54.7015	478
	214	49001	-2.3089	54.7014	480
	215	48989	-2.3089	54.7013	482
	216	48996	-2.3095	54.7011	482
	217	49009	-2.3098	54.7010	483
	218	49023	-2.3103	54.7008	484
	219	49028	-2.3108	54.7006	484
	220	49035	-2.3112	54.7004	485
	221	49007	-2.3117	54.7002	486
	222	49000	-2.3121	54.7000	486
	223	49007	-2.3126	54.6998	488
	224	49002	-2.3130	54.6996	489
	225	49003	-2.3135	54.6994	489
	226	49002	-2.3139	54.6992	486
	227	49004	-2.3144	54.6990	467
	228	49014	-2.3148	54.6988	466
	229	49006	-2.3153	54.6986	466
	230	48978	-2.3157	54.6984	465
11	231	49006	-2.3057	54.7061	500
	232	49011	-2.3060	54.7060	500
	233	49002	-2.3062	54.7059	498

	234	49004	-2.3063	54.7059	497
	235	49012	-2.3065	54.7058	493
	236	49005	-2.3066	54.7058	491
	237	49001	-2.3068	54.7057	487
	238	48991	-2.3069	54.7057	483
	239	49004	-2.3071	54.7056	482
	240	49034	-2.3072	54.7056	475
	241	48964	-2.3074	54.7055	472
	242	48947	-2.3075	54.7055	472
	243	48881	-2.3077	54.7054	470
	244	48989	-2.3078	54.7054	471
	245	48987	-2.3080	54.7053	474
	246	48989	-2.3081	54.7053	474
	247	49018	-2.3083	54.7052	475
	248	48987	-2.3084	54.7052	475
	249	48995	-2.3086	54.7051	474
	250	49032	-2.3087	54.7051	478
	251	49023	-2.3090	54.7050	478
	252	49031	-2.3089	54.7050	480
	253	49043	-2.3093	54.7049	482
	254	49020	-2.3098	54.7048	484
	255	48958	-2.3096	54.7048	484
	256	48849	-2.3104	54.7047	484
	257	48718	-2.3102	54.7047	484
12	258	48692	-2.3115	54.7045	484
	259	48741	-2.3119	54.7044	486
	260	48832	-2.3119	54.7043	490
	261	48888	-2.3125	54.7041	491
	262	48927	-2.3128	54.7040	492
	263	48947	-2.3133	54.7038	493
	264	48964	-2.3138	54.7036	495
	265	48980	-2.3142	54.7034	496
	266	48985	-2.3147	54.7032	497
	267	48996	-2.3151	54.7030	498
	268	49013	-2.3156	54.7028	499
	269	49018	-2.3160	54.7026	501
	270	49031	-2.3165	54.7024	503
	271	49033	-2.3169	54.7022	502
	272	49030	-2.3174	54.7020	503
	273	49044	-2.3178	54.7018	500
	274	49044	-2.3183	54.7016	503
	275	49042	-2.3187	54.7014	507
	276	49044	-2.3192	54.7012	511
13	277	49008	-2.3105	54.7083	477
	278	49008	-2.3107	54.7082	478
	279	49002	-2.3109	54.7082	479
	280	49002	-2.3111	54.7081	480
	281	49007	-2.3114	54.7080	484

	282	49013	-2.3116	54.7079	486
	283	49014	-2.3117	54.7079	490
	284	49007	-2.3119	54.7078	492
	285	49004	-2.3120	54.7078	494
	286	48990	-2.3122	54.7077	496
	287	48963	-2.3123	54.7077	500
	288	48923	-2.3125	54.7076	504
	289	48860	-2.3126	54.7076	506
	290	48780	-2.3128	54.7075	510
	291	48746	-2.3129	54.7075	509
	292	48714	-2.3131	54.7074	510
	293	48691	-2.3132	54.7074	511
	294	48683	-2.3134	54.7073	512
	295	48696	-2.3135	54.7073	514
	296	48726	-2.3137	54.7072	516
	297	48771	-2.3138	54.7072	517
	298	48824	-2.3140	54.7071	518
	299	48863	-2.3141	54.7071	519
	300	48900	-2.3143	54.7070	518
	301	48931	-2.3144	54.7070	516
	302	48964	-2.3147	54.7069	509
	303	48978	-2.3150	54.7068	509
	304	49000	-2.3152	54.7068	509
	305	49005	-2.3156	54.7067	508
	306	49036	-2.3168	54.7067	508
	307	49032	-2.3169	54.7065	510
	308	49034	-2.3173	54.7064	514
14	1	49196	-2.3123	54.7081	526
	2	49060	-2.3125	54.7080	532
	3	48880	-2.3126	54.7080	530
	4	48656	-2.3129	54.7079	532
	5	48490	-2.3132	54.7078	529
	6	48512	-2.3134	54.7078	528
	7	48391	-2.3138	54.7077	519
	8	48505	-2.3150	54.7077	518
	9	48730	-2.3151	54.7075	524
	10	48855	-2.3155	54.7074	529
	11	48944	-2.3155	54.7073	530
	12	48990	-2.3161	54.7071	532
	13	49043	-2.3166	54.7070	533
	14	49032	-2.3186	54.7074	541
	15	48973	-2.3183	54.7075	540
	16	48861	-2.3183	54.7078	534
	17	48804	-2.3179	54.7081	537
	18	48983	-2.3176	54.7081	540
	19	49059	-2.3172	54.7082	541
	20	49133	-2.3169	54.7083	544
	21	49195	-2.3165	54.7084	546

	22	49228	-2.3160	54.7085	544
	23	49259	-2.3157	54.7086	545
	24	49279	-2.3151	54.7087	547
15	25	49172	-2.3200	54.7094	580
	26	49230	-2.3203	54.7093	576
	27	49198	-2.3206	54.7092	568
	28	49196	-2.3208	54.7090	559
	29	49171	-2.3210	54.7089	556
	30	49154	-2.3213	54.7088	552
	31	49110	-2.3216	54.7087	543
	32	48861	-2.3216	54.7084	546
	33	48811	-2.3218	54.7083	549
	34	48885	-2.3220	54.7081	546
	35	48951	-2.3222	54.7079	551
	36	49004	-2.3224	54.7077	554
	37	49040	-2.3226	54.7075	560
	38	49072	-2.3228	54.7074	562
	39	49113	-2.3229	54.7073	565
	40	49143	-2.3231	54.7071	571
	41	49180	-2.3233	54.7069	575
	42	48721	-2.3232	54.7090	546
	43	48674	-2.3241	54.7087	543
	44	48675	-2.3234	54.7086	543
	45	48753	-2.3229	54.7083	544
	46	48835	-2.3221	54.7083	545
	47	48777	-2.3215	54.7082	545
	48	48725	-2.3203	54.7081	544
	49	48721	-2.3193	54.7081	543
	50	48731	-2.3176	54.7078	536
	51	48310	-2.3161	54.7076	526
	52	48263	-2.3149	54.7077	514
	133	49186	-2.3267	54.7122	614
	134	49195	-2.3268	54.7120	612
	135	49201	-2.3270	54.7118	611
	136	49199	-2.3271	54.7117	609
	137	49222	-2.3273	54.7115	606
	138	49220	-2.3276	54.7114	601
	139	49232	-2.3278	54.7113	599
	140	49212	-2.3281	54.7111	598
	141	49223	-2.3283	54.7110	597
	142	49215	-2.3286	54.7108	594
	143	49207	-2.3288	54.7108	592
	144	49204	-2.3290	54.7106	588
	145	49201	-2.3291	54.7104	584
	146	49175	-2.3292	54.7102	579
	147	49151	-2.3295	54.7100	574
	148	49166	-2.3296	54.7098	566
	149	49003	-2.3298	54.7097	558

	150	49023	-2.3300	54.7095	558
	151	49056	-2.3302	54.7094	560
	152	49077	-2.3303	54.7092	566
	153	49093	-2.3305	54.7091	573
	154	49101	-2.3306	54.7089	575
	155	49105	-2.3307	54.7087	575
	156	49122	-2.3309	54.7085	576
	157	49137	-2.3310	54.7083	576
	159	49168	-2.3313	54.7079	581
	160	49165	-2.3315	54.7078	582
	161	49173	-2.3316	54.7076	584
	162	49178	-2.3318	54.7073	585
	163	49179	-2.3319	54.7072	590
	164	49176	-2.3320	54.7070	595
	165	49188	-2.3322	54.7068	598
	166	49188	-2.3322	54.7067	600
	167	49150	-2.3046	54.7130	493
	168	49158	-2.3048	54.7129	495
	169	49154	-2.3049	54.7127	495
	170	49142	-2.3051	54.7125	497
	171	49084	-2.3053	54.7123	499
	172	49055	-2.3056	54.7121	498
	173	49004	-2.3057	54.7120	498
	174	48957	-2.3059	54.7118	497
	175	48965	-2.3062	54.7115	495
	176	48993	-2.3064	54.7113	494
	177	49005	-2.3066	54.7111	491
	178	49046	-2.3067	54.7109	493
	179	49080	-2.3070	54.7107	496
	180	49094	-2.3072	54.7105	499
	181	49136	-2.3074	54.7103	498
	182	49165	-2.3076	54.7102	496
	183	49163	-2.3078	54.7100	499
	184	49157	-2.3079	54.7098	501
	185	49160	-2.3081	54.7096	499
Langdon Beck					
	Stn. No.	magav.nT	long deg.	lat deg.	alt.m
16	170	49020	-2.2334	54.6818	440
	171	49092	-2.2336	54.6816	439
	172	49095	-2.2337	54.6814	420
	173	49048	-2.2339	54.6812	421
	174	49075	-2.2341	54.6810	431
	175	49086	-2.2343	54.6808	432
	176	49061	-2.2344	54.6806	430
	177	49034	-2.2346	54.6804	422
	178	49028	-2.2348	54.6801	419

	179	48934	-2.2349	54.6800	417
	180	48921	-2.2351	54.6798	417
	181	48947	-2.2353	54.6796	417
	182	48930	-2.2354	54.6793	417
	183	48980	-2.2356	54.6792	415
	184	49015	-2.2358	54.6790	411
	185	48998	-2.2360	54.6787	409
	186	48986	-2.2361	54.6785	407
	187	48952	-2.2363	54.6787	405
	188	48882	-2.2365	54.6781	403
	189	48798	-2.2366	54.6779	401
	190	48831	-2.2368	54.6777	404
	191	48901	-2.2370	54.6775	406
	192	48973	-2.2371	54.6773	404
	193	49078	-2.2373	54.6771	401
	194	49144	-2.2375	54.6769	398
	195	49248	-2.2377	54.6767	396
	196	49322	-2.2378	54.6765	393
	197	49249	-2.2380	54.6764	373
	198	49265	-2.2382	54.6761	371
	199	49129	-2.2383	54.6759	371
	200	49009	-2.2385	54.6757	370
	201	49137	-2.2387	54.6755	371
	202	49253	-2.2388	54.6753	373
	203	49324	-2.2390	54.6751	373
	204	49264	-2.2392	54.6749	381
	205	49253	-2.2394	54.6747	386
	206	49235	-2.2395	54.6745	387
	207	49256	-2.2397	54.6743	389
	208	49246	-2.2399	54.6740	389
	209	49271	-2.2400	54.6738	387
	210	49282	-2.2402	54.6736	386
	211	49235	-2.2404	54.6734	386
	212	48914	-2.2405	54.6732	386
	213	48960	-2.2407	54.6730	386
	214	49097	-2.2409	54.6728	386
	215	49120	-2.2411	54.6726	386
	216	49136	-2.2412	54.6724	388
	217	49125	-2.2414	54.6722	388
	218	49135	-2.2416	54.6720	388
17	64	49022	-2.1957	54.6683	415
	65	49068	-2.1958	54.6679	415
	66	49066	-2.1958	54.6677	416
	67	49058	-2.1958	54.6675	418
	68	49047	-2.1959	54.6673	420
	69	49036	-2.1959	54.6672	420
	70	49002	-2.1960	54.6670	418
	71	48961	-2.1961	54.6667	416

	72	48989	-2.1962	54.6665	414
	73	49020	-2.1964	54.6663	413
	74	48646	-2.1964	54.6660	413
	75	48921	-2.1966	54.6655	413
	76	49072	-2.1967	54.6653	414
	77	49173	-2.1968	54.6651	415
	78	49210	-2.1970	54.6649	417
	79	49230	-2.1971	54.6647	419
	80	49211	-2.1972	54.6645	421
	81	49203	-2.1973	54.6643	421
	82	49203	-2.1974	54.6640	419
	83	49193	-2.1975	54.6638	416
	84	49187	-2.1976	54.6636	414
	85	49173	-2.1978	54.6635	412
	86	49167	-2.1978	54.6632	410
	87	49186	-2.1979	54.6630	408
	88	49196	-2.1980	54.6626	406
18	97	49145	-2.2009	54.6604	378
	98	49080	-2.2011	54.6604	373
	99	49213	-2.2014	54.6603	370
	100	49215	-2.2018	54.6603	372
	101	49243	-2.2024	54.6601	371
	102	49447	-2.2031	54.6601	374
	103	49386	-2.2038	54.6601	374
	104	49299	-2.2044	54.6599	371
	105	49166	-2.2050	54.6598	368
	106	48927	-2.2057	54.6596	368
	107	49342	-2.2062	54.6593	368
	108	49095	-2.2070	54.6592	367
	109	48938	-2.2076	54.6590	364
	110	48927	-2.2079	54.6589	364
	111	48918	-2.2083	54.6589	364
	112	48905	-2.2089	54.6591	364
	113	48967	-2.2096	54.6592	365
	114	49063	-2.2102	54.6594	363
	115	48755	-2.2108	54.6595	363
	116	48924	-2.2118	54.6597	361
	117	48881	-2.2125	54.6597	360
	118	48996	-2.2130	54.6600	363
	119	48889	-2.2134	54.6599	362
	120	48835	-2.2137	54.6598	361
	121	48835	-2.2139	54.6598	359
	122	48880	-2.2141	54.6597	355
	123	48925	-2.2144	54.6595	353
	124	48903	-2.2146	54.6594	353
	125	49042	-2.2149	54.6592	355
	126	48872	-2.2151	54.6592	360
	127	48878	-2.2154	54.6589	360

	128	48956	-2.2158	54.6589	352
	129	48985	-2.2161	54.6589	352
	130	48985	-2.2164	54.6589	353
	131	48943	-2.2168	54.6589	351
	132	48994	-2.2172	54.6587	353
	133	49039	-2.2175	54.6684	386
	134	48936	-2.2177	54.6683	384
	135	48772	-2.2180	54.6681	383
	136	48930	-2.2184	54.6681	379
	137	49058	-2.2187	54.6679	379
	138	49032	-2.2190	54.6678	377
	139	49133	-2.2192	54.6677	377
	140	49095	-2.2195	54.6675	377
	141	49094	-2.2198	54.6674	377
	142	49219	-2.2201	54.6673	378
	143	49219	-2.2204	54.6672	378
	144	49226	-2.2207	54.6671	379
	145	49180	-2.2210	54.6670	380
	146	49088	-2.2213	54.6669	380
	147	49089	-2.2216	54.6669	381
	148	49046	-2.2218	54.6667	380
	149	49284	-2.2221	54.6666	378
	150	49337	-2.2224	54.6665	372
	151	49162	-2.2228	54.6664	371
	152	49155	-2.2231	54.6663	371
	153	49269	-2.2234	54.6662	370
	154	49267	-2.2237	54.6661	370
	155	49207	-2.2240	54.6659	369
	156	49183	-2.2243	54.6658	368
	157	49038	-2.2251	54.6664	377
	158	49128	-2.2254	54.6664	374
	159	49120	-2.2258	54.6665	374
	160	49024	-2.2262	54.6665	365
	161	48638	-2.2265	54.6667	365
	162	48778	-2.2266	54.6667	360
	163	48701	-2.2268	54.6668	360
	164	49046	-2.2272	54.6667	364
	165	49110	-2.2275	54.6666	362
	166	48912	-2.2278	54.6664	362
	167	48792	-2.2281	54.6664	364
	168	48774	-2.2284	54.6662	365
	169	48829	-2.2286	54.6661	369
	170	48921	-2.2289	54.6660	368
	171	48942	-2.2283	54.6658	368
	172	48997	-2.2284	54.6656	368
	173	49030	-2.2286	54.6654	365
	174	49029	-2.2287	54.6652	368
	175	49053	-2.2287	54.6651	370

	176	49050	-2.2287	54.6648	367
	177	49097	-2.2289	54.6646	365
	178	49130	-2.2290	54.6644	367
	179	49111	-2.2291	54.6642	366
	180	49096	-2.2293	54.6640	365
	181	49057	-2.2294	54.6639	365
	182	49012	-2.2296	54.6637	365
	183	49013	-2.2297	54.6636	365
19	183	48985	-2.2321	54.6744	387
	184	49020	-2.2324	54.6743	388
	185	49009	-2.2326	54.6741	389
	186	48853	-2.2329	54.6740	390
	187	48895	-2.2330	54.6738	390
	188	49033	-2.2332	54.6736	391
	189	49018	-2.2334	54.6734	390
	190	49052	-2.2336	54.6732	386
	191	48904	-2.2338	54.6731	380
	192	48790	-2.2341	54.6730	377
	193	48602	-2.2342	54.6729	373
	194	48699	-2.2334	54.6728	374
	195	49043	-2.2348	54.6728	375
	196	49157	-2.2351	54.6727	382
	197	49038	-2.2350	54.6724	385
	198	49268	-2.2352	54.6722	385
	199	49424	-2.2353	54.6721	385
	200	49414	-2.2355	54.6719	382
	201	49155	-2.2357	54.6717	383
	202	49050	-2.2358	54.6715	387
	203	49034	-2.2357	54.6712	387
	204	48942	-2.2359	54.6710	387
	205	48895	-2.2360	54.6709	389
	206	48961	-2.2362	54.6707	389
	207	48988	-2.2365	54.6705	389
	208	48910	-2.2368	54.6703	388
	209	48898	-2.2369	54.6702	385
	210	48845	-2.2371	54.6701	379
	211	48858	-2.2376	54.6700	378
	212	48890	-2.2376	54.6698	379
	213	48879	-2.2377	54.6696	380
20	2001	49156	-2.2221	54.6714	382
	2002	49153	-2.2219	54.6715	382
	2003	49159	-2.2215	54.6716	382
	2004	49176	-2.2213	54.6717	381
	2005	49237	-2.2210	54.6718	382
	2006	49200	-2.2208	54.6719	382
	2007	49164	-2.2206	54.6720	383
	2008	49088	-2.2204	54.6721	384
	2009	49080	-2.2201	54.6722	384

	2010	49150	-2.2199	54.6723	384
	2011	49172	-2.2197	54.6724	385
	2012	49177	-2.2194	54.6725	385
	2013	49150	-2.2192	54.6726	385
	2014	49120	-2.2190	54.6727	385
	2015	49155	-2.2187	54.6728	385
	2016	49143	-2.2185	54.6729	386
	2017	49133	-2.2183	54.6730	386
	2018	49147	-2.2181	54.6731	386
	2019	49158	-2.2178	54.6732	386
	2020	49189	-2.2176	54.6733	385
	2021	49195	-2.2174	54.6734	386
	2022	49195	-2.2171	54.6735	387
	2023	49197	-2.2169	54.6736	388
	2024	49198	-2.2167	54.6737	389
	2025	49230	-2.2164	54.6738	389
	2026	49208	-2.2162	54.6739	390
	2027	49205	-2.2160	54.6740	391
	2028	49209	-2.2158	54.6741	392
	2029	49190	-2.2155	54.6742	393
	2030	49162	-2.2153	54.6743	394
	2031	49146	-2.2151	54.6744	395
	2032	49130	-2.2148	54.6745	396
	2033	49090	-2.2146	54.6746	397
	2034	49063	-2.2144	54.6747	398
	2035	49038	-2.2141	54.6748	399
	2036	49020	-2.2139	54.6749	400
	2037	49002	-2.2137	54.6750	402
	2038	48992	-2.2135	54.6751	404
	2039	48973	-2.2132	54.6752	406
	2040	48972	-2.2130	54.6753	410
	2041	48975	-2.2128	54.6754	414
	2042	48975	-2.2125	54.6755	420
	2043	48984	-2.2123	54.6756	425
	2044	49005	-2.2121	54.6757	432
	2045	49031	-2.2118	54.6758	440
	2046	49023	-2.2116	54.6759	445
	2047	49029	-2.2114	54.6760	449
	2048	49048	-2.2112	54.6761	453
	2049	49061	-2.2109	54.6762	460
	2050	49065	-2.2107	54.6763	467
	2051	49079	-2.2105	54.6764	471
	2052	49088	-2.2102	54.6765	474
	2053	49074	-2.2100	54.6766	477
	2054	49092	-2.2098	54.6767	479
	2055	49090	-2.2095	54.6768	481
	2056	49092	-2.2093	54.6769	483
	2057	49071	-2.2091	54.6770	484

	2058	49084	-2.2089	54.6771	485
	2059	49088	-2.2086	54.6772	485
	2060	49080	-2.2084	54.6773	486
	2061	49090	-2.2082	54.6774	488
	2062	49089	-2.2079	54.6775	489
	2063	49086	-2.2077	54.6775	490
21	2101	49059	-2.2166	54.6777	445
	2102	49050	-2.2168	54.6776	444
	2103	49052	-2.2169	54.6775	442
	2104	49058	-2.2171	54.6774	440
	2105	49049	-2.2172	54.6772	438
	2106	49060	-2.2174	54.6771	440
	2107	49057	-2.2176	54.6770	443
	2108	49058	-2.2177	54.6769	445
	2109	49046	-2.2179	54.6768	443
	2110	49051	-2.2180	54.6767	440
	2111	49044	-2.2182	54.6766	437
	2112	49050	-2.2184	54.6764	431
	2113	49037	-2.2185	54.6763	428
	2114	49031	-2.2187	54.6762	422
	2115	49016	-2.2188	54.6761	420
	2116	49008	-2.2190	54.6760	419
	2117	48988	-2.2192	54.6759	418
	2118	48978	-2.2193	54.6757	416
	2119	48964	-2.2195	54.6756	419
	2120	48947	-2.2196	54.6755	421
	2121	48938	-2.2198	54.6754	426
	2122	48948	-2.2200	54.6753	430
	2123	48935	-2.2201	54.6752	434
	2124	48953	-2.2203	54.6751	430
	2125	48984	-2.2204	54.6749	430
	2126	49017	-2.2206	54.6748	428
	2127	49050	-2.2208	54.6747	426
	2128	49059	-2.2209	54.6746	425
	2129	49094	-2.2211	54.6745	423
	2130	49102	-2.2212	54.6744	421
	2131	49114	-2.2214	54.6743	417
	2132	49112	-2.2216	54.6741	415
	2133	49124	-2.2217	54.6740	412
	2134	49112	-2.2219	54.6739	409
	2135	49115	-2.2220	54.6738	406
	2136	49132	-2.2222	54.6737	400
	2137	49145	-2.2224	54.6736	396
	2138	49155	-2.2225	54.6735	394
	2139	49167	-2.2227	54.6733	389
	2140	49176	-2.2228	54.6732	387
	2141	49160	-2.2230	54.6731	385
	2142	49168	-2.2232	54.6730	384

	2143	49161	-2.2233	54.6729	383
	2144	49157	-2.2235	54.6728	382
22	1	49040	-2.2721	54.6853	430
	2	49043	-2.2720	54.6854	424
	3	49105	-2.2719	54.6855	420
	4	49117	-2.2717	54.6856	419
	5	48997	-2.2716	54.6856	404
	6	49159	-2.2715	54.6857	403
	7	49196	-2.2714	54.6857	399
	8	49234	-2.2713	54.6859	399
	9	49248	-2.2713	54.6861	400
	10	49132	-2.2708	54.6862	399
	11	49151	-2.2706	54.6863	400
	12	49102	-2.2706	54.6864	399
	13	48779	-2.2706	54.6865	397
	14	48726	-2.2706	54.6866	398
	15	48956	-2.2705	54.6867	400
	16	48908	-2.2704	54.6869	399
	17	48852	-2.2705	54.6870	396
	18	48944	-2.2705	54.6870	397
	19	48940	-2.2704	54.6870	413
	20	49035	-2.2704	54.6870	430
	21	49083	-2.2702	54.6871	441
	22	49083	-2.2700	54.6873	443
	23	49102	-2.2699	54.6874	445
	24	49118	-2.2671	54.6864	416
	25	49107	-2.2671	54.6863	423
	26	49083	-2.2672	54.6863	420
	27	49111	-2.2672	54.6861	422
	28	49039	-2.2673	54.6860	419
	29	49045	-2.2674	54.6859	415
	30	49027	-2.2675	54.6858	415
	31	49024	-2.2676	54.6857	411
	32	49011	-2.2677	54.6856	406
	33	49013	-2.2677	54.6855	405
	34	48982	-2.2678	54.6854	408
	35	48947	-2.2679	54.6853	407
	36	48907	-2.2680	54.6852	408
	37	48888	-2.2681	54.6851	407
	38	48783	-2.2682	54.6851	407
	39	48804	-2.2683	54.6849	408
	40	48948	-2.2684	54.6849	406
	41	49296	-2.2684	54.6848	408
	42	49261	-2.2684	54.6847	410
	43	49428	-2.2685	54.6846	410
	44	49424	-2.2686	54.6845	413
	45	49473	-2.2663	54.6840	411
	46	49479	-2.2661	54.6841	410

	47	49321	-2.2660	54.6842	409
	48	48925	-2.2659	54.6843	407
	49	48781	-2.2656	54.6843	408
	50	48760	-2.2656	54.6845	407
	51	48864	-2.2656	54.6845	407
	52	48883	-2.2655	54.6846	406
	53	48920	-2.2654	54.6847	407
	54	48959	-2.2653	54.6848	408
	55	48990	-2.2652	54.6849	406
	56	48979	-2.2652	54.6850	406
	57	49000	-2.2650	54.6851	412
	58	49002	-2.2649	54.6852	415
	59	49022	-2.2647	54.6853	417
	60	49016	-2.2647	54.6854	419
	61	49090	-2.2646	54.6855	422
	62	49060	-2.2645	54.6857	422
	63	49085	-2.2644	54.6857	423
	64	49096	-2.2643	54.6858	423
23	0	48868	-2.2164	54.6589	350
	25	48886	-2.2168	54.6589	350
	50	48912	-2.2172	54.6587	351
	75	48889	-2.2175	54.6588	352
	100	48871	-2.2178	54.6590	353
	125	48887	-2.2181	54.6591	353
	150	48929	-2.2184	54.6592	354
	175	48967	-2.2187	54.6594	354
	200	48989	-2.2189	54.6595	355
	225	49014	-2.2192	54.6596	355
	250	49016	-2.2195	54.6597	355
	275	49009	-2.2198	54.6599	355
	300	49005	-2.2201	54.6600	356
	325	49049	-2.2204	54.6601	356
	350	49115	-2.2207	54.6603	356
	375	49190	-2.2210	54.6604	356
	400	49177	-2.2213	54.6605	357
	425	49148	-2.2216	54.6607	357
	450	49150	-2.2218	54.6608	357
	475	49182	-2.2221	54.6609	358
	500	49187	-2.2224	54.6610	359
	525	49129	-2.2227	54.6612	359
	550	49034	-2.2230	54.6613	360
	575	48983	-2.2233	54.6614	361
	600	48936	-2.2236	54.6616	362
	625	48964	-2.2239	54.6616	363
	650	48931	-2.2242	54.6616	364
	675	48893	-2.2245	54.6617	364
	700	48857	-2.2247	54.6617	365
	725	48873	-2.2250	54.6617	365

	750	48911	-2.2253	54.6617	365
	775	48936	-2.2256	54.6618	365
	800	48957	-2.2259	54.6618	365
	825	48986	-2.2262	54.6618	365
	850	49028	-2.2265	54.6619	365
	875	49052	-2.2268	54.6619	365
	900	49040	-2.2271	54.6619	365
	925	49014	-2.2274	54.6620	365
	950	49001	-2.2276	54.6620	365
	975	48971	-2.2279	54.6620	365
	1000	48968	-2.2282	54.6620	365
	1025	48965	-2.2285	54.6621	365
	1050	48981	-2.2288	54.6621	365
	1075	48977	-2.2291	54.6621	365
	1100	48975	-2.2294	54.6622	365
	1125	48983	-2.2297	54.6622	365
	1150	48970	-2.2300	54.6622	356
	1175	48941	-2.2303	54.6623	365
	1200	48921	-2.2305	54.6623	365
24	0	48897	-2.2198	54.6590	357
	25	48886	-2.2201	54.6590	359
	50	48842	-2.2205	54.6590	360
	75	48848	-2.2208	54.6590	363
	100	48850	-2.2212	54.6590	365
	125	48847	-2.2215	54.6590	367
	150	48847	-2.2219	54.6590	368
	175	48890	-2.2222	54.6590	370
	200	48933	-2.2226	54.6590	371
	225	48942	-2.2230	54.6590	373
	250	48925	-2.2233	54.6589	374
	275	48926	-2.2237	54.6589	376
	300	48946	-2.2240	54.6589	378
	325	48920	-2.2244	54.6589	379
	350	48933	-2.2247	54.6589	380
	375	48927	-2.2251	54.6589	382
	400	48940	-2.2254	54.6589	383
	425	48930	-2.2258	54.6589	383
	450	48938	-2.2262	54.6589	384
	475	48943	-2.2265	54.6589	384
	500	48929	-2.2269	54.6589	385
	525	48915	-2.2272	54.6589	385
	550	48884	-2.2276	54.6589	386
	575	48909	-2.2279	54.6589	386
	600	48926	-2.2283	54.6588	386
	625	48973	-2.2286	54.6588	386
	650	48954	-2.2290	54.6588	386
	675	48925	-2.2293	54.6588	386
	700	48902	-2.2297	54.6588	386

25	0	49020	-2.2155	54.6577	358
	25	49009	-2.2159	54.6577	359
	50	48978	-2.2162	54.6577	360
	75	48949	-2.2165	54.6577	362
	100	48931	-2.2169	54.6577	363
	125	48924	-2.2172	54.6577	364
	150	48932	-2.2176	54.6577	365
	175	48944	-2.2179	54.6578	367
	200	48953	-2.2183	54.6578	368
	225	48910	-2.2186	54.6578	369
	250	48901	-2.2190	54.6578	370
	275	48903	-2.2193	54.6578	371
	300	48932	-2.2197	54.6578	372
	325	48917	-2.2200	54.6578	372
	350	48915	-2.2204	54.6578	373
	375	48915	-2.2207	54.6578	373
	400	48924	-2.2210	54.6579	374
	425	48926	-2.2214	54.6579	374
	450	48948	-2.2217	54.6579	375
	475	48965	-2.2221	54.6579	376
	500	48993	-2.2224	54.6579	377
	525	49009	-2.2228	54.6579	377
	550	49024	-2.2231	54.6579	378
	575	49009	-2.2235	54.6579	380
	600	48998	-2.2238	54.6580	381
	625	48989	-2.2242	54.6580	381
	650	48990	-2.2245	54.6580	382
	675	48994	-2.2248	54.6580	383
	700	48990	-2.2252	54.6580	384
	725	48979	-2.2255	54.6580	385
	750	48953	-2.2259	54.6580	386
	775	48938	-2.2262	54.6580	386
	800	48936	-2.2266	54.6581	387
	825	48950	-2.2269	54.6581	387
	850	48963	-2.2273	54.6581	388
	875	48961	-2.2276	54.6581	389
	900	48951	-2.2280	54.6581	390
	925	48938	-2.2283	54.6581	391
	950	48927	-2.2287	54.6581	392
	975	48925	-2.2290	54.6581	393
	1000	48921	-2.2293	54.6582	394
26	0	48955	-2.2151	54.6563	367
	25	48956	-2.2155	54.6563	368
	50	48957	-2.2158	54.6563	369
	75	48955	-2.2162	54.6563	371
	100	48957	-2.2166	54.6563	372
	125	48962	-2.2169	54.6563	373
	150	48952	-2.2173	54.6563	375

	175	48935	-2.2177	54.6563	377
	200	48920	-2.2180	54.6563	378
	225	48911	-2.2184	54.6563	379
	250	48918	-2.2188	54.6562	380
	275	48932	-2.2191	54.6562	381
	300	48947	-2.2195	54.6562	383
	325	48962	-2.2198	54.6562	384
	350	48971	-2.2202	54.6562	385
	375	48988	-2.2206	54.6562	387
	400	48992	-2.2209	54.6562	388
	425	48992	-2.2213	54.6562	389
	450	48985	-2.2217	54.6562	390
	475	48969	-2.2220	54.6562	391
	500	48956	-2.2224	54.6562	392
	525	48948	-2.2228	54.6562	392
	550	48951	-2.2231	54.6562	393
	575	48949	-2.2235	54.6562	394
	600	48946	-2.2238	54.6562	395
	625	48942	-2.2242	54.6562	396
	650	48938	-2.2246	54.6561	397
	675	48925	-2.2249	54.6561	399
	700	48910	-2.2253	54.6561	401
	725	48911	-2.2257	54.6561	402
	750	48900	-2.2260	54.6561	403
	775	48913	-2.2264	54.6561	405
	800	48908	-2.2268	54.6561	407
	825	48943	-2.2271	54.6561	408
	850	48951	-2.2275	54.6561	409
	875	48940	-2.2278	54.6561	410
	900	48920	-2.2282	54.6561	412
27	3	48978	-2.2333	54.6746	413
	7	48960	-2.2335	54.6744	412
	11	48899	-2.2336	54.6743	408
	15	48895	-2.2337	54.6741	403
	19	49024	-2.2338	54.6740	398
	23	49214	-2.2340	54.6738	397
	27	49364	-2.2341	54.6737	399
	31	49391	-2.2342	54.6735	399
	35	49359	-2.2343	54.6734	395
	39	49274	-2.2345	54.6732	392
	43	49116	-2.2346	54.6731	390
	47	48934	-2.2347	54.6729	388
	51	48795	-2.2349	54.6728	387
	55	48731	-2.2350	54.6726	387
	59	48751	-2.2351	54.6725	387
	63	48822	-2.2352	54.6723	389
	25	48918	-2.2354	54.6722	387
	29	48991	-2.2355	54.6720	385

	32	49017	-2.2356	54.6719	383
	34	49000	-2.2357	54.6717	380
	38	48968	-2.2359	54.6716	378
	42	48926	-2.2360	54.6714	377
	46	48891	-2.2361	54.6713	377
	49	48869	-2.2362	54.6711	378
	51	48862	-2.2364	54.6710	375
	53	48870	-2.2365	54.6708	374
	55	48884	-2.2366	54.6707	377
	57	48911	-2.2368	54.6705	380
	59	48936	-2.2369	54.6704	380
	61	48946	-2.2370	54.6702	383
	65	48942	-2.2371	54.6701	388
	69	48941	-2.2373	54.6699	388
	73	48952	-2.2374	54.6698	389
	77	48978	-2.2375	54.6696	387
	81	48997	-2.2376	54.6695	385
	85	49015	-2.2378	54.6693	386
	89	49006	-2.2379	54.6692	387
	91	49004	-2.2380	54.6690	388
	95	48998	-2.2381	54.6689	387
	99	49012	-2.2383	54.6687	387
	103	49013	-2.2384	54.6686	386
	107	49016	-2.2385	54.6684	386
	111	49007	-2.2387	54.6683	386
	115	49001	-2.2388	54.6681	388
	119	49010	-2.2389	54.6680	388
	124	49012	-2.2390	54.6678	388
	128	49016	-2.2392	54.6677	387
	132	48998	-2.2393	54.6675	385
	136	48989	-2.2394	54.6674	387
	140	48981	-2.2395	54.6672	385
	144	48979	-2.2397	54.6671	388
	148	48990	-2.2398	54.6669	388
	152	49008	-2.2399	54.6668	388
	156	49015	-2.2400	54.6666	389
	159	49013	-2.2402	54.6665	389
	161	49003	-2.2403	54.6663	390
	163	49013	-2.2404	54.6662	390
	165	49006	-2.2406	54.6660	391
	167	49005	-2.2407	54.6659	390
	169	48993	-2.2408	54.6657	391
28	3	48920	-2.2372	54.6732	382
	5	48904	-2.2373	54.6730	383
	7	48845	-2.2375	54.6729	385
	11	48794	-2.2376	54.6727	380
	15	48751	-2.2377	54.6725	378
	19	48761	-2.2379	54.6724	377

	21	48826	-2.2380	54.6722	378
	25	48916	-2.2381	54.6720	380
	29	48991	-2.2383	54.6719	383
	32	49017	-2.2384	54.6717	385
	34	49000	-2.2385	54.6715	384
	38	48968	-2.2387	54.6714	385
	42	48926	-2.2388	54.6712	386
	46	48891	-2.2389	54.6710	385
	49	48869	-2.2391	54.6709	385
	51	48862	-2.2392	54.6707	385
	53	48870	-2.2393	54.6705	385
	55	48884	-2.2394	54.6703	385
	57	48911	-2.2396	54.6702	384
	59	48936	-2.2397	54.6700	384
	61	48959	-2.2398	54.6698	384
	62	48955	-2.2400	54.6697	384
	65	48947	-2.2401	54.6695	384
	69	48941	-2.2402	54.6693	384
	73	48952	-2.2404	54.6692	383
	77	48978	-2.2405	54.6690	383
	81	48997	-2.2406	54.6688	383
	85	49020	-2.2408	54.6687	383
	88	49010	-2.2409	54.6685	383
	91	49008	-2.2410	54.6683	383
	95	48998	-2.2412	54.6682	382
	99	49012	-2.2413	54.6680	382
	103	49013	-2.2414	54.6678	382
	107	49016	-2.2416	54.6677	382
	111	49007	-2.2417	54.6675	382
	115	49001	-2.2418	54.6673	382
	119	49010	-2.2419	54.6671	381
	124	49012	-2.2421	54.6670	381
	128	49016	-2.2422	54.6668	381
	132	48998	-2.2423	54.6666	381
	136	48989	-2.2425	54.6665	381
	140	48981	-2.2426	54.6663	381
	144	48979	-2.2427	54.6661	380
	148	48990	-2.2429	54.6660	380
	152	49008	-2.2430	54.6658	380
	156	49015	-2.2431	54.6656	380
	159	49013	-2.2433	54.6655	380
	161	49003	-2.2434	54.6653	380
	163	49013	-2.2435	54.6651	379
	165	49006	-2.2437	54.6650	379
	167	49005	-2.2438	54.6648	379
	169	48993	-2.2439	54.6646	379
29	3	49074	-2.2334	54.6818	440
	7	49076	-2.2336	54.6817	439

	10	49077	-2.2337	54.6815	420
	13	49084	-2.2339	54.6814	421
	15	49086	-2.2340	54.6812	431
	17	49087	-2.2342	54.6811	432
	18	49087	-2.2344	54.6809	430
	19	49085	-2.2345	54.6808	422
	20	49080	-2.2347	54.6806	419
	22	49070	-2.2348	54.6805	417
	24	49069	-2.2350	54.6804	417
	26	49060	-2.2352	54.6802	417
	28	49055	-2.2353	54.6801	417
	30	49037	-2.2355	54.6799	415
	32	49034	-2.2356	54.6798	411
	34	49026	-2.2358	54.6796	409
	36	49017	-2.2360	54.6795	407
	38	48998	-2.2361	54.6793	405
	40	48976	-2.2363	54.6792	403
	42	48951	-2.2364	54.6791	401
	44	48926	-2.2366	54.6789	404
	46	48906	-2.2368	54.6788	406
	49	48897	-2.2369	54.6786	404
	51	48900	-2.2371	54.6785	401
	53	48910	-2.2372	54.6783	398
	55	48918	-2.2374	54.6782	396
	57	48924	-2.2376	54.6781	393
	59	48923	-2.2377	54.6779	373
	61	48918	-2.2379	54.6778	371
	63	48905	-2.2380	54.6776	371
	65	48864	-2.2382	54.6775	370
	67	48783	-2.2384	54.6773	371
	70	48752	-2.2385	54.6772	373
	74	48752	-2.2387	54.6770	373
	78	48813	-2.2388	54.6769	381
	82	48859	-2.2390	54.6768	386
	86	48916	-2.2392	54.6766	387
	90	48969	-2.2393	54.6765	389
	94	49023	-2.2395	54.6763	389
	98	49081	-2.2396	54.6762	387
	102	49148	-2.2398	54.6760	386
	106	49202	-2.2400	54.6759	386
	110	49229	-2.2401	54.6757	386
	114	49199	-2.2403	54.6756	386
	118	49126	-2.2404	54.6755	386
	119	49075	-2.2406	54.6753	386
	120	49112	-2.2408	54.6752	388
	124	49207	-2.2409	54.6750	388
	127	49283	-2.2411	54.6749	388
	131	49290	-2.2412	54.6747	390

	135	49259	-2.2414	54.6746	391
	139	49240	-2.2416	54.6744	390
	141	49238	-2.2417	54.6743	389
	144	49241	-2.2419	54.6742	389
	146	49247	-2.2420	54.6740	389
	148	49253	-2.2422	54.6739	388
	150	49237	-2.2424	54.6737	389
	152	49213	-2.2425	54.6736	390
	154	49190	-2.2427	54.6734	390
	157	49188	-2.2428	54.6733	389
	161	49173	-2.2430	54.6731	388
	165	49126	-2.2432	54.6730	389
	170	49067	-2.2433	54.6729	390
	174	48997	-2.2435	54.6727	390
	177	48949	-2.2436	54.6726	391
	181	48872	-2.2438	54.6724	391
	185	48804	-2.2440	54.6723	390
	189	48719	-2.2441	54.6721	390
	193	48709	-2.2443	54.6720	390
	197	48753	-2.2444	54.6718	392
	201	48844	-2.2446	54.6717	393
	205	48915	-2.2448	54.6716	394
	209	48962	-2.2449	54.6714	394
	213	48993	-2.2451	54.6713	395
	217	49020	-2.2452	54.6711	396
	221	49051	-2.2454	54.6710	396
	225	49048	-2.2456	54.6708	396
	229	49038	-2.2457	54.6707	397
	233	49008	-2.2459	54.6705	397
	237	49012	-2.2460	54.6704	397
	241	49015	-2.2462	54.6703	397
	245	49024	-2.2464	54.6701	398
	249	49025	-2.2465	54.6700	399
30	4	48935	-2.2388	54.6815	462
	6	48937	-2.2389	54.6814	459
	7	48941	-2.2390	54.6812	457
	8	48946	-2.2392	54.6811	454
	9	48955	-2.2393	54.6809	452
	10	48969	-2.2395	54.6808	449
	12	48986	-2.2396	54.6806	447
	13	49009	-2.2397	54.6805	444
	15	49034	-2.2399	54.6803	442
	17	49066	-2.2400	54.6802	439
	21	49093	-2.2402	54.6800	437
	25	49121	-2.2403	54.6799	434
	29	49152	-2.2404	54.6797	432
	33	49207	-2.2406	54.6796	429
	37	49261	-2.2407	54.6794	427

	41	49281	-2.2409	54.6793	424
	45	49243	-2.2410	54.6791	422
	49	49157	-2.2411	54.6790	419
	53	49024	-2.2413	54.6788	417
	57	48806	-2.2414	54.6787	414
	61	48597	-2.2416	54.6785	412
	65	48505	-2.2417	54.6784	409
	69	48566	-2.2418	54.6782	407
	73	48698	-2.2420	54.6781	404
	77	48798	-2.2421	54.6779	402
	81	48870	-2.2423	54.6777	399
	85	48926	-2.2424	54.6776	400
	89	49010	-2.2425	54.6774	401
	93	49139	-2.2427	54.6773	402
	97	49269	-2.2428	54.6771	403
	101	49357	-2.2430	54.6770	403
	105	49367	-2.2431	54.6768	404
	109	49329	-2.2433	54.6767	405
	113	49272	-2.2434	54.6765	406
	117	49229	-2.2435	54.6764	407
	121	49206	-2.2437	54.6762	408
	125	49195	-2.2438	54.6761	408
	129	49189	-2.2440	54.6759	409
	133	49192	-2.2441	54.6758	410
	137	49203	-2.2442	54.6756	411
	141	49208	-2.2444	54.6755	412
	145	49203	-2.2445	54.6753	413
	149	49188	-2.2447	54.6752	413
	153	49174	-2.2448	54.6750	414
	157	49167	-2.2449	54.6749	415
	161	49162	-2.2451	54.6747	416
	164	49155	-2.2452	54.6746	417
	167	49124	-2.2454	54.6744	418
	171	49085	-2.2455	54.6743	418
	175	49024	-2.2456	54.6741	419
	180	48935	-2.2458	54.6740	419
	184	48824	-2.2459	54.6738	419
	188	48785	-2.2461	54.6737	419
	191	48837	-2.2462	54.6735	419
	195	48968	-2.2463	54.6734	419
	199	49079	-2.2465	54.6732	419
	203	49152	-2.2466	54.6731	419
	207	49173	-2.2468	54.6729	419
	211	49124	-2.2469	54.6727	419
	215	49074	-2.2470	54.6726	419
	219	49022	-2.2472	54.6724	419
	223	49000	-2.2473	54.6723	419
	227	48959	-2.2475	54.6721	419

	231	48916	-2.2476	54.6720	419
	235	48903	-2.2477	54.6718	419
	239	48899	-2.2479	54.6717	419
	242	48902	-2.2480	54.6715	419
	246	48897	-2.2482	54.6714	420
	250	48939	-2.2483	54.6712	420
	252	48980	-2.2484	54.6711	420
	254	49008	-2.2486	54.6709	420
	258	48967	-2.2487	54.6708	420
	262	48918	-2.2489	54.6706	420
	266	48897	-2.2490	54.6705	420
	270	48902	-2.2491	54.6703	420
	274	48938	-2.2493	54.6702	420
	279	48967	-2.2494	54.6700	420
	283	48998	-2.2496	54.6699	420
	286	49005	-2.2497	54.6697	420
	288	48994	-2.2498	54.6696	420
	290	49005	-2.2500	54.6694	420
	292	49013	-2.2501	54.6693	420
	294	49017	-2.2503	54.6691	420
	296	48985	-2.2504	54.6690	420
	298	48963	-2.2505	54.6688	420
	300	48962	-2.2507	54.6687	421
	302	48976	-2.2508	54.6685	421
	304	48999	-2.2510	54.6684	421
	306	48998	-2.2511	54.6682	421
	308	48997	-2.2512	54.6681	421
	310	48985	-2.2514	54.6679	421
	312	48992	-2.2515	54.6677	421
	314	48990	-2.2517	54.6676	421
	316	48998	-2.2518	54.6674	421
	318	48990	-2.2519	54.6673	421
	320	49005	-2.2521	54.6671	421
	322	48991	-2.2522	54.6670	421
	324	48985	-2.2524	54.6668	421
	326	48973	-2.2525	54.6667	421
	328	48990	-2.2527	54.6665	421
	330	49012	-2.2528	54.6664	421
	332	49026	-2.2529	54.6662	421
	334	49028	-2.2531	54.6661	421
31	3	48978	-2.2411	54.6833	479
	5	48985	-2.2412	54.6832	475
	7	48999	-2.2414	54.6831	472
	9	49011	-2.2415	54.6829	468
	11	49022	-2.2417	54.6828	465
	13	49033	-2.2418	54.6827	461
	15	49039	-2.2420	54.6825	458
	17	49042	-2.2421	54.6824	454

	19	49039	-2.2422	54.6823	451
	21	49040	-2.2424	54.6821	447
	23	49040	-2.2425	54.6820	444
	28	49048	-2.2427	54.6819	444
	31	49063	-2.2428	54.6817	437
	35	49090	-2.2430	54.6816	433
	39	49128	-2.2431	54.6815	430
	43	49178	-2.2433	54.6813	426
	47	49226	-2.2434	54.6812	423
	51	49258	-2.2435	54.6811	419
	55	49266	-2.2437	54.6809	416
	60	49238	-2.2438	54.6808	412
	64	49179	-2.2440	54.6807	409
	68	49110	-2.2441	54.6805	405
	72	49069	-2.2443	54.6804	406
	76	49053	-2.2444	54.6803	402
	80	49054	-2.2446	54.6801	403
	84	49048	-2.2447	54.6800	403
	87	49028	-2.2448	54.6799	404
	91	48998	-2.2450	54.6797	404
	95	48952	-2.2451	54.6796	405
	99	48915	-2.2453	54.6795	405
	103	48917	-2.2454	54.6793	406
	107	48977	-2.2456	54.6792	406
	111	49079	-2.2457	54.6791	407
	115	49164	-2.2459	54.6789	407
	119	49203	-2.2460	54.6788	407
	123	49189	-2.2462	54.6787	408
	127	49164	-2.2463	54.6785	408
	132	49158	-2.2464	54.6784	409
	136	49193	-2.2466	54.6783	409
	139	49198	-2.2467	54.6781	410
	142	49228	-2.2469	54.6780	410
	145	49208	-2.2470	54.6779	411
	148	49198	-2.2472	54.6777	411
	149	49151	-2.2473	54.6776	412
	153	49141	-2.2475	54.6775	412
	155	49156	-2.2476	54.6773	413
	157	49186	-2.2477	54.6772	413
	159	49217	-2.2479	54.6771	414
	161	49233	-2.2480	54.6769	414
	163	49227	-2.2482	54.6768	414
	165	49212	-2.2483	54.6767	415
	168	49194	-2.2485	54.6765	415
	172	49173	-2.2486	54.6764	416
	176	49150	-2.2488	54.6763	416
	179	49125	-2.2489	54.6761	417
	182	49100	-2.2490	54.6760	417

	186	49055	-2.2492	54.6759	418
	190	49001	-2.2493	54.6757	418
	194	48964	-2.2495	54.6756	419
	198	48968	-2.2496	54.6755	419
	202	49008	-2.2498	54.6753	420
	206	49075	-2.2499	54.6752	420
	210	49149	-2.2501	54.6751	421
	214	49179	-2.2502	54.6749	421
	218	49128	-2.2503	54.6748	421
	222	49076	-2.2505	54.6747	422
	226	49060	-2.2506	54.6745	422
	230	49072	-2.2508	54.6744	423
	234	49064	-2.2509	54.6743	423
	238	49007	-2.2511	54.6741	424
	242	48960	-2.2512	54.6740	424
	245	48941	-2.2514	54.6739	425
	248	48980	-2.2515	54.6737	425
	251	49014	-2.2517	54.6736	426
	255	49011	-2.2518	54.6735	426
	259	48975	-2.2519	54.6733	427
	263	48955	-2.2521	54.6732	427
	267	48932	-2.2522	54.6731	428
	271	48908	-2.2524	54.6729	428
	275	48895	-2.2525	54.6728	428
	279	48910	-2.2527	54.6727	429
	283	48907	-2.2528	54.6725	429
	287	48907	-2.2530	54.6724	430
	291	48918	-2.2531	54.6723	430
	295	48967	-2.2532	54.6721	431
	301	48999	-2.2534	54.6720	431
	303	49010	-2.2535	54.6719	432
	305	49019	-2.2537	54.6717	432
	307	49014	-2.2538	54.6716	433
	309	49006	-2.2540	54.6715	433
	311	48977	-2.2541	54.6713	434
	313	48972	-2.2543	54.6712	434
	315	48949	-2.2544	54.6711	435
	317	48920	-2.2545	54.6709	435
	319	48902	-2.2547	54.6708	435
	321	48927	-2.2548	54.6707	436
	323	48989	-2.2550	54.6705	436
	325	49048	-2.2551	54.6704	437
	327	49073	-2.2553	54.6703	437
	329	49068	-2.2554	54.6701	438
	331	49034	-2.2556	54.6700	438
	333	48980	-2.2557	54.6699	439
	335	48933	-2.2558	54.6697	439
	337	48913	-2.2560	54.6696	440

	339	48932	-2.2561	54.6695	440
	341	48964	-2.2563	54.6693	441
	343	48978	-2.2564	54.6692	441
	345	48983	-2.2566	54.6691	442
	347	48994	-2.2567	54.6689	442
	349	49008	-2.2569	54.6688	442
32	5	49116	-2.2488	54.6845	470
	7	49111	-2.2490	54.6844	468
	8	49099	-2.2491	54.6842	464
	9	49086	-2.2493	54.6841	461
	11	49072	-2.2494	54.6840	459
	13	49066	-2.2496	54.6839	456
	15	49069	-2.2497	54.6838	453
	17	49077	-2.2498	54.6837	450
	19	49079	-2.2500	54.6836	447
	20	49082	-2.2501	54.6835	444
	21	49085	-2.2503	54.6834	441
	22	49092	-2.2504	54.6833	438
	24	49091	-2.2506	54.6832	435
	25	49092	-2.2507	54.6830	432
	27	49096	-2.2508	54.6829	430
	29	49103	-2.2510	54.6828	427
	31	49104	-2.2511	54.6827	424
	34	49094	-2.2513	54.6826	421
	38	49071	-2.2514	54.6825	418
	42	49057	-2.2516	54.6824	415
	46	49038	-2.2517	54.6823	412
	50	49065	-2.2518	54.6822	409
	54	48976	-2.2520	54.6821	406
	58	48867	-2.2521	54.6819	403
	62	48888	-2.2523	54.6818	401
	66	49184	-2.2524	54.6817	398
	70	49445	-2.2526	54.6816	400
	73	49464	-2.2527	54.6815	402
	77	49318	-2.2528	54.6814	405
	81	49172	-2.2530	54.6813	407
	85	49039	-2.2531	54.6812	409
	89	49053	-2.2533	54.6811	412
	93	49141	-2.2534	54.6810	414
	97	49244	-2.2535	54.6809	416
	101	49230	-2.2537	54.6807	419
	105	49231	-2.2538	54.6806	421
	109	49147	-2.2540	54.6805	423
	113	49077	-2.2541	54.6804	426
	117	49017	-2.2543	54.6803	426
	122	49090	-2.2544	54.6802	426
	126	49127	-2.2545	54.6801	427
	129	49140	-2.2547	54.6800	427

	131	49152	-2.2548	54.6799	427
	133	49155	-2.2550	54.6798	428
	135	49145	-2.2551	54.6796	428
	137	49135	-2.2553	54.6795	428
	139	49137	-2.2554	54.6794	429
	141	49145	-2.2555	54.6793	429
	143	49149	-2.2557	54.6792	429
	145	49153	-2.2558	54.6791	430
	147	49153	-2.2560	54.6790	430
	149	49146	-2.2561	54.6789	430
	151	49114	-2.2563	54.6788	431
	153	49062	-2.2564	54.6787	431
	155	49010	-2.2565	54.6786	431
	158	48979	-2.2567	54.6784	432
	162	48966	-2.2568	54.6783	432
	166	48952	-2.2570	54.6782	432
	170	48913	-2.2571	54.6781	433
	173	48877	-2.2573	54.6780	433
	175	48859	-2.2574	54.6779	433
	177	48861	-2.2575	54.6778	434
	179	48871	-2.2577	54.6777	434
	181	48892	-2.2578	54.6776	434
	183	48930	-2.2580	54.6775	435
	185	48960	-2.2581	54.6774	435
	187	48976	-2.2583	54.6772	435
	189	48973	-2.2584	54.6771	436
	191	48971	-2.2585	54.6770	436
	193	48972	-2.2587	54.6769	436
	195	48985	-2.2588	54.6768	437
	197	48988	-2.2590	54.6767	437
	199	48978	-2.2591	54.6766	437
	201	48983	-2.2593	54.6765	438
	203	48980	-2.2594	54.6764	438
	205	48998	-2.2595	54.6763	438
	207	49013	-2.2597	54.6761	439
	208	49007	-2.2598	54.6760	439
	210	48988	-2.2600	54.6759	439
	212	48945	-2.2601	54.6758	440
	214	48964	-2.2603	54.6757	440
	216	48958	-2.2604	54.6756	440
	218	48981	-2.2605	54.6755	441
	220	49003	-2.2607	54.6754	441
	222	49034	-2.2608	54.6753	441
	224	49011	-2.2610	54.6752	442
	226	48935	-2.2611	54.6751	442
	228	48926	-2.2613	54.6749	442
	230	48901	-2.2614	54.6748	443
	232	48942	-2.2615	54.6747	443

	234	48955	-2.2617	54.6746	443
	236	49011	-2.2618	54.6745	444
	238	49046	-2.2620	54.6744	444
	240	49016	-2.2621	54.6743	444
	242	49010	-2.2623	54.6742	445
33	4	49149	-2.2450	54.6842	473
	7	49150	-2.2451	54.6841	470
	9	49149	-2.2452	54.6839	466
	11	49144	-2.2454	54.6838	463
	12	49142	-2.2455	54.6836	459
	13	49130	-2.2457	54.6835	456
	14	49121	-2.2458	54.6833	453
	16	49105	-2.2459	54.6832	450
	18	49096	-2.2461	54.6830	447
	20	49095	-2.2462	54.6829	444
	22	49096	-2.2463	54.6827	441
	24	49111	-2.2465	54.6825	438
	26	49107	-2.2466	54.6824	435
	27	49100	-2.2468	54.6822	432
	28	49076	-2.2469	54.6821	430
	30	49054	-2.2470	54.6819	427
	34	49026	-2.2472	54.6818	424
	38	49005	-2.2473	54.6816	421
	41	49006	-2.2475	54.6815	418
	44	49016	-2.2476	54.6813	415
	46	49050	-2.2477	54.6812	412
	50	49052	-2.2479	54.6810	409
	54	49043	-2.2480	54.6808	406
	58	49045	-2.2482	54.6807	403
	62	48995	-2.2483	54.6805	401
	66	48892	-2.2484	54.6804	398
	70	48802	-2.2486	54.6802	400
	74	48864	-2.2487	54.6801	402
	78	49024	-2.2488	54.6799	405
	82	49153	-2.2490	54.6798	407
	86	49208	-2.2491	54.6796	409
	88	49240	-2.2493	54.6795	412
	92	49256	-2.2494	54.6793	414
	96	49273	-2.2495	54.6792	416
	100	49270	-2.2497	54.6790	419
	104	49249	-2.2498	54.6788	421
	108	49202	-2.2500	54.6787	423
	112	49179	-2.2501	54.6785	426
	116	49190	-2.2502	54.6784	426
	120	49171	-2.2504	54.6782	426
	124	49130	-2.2505	54.6781	427
	127	49052	-2.2507	54.6779	427
	128	49023	-2.2508	54.6778	427

	130	49010	-2.2509	54.6776	428
	134	49026	-2.2511	54.6775	428
	138	49062	-2.2512	54.6773	428
	142	49102	-2.2513	54.6771	429
	145	49140	-2.2515	54.6770	429
	148	49163	-2.2516	54.6768	429
	152	49171	-2.2518	54.6767	430
	154	49169	-2.2519	54.6765	430
	156	49164	-2.2520	54.6764	430
	159	49151	-2.2522	54.6762	431
	163	49126	-2.2523	54.6761	431
	167	49077	-2.2525	54.6759	431
	171	49034	-2.2526	54.6758	432
	175	49014	-2.2527	54.6756	432
	178	49019	-2.2529	54.6754	432
	179	49013	-2.2530	54.6753	433
	183	49009	-2.2531	54.6751	433
	186	49002	-2.2533	54.6750	433
	189	49001	-2.2534	54.6748	434
	193	48986	-2.2536	54.6747	434
	196	48951	-2.2537	54.6745	434
	198	48926	-2.2538	54.6744	435
	200	48947	-2.2540	54.6742	435
	202	49013	-2.2541	54.6741	435
	204	49097	-2.2543	54.6739	436
	206	49126	-2.2544	54.6738	436
	208	49111	-2.2545	54.6736	436
	210	49064	-2.2547	54.6734	437
	212	49031	-2.2548	54.6733	437
	214	49016	-2.2550	54.6731	437
	216	49015	-2.2551	54.6730	438
Ettersgill					
	Stn. No.	magred.nT	long deg.	lat deg.	alt.m
34	103	49581	-2.1832	54.6622	351
	104	49581	-2.1831	54.6622	351
	105	49499	-2.1830	54.6623	353
	106	49497	-2.1829	54.6621	350
	107	49554	-2.1830	54.6620	351
	108	49556	-2.1829	54.6620	350
	109	48821	-2.1826	54.6619	340
	110	47496	-2.1825	54.6619	340
35	111	48401	-2.1818	54.6616	356
	112	47889	-2.1818	54.6617	358
	113	47958	-2.1818	54.6619	360
	114	48202	-2.1818	54.6620	362
	115	48594	-2.1819	54.6620	363
	116	48908	-2.1818	54.6621	364

	117	49036	-2.1817	54.6622	364
36	118	49086	-2.1817	54.6623	364
	119	49099	-2.1811	54.6624	364
	120	49021	-2.1811	54.6623	366
	121	48888	-2.1808	54.6622	363
	122	48592	-2.1808	54.6621	363
	123	48370	-2.1805	54.6620	361
	124	48340	-2.1805	54.6619	361
	125	48356	-2.1802	54.6619	360
	126	48452	-2.1801	54.6617	359
	stn		Long.	Lat.	Alt.
37	2201	49079	-2.1419	54.6576	351
	2202	48998	-2.1419	54.6575	350
	2203	48828	-2.1419	54.6574	349
	2204	48475	-2.1419	54.6573	351
	2205	48515	-2.1419	54.6573	348
	2206	48655	-2.1419	54.6572	349
	2207	48734	-2.1419	54.6571	350
	2208	48794	-2.1419	54.6570	350
	2209	48846	-2.1419	54.6569	351
	2210	48884	-2.1419	54.6568	350
	2211	48910	-2.1419	54.6567	350
	2212	48932	-2.1419	54.6566	349
	2213	48942	-2.1419	54.6565	349
	2214	48945	-2.1419	54.6564	350
	2215	48943	-2.1419	54.6564	350
	2216	48939	-2.1419	54.6563	351
38	2301	48872	-2.1403	54.6563	365
	2302	48873	-2.1403	54.6564	364
	2303	48870	-2.1403	54.6565	363
	2304	48877	-2.1403	54.6566	362
	2305	48876	-2.1403	54.6567	361
	2306	48872	-2.1403	54.6569	359
	2307	48878	-2.1403	54.6570	360
	2308	48879	-2.1403	54.6571	362
	2309	48880	-2.1403	54.6572	363
	2310	48889	-2.1403	54.6573	362
	2311	48896	-2.1403	54.6574	363
	2312	48856	-2.1403	54.6575	363
	2313	48806	-2.1403	54.6576	362
	2314	48704	-2.1403	54.6577	361
	2315	48865	-2.1403	54.6578	362
	2316	48979	-2.1403	54.6579	362
39	2401	49124	-2.1387	54.6581	376
	2402	49102	-2.1387	54.6580	374
	2403	49081	-2.1387	54.6579	372
	2404	49057	-2.1387	54.6577	370
	2405	49028	-2.1387	54.6576	367

	2406	49004	-2.1387	54.6575	368
	2407	48978	-2.1387	54.6574	366
	2408	48952	-2.1387	54.6573	364
	2409	48930	-2.1387	54.6571	362
	2410	48891	-2.1387	54.6570	361
	2411	48839	-2.1387	54.6569	360
	2412	48774	-2.1387	54.6568	359
	2413	48725	-2.1387	54.6567	358
	2414	48661	-2.1387	54.6565	359
	2415	48310	-2.1387	54.6564	358
	2416	48808	-2.1387	54.6563	359
40	2417	48806	-2.1387	54.6562	359
	2501	48973	-2.1371	54.6564	384
	2502	49020	-2.1371	54.6566	382
	2503	49047	-2.1371	54.6567	379
	2504	49074	-2.1371	54.6569	376
	2505	49103	-2.1371	54.6570	374
	2506	49101	-2.1371	54.6572	371
	2507	49107	-2.1371	54.6574	370
	2508	49108	-2.1371	54.6575	370
	2509	49104	-2.1371	54.6577	369
	2510	49107	-2.1371	54.6578	368
	2511	49107	-2.1371	54.6580	366
	2512	49104	-2.1371	54.6582	365
	2513	49109	-2.1371	54.6583	365
	2514	49127	-2.1371	54.6585	365
	2515	49134	-2.1371	54.6586	365
	2516	49142	-2.1371	54.6588	364